TTI: 0-6941

Texas A&M Transportation Institute

Direct Determination of Cement Composition by X-ray Diffraction

Technical Report 0-6941-R1

Cooperative Research Program

TEXAS A&M TRANSPORTATION INSTITUTE
COLLEGE STATION, TEXAS

in cooperation with the
Federal Highway Administration and the
Texas Department of Transportation
http://tti.tamu.edu/documents/0-6941-R1.pdf

Technical Report Documentation Page

1. Report No.	2. Government Accession No.	3. Recipient's Catalog No.
FHWA/TX-19/0-6941-R1		

4. Title and Subtitle	5. Report Date
DIRECT DETERMINATION OF CEMENT COMPOSITION BY X-RAY DIFFRACTION	Published: June 2019
	6. Performing Organization Code

7. Author(s)	8. Performing Organization Report No.
Anol Mukhopadhyay, Ramnath Mylapore Ganesh, Kai-Wei Liu, and Youjun Deng	Report 0-6941-R1

9. Performing Organization Name and Address	10. Work Unit No. (TRAIS)
Texas A&M Transportation Institute The Texas A&M University System College Station, Texas 77843-3135	11. Contract or Grant No. Project 0-6941

12. Sponsoring Agency Name and Address	13. Type of Report and Period Covered
Texas Department of Transportation Research and Technology Implementation Office 125 E. 11th Street Austin, Texas 78701-2483	Technical Report: September 2016–August 2018
	14. Sponsoring Agency Code

15. Supplementary Notes

Project performed in cooperation with the Texas Department of Transportation.
Project Title: Direct Determination of Cement Composition by X-ray Diffraction
URL: http://tti.tamu.edu/documents/0-6941-R1.pdf

16. Abstract

This project established protocols and specifications for the direct determination of cement composition by Quantitative X-ray Diffraction (QXRD). The main objectives of this research were: 1) developing protocols for routinely performing QXRD testing, 2) testing the effectiveness of the protocols using commercial cement samples, and 3) documenting the potential qualitative and economic benefits of utilizing QXRD. Researchers developed a state of the art QXRD methodology through regular collaboration and knowledge transfer with industrial experts. In addition to the important findings, further recommendations to improve the current phase quantification were proposed to address some of the gaps in existing research and testing. Researchers predicted the financial implications using life-cycle cost analysis procedures if industrial quality control adopts these protocols. The conclusions, both important and supplementary, were recorded with recommendations for future implementation projects.

17. Key Words	18. Distribution Statement
Cement, Blended Cements, Quantitative X-ray Diffraction, ASTM C150, Fly Ash, Pressed Pellet QXRD, TGA, Calorimetry, Bogue	No restrictions. This document is available to the public through NTIS: National Technical Information Service Alexandria, Virginia http://www.ntis.gov

19. Security Classification (of this report)	20. Security Classification (of this page)	21. No. of Pages	22. Price
Unclassified	Unclassified	102	

Form DOT F 1700.7 (8-72) Reproduction of completed page authorized

DIRECT DETERMINATION OF CEMENT COMPOSITION BY X-RAY DIFFRACTION

by

Anol Mukhopadhyay
Research Scientist
Texas A&M Transportation Institute

Ramnath Mylapore Ganesh
Graduate Assistant – Research
Texas A&M Transportation Institute

Kai-Wei Liu
Assistant Transportation Engineer
Texas A&M Transportation Institute

and

Youjun Deng
Professor, Department of Soil & Agricultural Sciences
Texas A&M University - College Station

Product 0-6941-R1
Project 0-6941
Project Title: Direct Determination of Cement Composition using X-ray Diffraction

Performed with financial assistance and cooperation from the
Texas Department of Transportation

Published: June 2019

TEXAS A&M TRANSPORTATION INSTITUTE
College Station, Texas 77843-3135

DISCLAIMER

This research was performed with assistance from the Texas Department of Transportation (TxDOT). The contents of this report reflect the views of the authors, who are responsible for the facts, and the accuracy of the data presented herein. The contents do not necessarily reflect the official view or policies of TxDOT. The research scientist in charge of the project was Dr. Anol K. Mukhopadhyay.

The United States Government and the State of Texas do not endorse products or manufacturers. Trade or manufacturers' names appear herein solely because they are considered essential to the object of this report.

ACKNOWLEDGMENTS

This project was completed with financial assistance from TxDOT. The authors wish to express their appreciation to TxDOT personnel for their support throughout this study. Special thanks are extended to Darrin Jensen as the project manager and to Andy Naranjo, Clifton Coward Jr., and Masoud Moradian for coordinating this project with their technical feedback. Acknowledgment is also due to all the staff at Texas A&M Transportation Institute (TTI). We would like to thank Dr. Kai-Wei Liu of TTI, and Dr. Youjun Deng of the Texas A&M University for their support at different stages of this project.

The authors would also like to acknowledge the strategic involvement of our industrial collaborators including, Jeff Hook, Andy Chafin (Lehigh Cement Company), Peter Lausser (Bruker AXS), Paul Stutzman (National Institute of Standards), Paul Tennis (Portland Cement Association), Greg Barger (Ash Grove Cement), and Victor Gonzalez (Leigh Cement Company).

TABLE OF CONTENTS

LIST OF FIGURES

Page

LIST OF TABLES

Page

CHAPTER 1. INTRODUCTION

BACKGROUND AND SIGNIFICANCE OF THE WORK

Determination of accurate cement phase composition (identification and quantification) using more accurate measurement techniques has the potential to improve our knowledge on cement hydration characteristics and capability to predict fresh and hardened (especially strength development) behavior and durability of concrete. Current protocols (ASTM C150) dictate that the Bogue method for quantifying cement phases is to be used to calculate clinker and cement phase compositions. The Bogue methodology uses elemental oxide weight percentages (wt.%) (i.e., bulk chemical composition) of clinker determined by a suitable test method recommended in ASTM C 114 (e.g., X-ray Fluorescence [XRF]) to generate (predominantly) the phase fraction estimates of alite, belite, aluminate, and ferrite. However, the phase abundance calculated by this method may be far from reality since the four main clinker phases are solid solutions with compositions significantly different from the stoichiometric composition of the pure phase. Several investigators had observed that the Bogue method incorporates various errors in its formulation, which lead to the generation of incomplete and inaccurate chemical composition information [1-4]. Furthermore, the Bogue method is incapable quantifying the amorphous contents (in blended cements), limestone phases (calcite and dolomite), calcium sulfates, and other additives/impurities.

Sometimes, changes to the chemistry of the melt inside the kiln can arise due to the variations in raw materials or burning conditions. These changes can lead to the clinker phases stabilizing in variant crystal structures that diverge from the actual or anticipated morphology. Such variants are called phase polymorphs. The polymorphic forms of the major clinker phases influence the hydration characteristics of the cement paste to a considerable extent [5-9]. This phenomenon was not well understood during the formulation of the Bogue method [10], which led to the method being developed discrediting such vital information.

The failure of the Bogue method to properly track such changes mean that the overwhelming control over cement performance properties is lost by the manufacturer. For instance, the accurate phase fraction determination of limestone phases can tell the difference between overuse or underuse of burning high-quality limestone to get the desired phases. In addition, the presence of sulfate phases, predominantly from the gypsum phase, poses as another challenge where the cement setting properties are directly affected. Furthermore, the complications involved with the different polymorphs of sulfate and their influence on ettringite formation (reaction with the aluminate phase) cannot be understood from the Bogue method.

Now, quantification through X-ray Diffraction (XRD) is a direct method of measurement that can overcome the disadvantages of the Bogue method. Quantitative X-ray Diffraction (QXRD) can directly identify and measure the limestone, sulfates, and the polymorphic variants in cement, thereby presenting as a natural solution to many problems with the Bogue method. Direct quantification of cement phases provides a more complete accounting of the actual phase compositions, which facilitates relating mineralogical composition to performance characteristics and improving predictive capability of cements. Still, certain disagreements prevail over the consistent application of QXRD protocols for cement quality control. This project documents proper QXRD protocols and the corresponding phase specifications similar to ASTM C150. In addition, several improvements were suggested as an extension of the research performed for this study, which can be directly incorporated during the QXRD analysis.

The overall goal of this project was to advance the use of QXRD method for cement phase quantification. This goal was accomplished through several stages followed as: 1) determination of the barriers preventing the progression of XRD in production testing and solutions to overcome these barriers through an extensive literature survey, 2) development of protocols for determining cement composition by QXRD for ASTM C150 and C595 types of cements, 3) determination of the effects on cement production if QXRD is used to quantify the cement phases, especially relating to C_3A-gypsum optimization and the influence of polymorphs, and finally 4) providing recommendations to the current specification based on QXRD based rather than Bogue based phase quantification information.

SCOPE OF THE PROJECT

Each chapter contains congregated information from the efforts performed according to the tasks in the proposal to maintain the flow of the report. A summary was provided at the end of each chapter to serve as a primer to the work described in the next chapter. The report outline is as follows:

- **Chapter 1**: **Introduction** provides a background on the problems with the Bogue method and the importance of modifying the current specifications.
- **Chapter 2: Literature Review** provides a historical overview of the cement phase quantification and introduces the application of QXRD in cement quality control. It also introduces the barriers preventing QXRD adoption and identifies the gaps in existing research.
- **Chapter 3: Protocols Development** addresses the errors or deficiencies of the current protocols (optimum fineness, amorphous quantification, extraction, etc.) and promotes experimental solutions to address the deficiencies or gaps. Improving the QXRD repeatability and reproducibility was identified as a major impediment that has not yet been addressed in existing literature. Hence, experiments using pressed pellets were pursued to address this issue, and the results were validated through microscopic investigations.
- **Chapter 4: Specification Development** contains step by step information of the QXRD protocols that were developed in this project along with steps to perform Rietveld refinement for quantifying the cement phases. In addition, the phase limits for the important ASTM C150 cement types were listed here with explanation behind the experimental model that was used to generate the phase limits.
- **Chapter 5: Specific Validation of QXRD Using Supportive Characterization Tools** addresses the outlying gaps in existing research using limited experimental data. The chapter includes information on the usage of QXRD-isothermal calorimetry for gypsum optimization, quick and accurate limestone quantification using QXRD, and its validation using thermogravimetric analysis (TGA). The outcomes of this chapter, although not directly related to the project, can be useful in highlighting the importance of QXRD for cement phase quantification.
- **Chapter 6: Determination of Effects on Cement Process Control** comprises case studies where the employment of QXRD in quality control can affect production testing. Examples of such areas include, grinding, gypsum optimization, cost of QXRD operation, etc. This chapter contains most of the information on process control

advantages offered by QXRD as per the most recent knowledge of cement chemistry and kiln process control.

- **Chapter 7: Cost Benefits Analysis** provides the financial implications of using QXRD for process control in cement manufacturing. In addition, several intangible yet important qualitative benefits of QXRD were summarized with proper justification.
- **Chapter 8: Summary** presents the observations and findings of this study and catalogues the conclusions derived from each chapter along with some observations for further implementation.

CHAPTER 2. LITERATURE REVIEW

Cement as a construction material has been in employment since pre-Roman times, as a lime-cement variant. At present, cement is the most common construction material in the world, which is evident from its carbon footprint. Burning of limestone, clay, shale, and iron ore in the kiln at elevated temperatures releases carbon dioxide and results in the generation of clinker compounds that vary widely in their phase compositions. Inter-blending or inter-grinding of gypsum to the cement clinker produces portland cement, which in combination with aggregates and water gains gradual strength to form concrete. ASTM C150M-17 [11] specifies compositional requirements covering five major types of commercial portland cement namely Types I, II, III, IV, and V. ASTM C595 specification pertains to blended hydraulic cements for both general and special applications, using slag, pozzolan, limestone, and prescribes ingredients and proportions with some performance requirements.

CEMENT PHASE QUANTIFICATION

The Bogue method, enshrined in ASTM C150M-17, is the current industrial standard for the determination of contents of different cement phases. This method uses oxide compositional estimates to compute the major cementitious phase fractions through a series of simultaneous equations. The original Bogue formulated matrix is reproduced in the following equations:

$$C3S = 4.071 \times \%CaO - 7.600 \times \%SiO_2 - 6.718 \times \%Al_2O_3 - 1.430 \times \%Fe_2O_3 - 2.852 \times \%SO_3 \quad \text{Eq. (1)}$$

$$C2S = 2.867 \times \%SiO_2 - 0.7544 \times \%C3S \quad \text{Eq. (2)}$$

$$C3A = 2.650 \times \%Al_2O_3 - 1.692 \times \%Fe_2O_3 \quad \text{Eq. (3)}$$

$$C4AF = 3.043 \times \%Fe_2O_3 \quad \text{Eq. (4)}$$

The Bogue equations were formulated with a small data set of samples, which meant that the quantification was limited only to four clinker phases and the estimation of the phases was not accurate for all cases. It was apparent when Taylor [1] found that the Bogue method consistently underpredicted the alite and overpredicted the aluminate contents in cement. The Modified Bogue method, proposed by Taylor [1], took the quantification of the sulfate and other minor phases into account for the cement coming from a finish mill. However, the equations of Modified Bogue were formulated in much the same way as the Bogue method, which meant that there was still not a large enough data set to be considered statistically reliable. Stutzman et al. [4] observed an error of ±9.6 wt.% for alite and belite, ±2.2 wt.% for aluminate, and ±1.6 wt.% for ferrite, from the actual stoichiometric composition of a commercial clinker, as the extent of errors contributed by the Bogue method to cement phase quantification. As a result, QXRD was developed as a more accurate and direct determination technique to quantify cement phases to overcome the pitfalls of the Bogue method.

QXRD is a fingerprint technique for the identification of crystalline phases in cement, and the phase quantity is directly proportional to the intensity of the X-ray reflections (i.e., commonly called as XRD peaks) from the major crystallographic planes in a phase. Preliminary analysis of cement through QXRD (in the 60s and 70s) was performed on bulk and chemically pre-treated cement by Hjorth [12], Aldridge [13], and Gutteridge [14], through the single-peak fitting method. With the arrival of micro-processor units, improved software programs for

cement QXRD were developed that engendered quantification through the Rietveld method and whole-pattern fitting [15-17]. Stutzman [18] in 1996 devised a QXRD methodology as a precursor for the employment of a standard QXRD protocol for quantitative cement analysis. Several researchers around the world [19-27] updated their best practices followed for cement QXRD to identify a quantification method that is better than ASTM C150 and lead to the development of the ASTM C1365 [28].

However, some issues relating to the morphology or properties of the cement phases remained unresolved in QXRD. For instance, the preferred orientation issue in the prismatic morphologies of the alite, gypsum, anhydrite, and hemihydrate phases. Preferred orientation is observed when the crystals of these phases align parallel to the sample holder surface and lead to a minor overestimation in the phase quantification through QXRD [29, 30]. This issue affects the alite phase the most among the discussed phases, while the other phases are often too low in quantity to be affected by preferred orientation. Similarly, increased X-ray absorption by the ferrite phase in cement can cause an underestimation of its quantity [31]. Although these issues are still prevalent in QXRD, the extent of inaccuracy in QXRD quantification is minimal compared to the Bogue method. Specifically, important phases such as limestone, sulfates, amorphous phases, and the C3A phase are not affected by the above issues associated with the QXRD method.

DIRECT APPLICATION OF QXRD

Application of QXRD can directly quantify the limestone and sulfate contents in the cement. Kumar et al. [32] perceived that QXRD incorporates an error of 0–5 wt.% in limestone in Type I-L cements after accounting for sample preparation errors. Huang et al. [33] and Soin et al. [34] identified the combination of TGA and QXRD to be a highly accurate tool for the quantification of limestone contents in cement and concrete. Similarly, TGA and QXRD were realized as the fastest tools for quantifying limestone comparing between combinations of BSE-SEM, TGA, QXRD, gamma ray densimetry, and isothermal calorimetry [32-38]. Hence, characterization of the cements using TGA and QXRD was performed in this project to generate a correlation between TGA and QXRD derived quantification for Type I-L cements.

Another important aspect is the control of the sulfate-aluminate ratio in cements leading to flash and false setting. Tang and Glasser [39] recognized that the inter-grinding of gypsum with the clinker in a finish mill can promote better control over cement setting than inter-blending. But the polymorphic transition of gypsum to anhydrite should be prevented during inter-grinding to avoid flash setting [40]. Gypsum-to-anhydrite conversion of the added calcium sulfate phase can occur as early 2 minutes into grinding, due to the rapid dehydration produced by the attrition heat [41]. Winnefeld et al. [42] observed that two cements with equal amounts of hemihydrate and gypsum generated ettringite within 5 minutes and 4 hours, respectively, through calorimetry measurements. Such a rapid reaction can often lead to false setting but can be recovered through gentle mixing or re-tempering. Hence in such cases, isothermal calorimetry measurements can accurately highlight the extent of reactivity differences between the gypsum and anhydrite before the cement is sent to the job site. Hence, the identification and quantification of sulfate polymorphs from QXRD can provide as an indicator of the setting issues, which can be understood from isothermal calorimetry.

In addition, the XRD technical shortcomings such as sample preparation inconsistencies, the ease of performing the analysis, and the reliability of the quantification also present a problem to industries (from Table 1). XRD sample preparation requires a diligent execution of

steps to generate reliable data and avoid systematic and random mistakes in sample preparation. Preferred orientation, micro-absorption, surface roughness, and sample porosity contribute to the most common differences in sample preparation. Whitfield and Mitchell [43] observed that fine-grinding to less than 10 µm can solve most of the QXRD sample preparation issues, including preferred orientation. Alternatively, preferred orientation effect can be minimized using alternative loading techniques such as backloading [44] or side loading [23] to mitigate the effect of the errors and improve the quantification accuracy. In a similar manner, extraction techniques were proposed to improve the quantification accuracy of the silicates (KOSH method [12]), aluminates (SAM method [14]), and the amorphous phases (HNO_3 method [45]), albeit being extremely time consuming. Luke and Glasser [46] elucidated that even binary and ternary blends of cement, fly ash, slag, and silica fume can all be quantified to ±1 wt.% accuracy through the dissolution of crystalline phases performed for hours. However, the observance of such time and labor-intensive techniques in conventional practice is waning, judging by the trends in important recent contributions to this field [47-49].

PRESSED PELLET QXRD

ASTM E177 [50] describes the reliability of a QXRD analysis using three terms: repeatability (within-lab variation), reproducibility (between-lab variation), and accuracy (variation from reference or actual values). Repeatability and reproducibility are often referred together as the precision of QXRD.

Several researchers [51-55] calculated the degree of repeatability and reproducibility variations in QXRD by performing round robin analyses. Petersen and Weber-Wisman [56] discovered that sampling and sample preparation inconsistencies contribute the highest percentage of variations/errors in phase quantification using X-ray methods (XRD and XRF) (see Figure 1). In particular, sample preparation imparts the most XRD errors if the sampling effects are considered negligible due to the homogeneity of commercial cements/clinkers. Indeed, the latest QXRD round robin analysis [57], which did not use a common sample preparation protocol, calculated the 95 percent repeatability variation to be ±2–3 wt.% and the 95 percent reproducibility variation of ±4–6 wt.% for the most abundant alite phase.

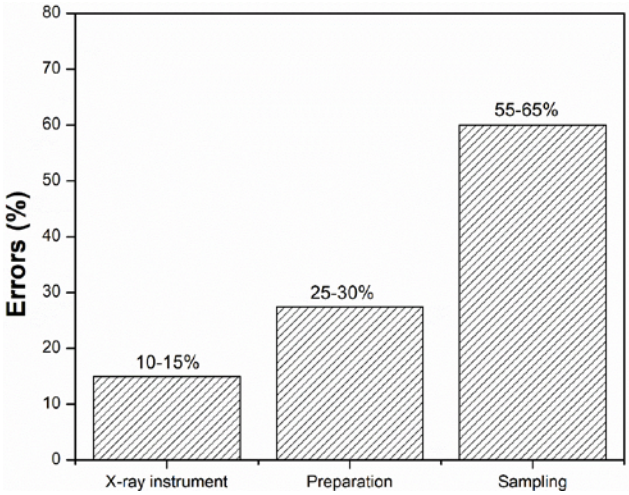

Figure 1. Distribution of Errors in X-ray Methodology as Calculated by Petersen and Weber-Wisman [56].

In order to improve the repeatability and reproducibility of QXRD, several European cement manufacturers use automated pressed pellet QXRD for routine cement analysis [41]. In the United States, the Lehigh Hanson cement plant at Maryland has been successfully using automatic pressed pellet QXRD for the past 3 years [58]. In the industry, pressing at a lower force (about 3–4 kN [59]) is performed directly in an XRD sample holder and the resulting pellet is automatically passed to the XRD instrument on a conveyor belt. Pressed pellet QXRD, although being a common practice in industry, does not enjoy full acceptance from the scientific community due to uncertainty about the effect of preferred orientation enhanced by pressing. Enders [60] observed that pressed pellets can impart an increased preferred orientation during pressing and advised on a low pressing force to make weak pellets for XRD analysis. Kocaba [61] generated pressed pellets and proved the increase in repeatability and reproducibility in clinker/cement pellet QXRD is unaffected by the pressing errors. However, no information was found on the pressing force used by Kocaba, which prevented the replication of the same experiment elsewhere. As a result, not much literature has been generated on pressed pellet sample preparation for QXRD and suspected issue of overestimation of alite due to preferred orientation needs be addressed through further work.

In this project, researchers generated a framework for strong pellet preparation (using pressing force around 130 kN) to improve the repeatability and reproducibility of powder QXRD and provide all information so that the technique is reproducible in a research and an industrial setting. A higher pressing force was desired to prepare pellet samples that are strong enough to be fit into the conventional XRD sample holders without breakage. Pressed pellets were analyzed using QXRD in three different labs using different instruments and the corresponding repeatability and reproducibility was quantified. A similar analysis was performed with powder QXRD and the comparison would be used to understand the effect of pelletizing on QXRD sample preparation. The issue of preferred orientation overestimating the alite quantification in pressed pellet QXRD was focused and its impact on repeatability and reproducibility was understood. In order to ascertain the accuracy of QXRD, supporting quantification using optical microscopic point counting and scanning electron microscopic image analysis (multispectral image analysis) were performed on the same samples. The accuracy analysis of pressed pellet and powder QXRD were performed to understand the difference between the two techniques.

Point-counting procedure to quantify the cement phase constituents is enshrined in two ASTM standard protocols, the C562 [62] and C1365 [63]. Backscattered electron microscopy (BSE-SEM) coupled with image analysis [64-67] is an effective tool to quantify cement phase composition. In this project, a recent technique called multispectral image analysis was used to spectrally distinguish the cement phases and quantify the phase contents based on [67].

BARRIERS PREVENTING QXRD ADOPTION IN PRODUCTION TESTING

The knowledge on the state of the art of cement phase composition in industrial quality control was collected from personal communication with industrial experts. The communications threw light on the barriers that preclude the widespread adoption of QXRD for online quality control. In spite of decades of research in the development of a universal QXRD protocol, ASTM still fails to recognize cement QXRD with a standard that is practicable in online quality control. This was put forward by some industrial experts as a major impediment for QXRD adoption during the course of the project. Table 1 categorizes the major disadvantages and advantages of QXRD as proposed by industrial experts. The underlying reasons can be classified into two major problems: 1) the systematic (preferred orientation, absorption contrast, etc.) and

random errors (surface roughness, height displacement, etc.) during sample preparation and measurement, and 2) the inconsistent results promulgated by QXRD due to the hardware and software discrepancies.

Table 1. Some of the Major Barriers Preventing QXRD and the Advantages of Using QXRD as Obtained from Industrial Experts.

Major Barriers
No standard calibration or a way to compare data from various XRD suppliers and methods
QXRD results are usually different than Bogue potentials, and this can cause confusion with personnel who are not familiar with QXRD
Lack of a good sample preparation procedure or the variability involved in QXRD sample preparation is large enough to cause confusion between supplier and consumer
Financial complications involved in justifying the purchase of a highly expensive equipment
Currently ASTM C150 and AASHTO M 85 do not include provisions for XRD-derived values of cement phase composition.
Advantages
Pressed pellet QXRD can be a routine quality control tool or a backup for the XRF [58]
QXRD is an accurate approach that can meet production QC time constraints [68]

Apart from the technical shortcomings, the financial burden of purchasing a fully automated XRD instrument along with its cost of operation is another major obstacle for industries.

SUMMARY OF CHAPTER 2

Personal communication with industrial experts identified sample preparation issues as the barriers that provided the most resistance toward the application of QXRD in online quality control. Errors arising due to sample preparation include fineness, preferred orientation, micro-absorption, peak shifts, asymmetric peaks, and random combinations of these errors. The prevalent mindset in industry was such that addressing some of the technical issues to make QXRD more reliable and easy to use can significantly increase the interest in QXRD adoption for online quality control.

Solutions to supplementary techniques discussed in this chapter such as extreme fine grinding, extraction methods, and backloading are required for the routine application of QXRD. However, a survey of the most recent literature [47-49] revealed that some of these techniques did not greatly influence the accuracy of QXRD, and consequently are expendable for routine analysis.

In industrial quality control, pressed pellets were identified to increase the repeatability and reproducibility of the QXRD. Since not much literature information could be found on pressed pellet QXRD, the reasoning behind its industrial adoption was investigated in this project experimentally. An experiment involving the QXRD analysis of a pressed pellet in three

different labs was proposed as a way to quantify the reproducibility of pellet QXRD. Comparison with a similar analysis of powder QXRD and comparing the accuracy of both pressed pellet and powder QXRD with microscopic investigations were also proposed.

CHAPTER 3. PROTOCOLS DEVELOPMENT

ISSUES WITH CURRENT PROTOCOLS

Researchers performed a precursor study on the state of the existing protocols for cement phase quantification using QXRD. Based on the knowledge gained in this study, the optimal sample preparation parameters existing in ASTM C1365 (standard for QXRD) [28] were deemed to be laborious for online testing. Some of the work intensive parameters include micro-grinding the cement to a particle size less than 5 μm, internal standard testing for amorphous phase quantification, different loading techniques for preferred orientation minimization, and selective extraction techniques. Workarounds were developed for such parameters, using basic engineering and the knowledge gained from the communications with industrial experts, so that the developed protocols obey the fundamental scientific principles of QXRD.

Sample Preparation

The following QXRD sample preparation practices were revisited and reworked in this project:

- Optimum fineness.
- Preferred orientation minimization.
- Reduction of absorption contrast effects.
- Selective dissolution or extraction techniques.
- Use of internal standard.

According to conventional QXRD protocols [49, 55], grinding a bulk cement clinker for around 10 minutes (5 μm median particle size) should effectively resolve the first three issues. Enders [69] explained about the loss of a sizeable proportion of the gypsum phases in cement during micronizing owing to the differential in hardness between phases. During grinding, the gypsum crystallites (with Moh's hardness of 2) get ground first as the strain imparted by the grinding elements is higher on the softer gypsum phase than the harder silicate phases. Le Saout et al. [23] found that the complete loss or conversion of the gypsum phase to its dehydrated transforms can occur as early as 60 seconds to 2 minutes into grinding. This development directly challenged the historical perception for accurate quantification: wet grinding must be proceeded for 10 minutes to produce cement size fractions in the 5 μm range. Hence, significant particle size reduction to around 5 μm in commercial cements cannot be considered an optimum QXRD sample preparation as it can affect the cement's phase contents.

Since the bulk commercial cements from the finish mill are at a fineness of around 10–15 μm, grinding is unnecessary for most QXRD purposes. This is exemplified in Figure 2 wherein the wet ground cement at a fineness of less than 5 μm displays suppressed gypsum and bassanite peaks indicating their reduced presence after grinding. Even a collapse of the bassanite or hemihydrate peak was observed. Whereas, the bulk cement of fineness around 10–15 μm provides a better signal to noise ratio than the wet ground cement, and the gypsum and hemihydrate peaks are properly represented without any major overlap or suppression.

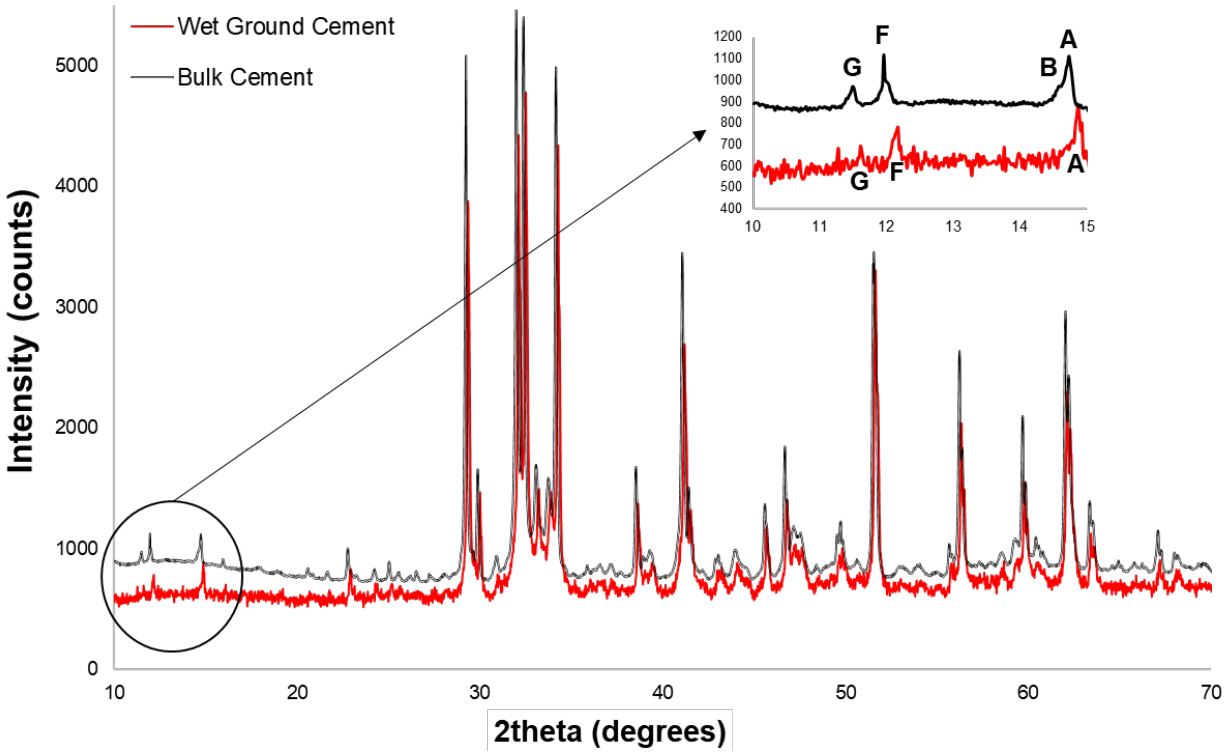

Note, the high amount of noise in the wet ground cement. G – gypsum, A – alite, B – basanite / hemihydrate, F – Brownmillerite.

Figure 2. The Suppression of the Gypsum Peak (G) to the Background Can Be Observed by Comparing the Relative Intensities of the G Peak between the Wet Ground and the Bulk Cements.

Dissolution and reprecipitation of the major cement phase groups to enrich the other phase groups is a very accurate mode of quantification. Individual methodologies exist for the dissolution of interstitial phases (the KOSH method, exemplified in Figure 3) [12], the silicate phases (the SAM method, exemplified in Figure 4) [14], and both silicate and interstitial phases (methanol-HNO3 method) [45] in cement and the supplementary cementing materials. Moreover, the techniques were found to be highly laborious, and sometimes inconsistent, thereby unsuitable for routine QXRD analysis. For instance, in the dissolution of all the crystalline phases through the HNO_3 method, a proper residue without any crystalline phases was unable to be obtained. Hence, selective dissolution of cements was not advised in the protocols.

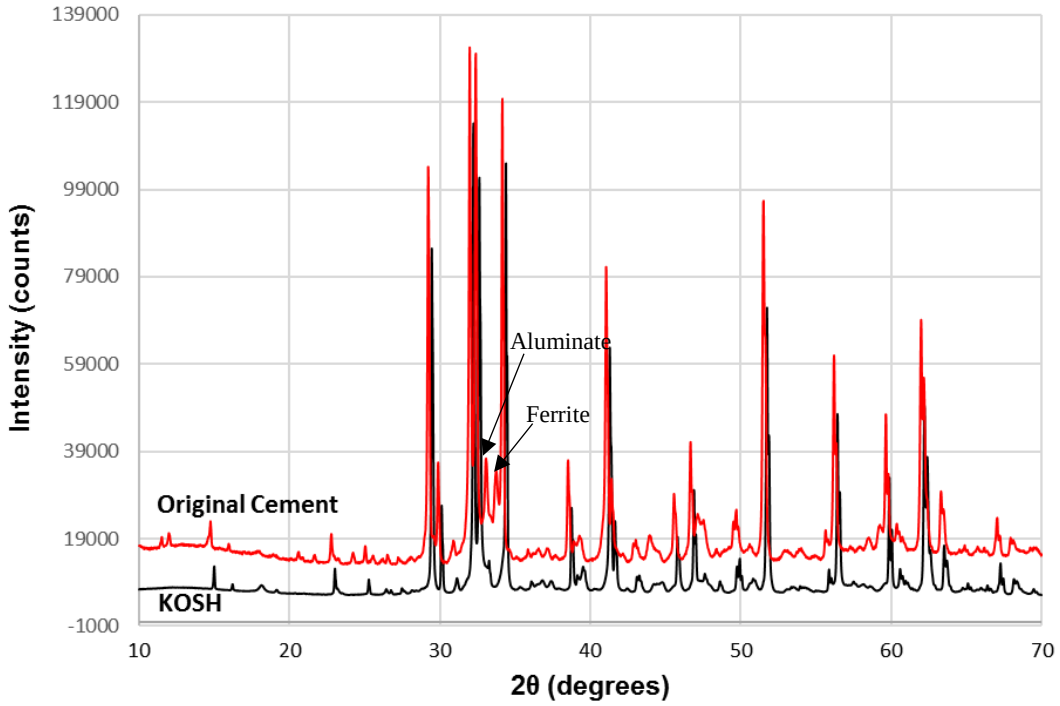

Figure 3. KOSH Method of Selective Dissolution of Interstitial Phases (Aluminate and Ferrite).

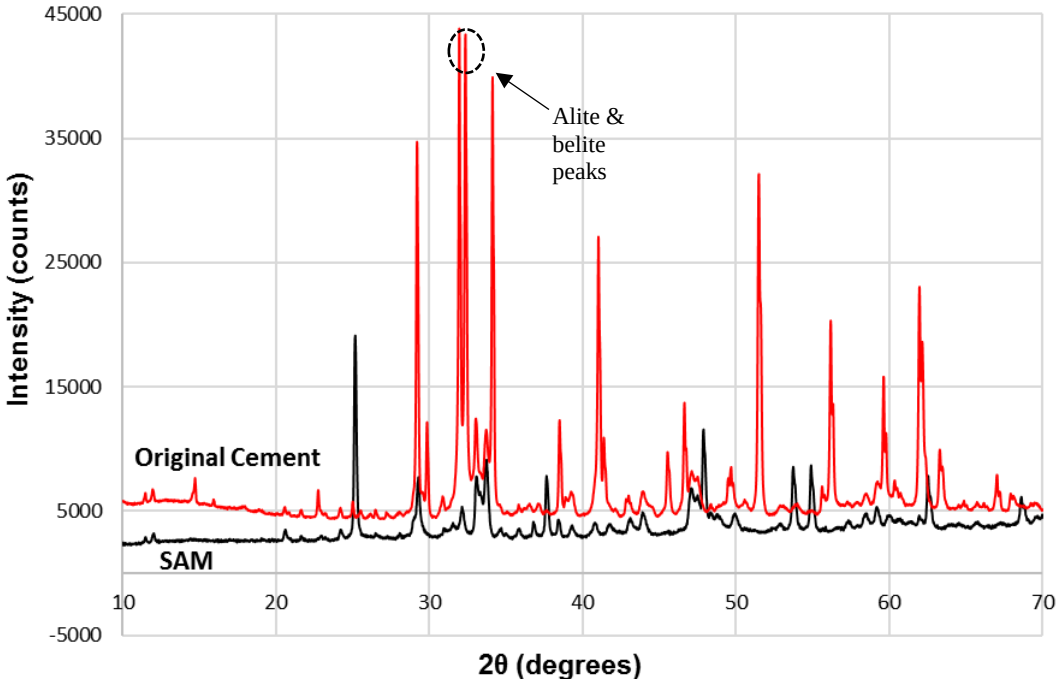

Figure 4. SAM Method of Selective Dissolution of Alite and Belite Phases.

Amorphous Phase Quantification

Since blended cements incorporate amorphous content (predominantly from fly ash and slag) in their constitution, conventional QXRD analysis often uses internal and external standard

techniques to quantify the amorphous phase. The internal standard technique involves the addition of a highly crystalline standard material to the blended cement and quantifying the amorphous phase retrospectively. The external standard technique requires a single addition of the standard material where the mass, X-ray absorption, and atomic number of the phase constituents of the standard are used for amorphous phase quantification.

Both techniques are known to be approximate, labor-intensive, and have well-known drawbacks [70]. While the internal standard method has a problem with the achievement of homogeneity of the standard material with the cement, the external standard method suffers from X-ray absorption differences between the standard material and cement leading to quantification errors. Westphal et al. [71] identified that for accurate quantification, a properly homogenous internal standard-cement mixture at a ratio of 1:1 is required. Jansen et al. [72] recognized the shortcomings of both standard methods and came up with a remastered external standard method modified from Suhermann et al. [73]. Jansen and co-workers [72, 74] generated the linear absorption coefficients of the cement phases and the standard material phase separately and derived a special relation called as the G-factor. The G-factor is a manifestation of the ZMV method [75] of external standard analysis that is popularly practiced in cement chemistry investigations using QXRD. The G-factor method requires the calibration of the absorption coefficients only once to get the approximate amorphous phase fraction.

The equation for calculating the internal standard phase composition is given by:

$$W_\alpha = \frac{S_\alpha (ZMV)_\alpha}{\sum_{j=1}^{n} S_j (ZMV)_j} \rightarrow Eq.(5)$$

Where, S_α = the scale factor for phase α.
Z = number of formula units per unit cell.
M = the mass of the formula unit.
V = the unit cell volume.
n = the number of phases in the analysis.

Eq. (6) provides the equation for calculating the phase constituent of the external standard using the G-factor calibration:

$$W_\alpha = \frac{S_\alpha (ZMV)_\alpha \mu_m^*}{G} \rightarrow Eq.(6)$$

Where, μ_m^* = the mass absorption coefficient of the entire sample.
G = normalization constant used to calculate the relative weight fraction of the amorphous phase.

A recent idea to directly quantify the amorphous phase fraction in blended cements is the Partially or No Known Crystalline structures (PONKCs) or pseudo-phase characterization [25, 47, 70, 75]. This technique records information about the mass, volume, and atomic number (ZMV) values of the commonly seen fly ash/slag amorphous phase and stores them into a pseudo crystal structure, called a PONKCs phase. The PONKCs amorphous phase can be refined similar to a crystalline phase to obtain the amorphous weight fraction.

Stetsko in 2016 [48] compared the internal, external, and PONKCs techniques and observed little variation between their amorphous phase fractions. However, there lies a caveat in

the PONKCs method with the creation of a proper amorphous pseudo-phase. The composition of the fly ashes produced in the United States vary considerably, and no single ASTM standard classifies the fly ashes or slags based on their mineralogical contents. Hence, the application of a single pseudo-phase for an amorphous fly ash or slag cannot be generalized over all fly ashes or slags obtained from different sources. Thus, one needs to be cautious when investigating the QXRD-generated amorphous phase fractions using PONKCs method and be mindful of these shortcomings.

QXRD Quantification of Fly Ash Added to Blended Cement

ASTM C595 specifies that fly ash addition to Type I cement should be between 20–40 wt.% replacement of cement. However, the exact quantity of fly ash addition is known only to the manufacturer. QXRD characterization of fly ash addition to Type I cement can provide an indication of the added fly ash quantity by the back-calculation of the cement and fly ash. Comparison between the determined and back-calculated fly ash can provide a relationship that can be generalized over Type I-P cements.

A source of low calcium fly ash was mixed with Portland cement at 5 percent, 10 percent, 20 percent, 30 percent, and 40 percent replacement ratios by weight. The phase fractions of the fly ash and the cement were pre-determined through QXRD, where a single PONKCs amorphous phase was used to characterize the amorphous component of fly ash. The PONKCs technique is better than the internal standard technique in rapidly quantifying low amorphous contents. An amorphous fraction less than 20 wt.% in the cement is difficult to detect using the internal standard method, unless proper intergrinding without damaging the mineral contents is performed, which is a labor-intensive and low efficiency method [71, 72, 74].

Comparison of the QXRD characterization of the added fly ash composition and the back-calculated fly ash composition yielded very good convergence. The back-calculated fly ash phase fractions were generated by multiplying the original phase fractions in cement and fly ash by their respective replacement ratios. Some of the observations that were made include:

1. Variation from added fly ash is least at commercial fly ash addition ranges (20–30 wt.%).
2. The QXRD calculation refers the quantification of the fly ash-cement mixture after replacement. It simulates the situation of performing QXRD where the phase contents of the original fly ash and cement are unknown, typical to what is commonly seen in TxDOT quality control of blended cements.
3. Back-calculation of fly ash was performed by multiplying the phase contents of the individual fly ash and cement before mixing. For example, at 5 percent fly ash replacement, the back-calculated fly ash is calculated by multiplying the phases in the original fly ash QXRD by 0.05 and the cement phases in the original cement QXRD by 0.95. Since the fly ash and cement did not have overlapping phases, this calculation is equivalent to the predicted fly ash content after mixing at 95 percent cement and 5 percent fly ash, respectively.
4. Amorphous fly ash phase was measurable by QXRD only when the added fly ash composition was >5 wt.% and closer to 10 wt.%. Therefore, the minimum detection limit of fly ash content is around 10 percent.

Table 2. Comparison of the Added Fly Ash Quantity against the Fly Ash Quantity from QXRD Direct Quantification and Back-Calculation from Replacement Ratios.

FLY ASH QUANTITY		
Replacement Levels	QXRD	Back-calculated FA
5	8.86	8.09
10	9.76	10.2
20	20.2	25.27
30	29.27	34.61
40	36.12	43.95

Table 2 illustrates a direct comparison of QXRD versus back-calculation of fly ash added to cement. The results suggest that QXRD determination of added fly ash suffers at additions less than 10 wt.% and greater than 40 wt.%. However, the determinations are extremely reliable in the mid-range and are better than calculated estimates. This points to the non-linearity of the distributed phase determination by QXRD. Figure 5 represents the back-calculation of added fly ash quantity from QXRD.

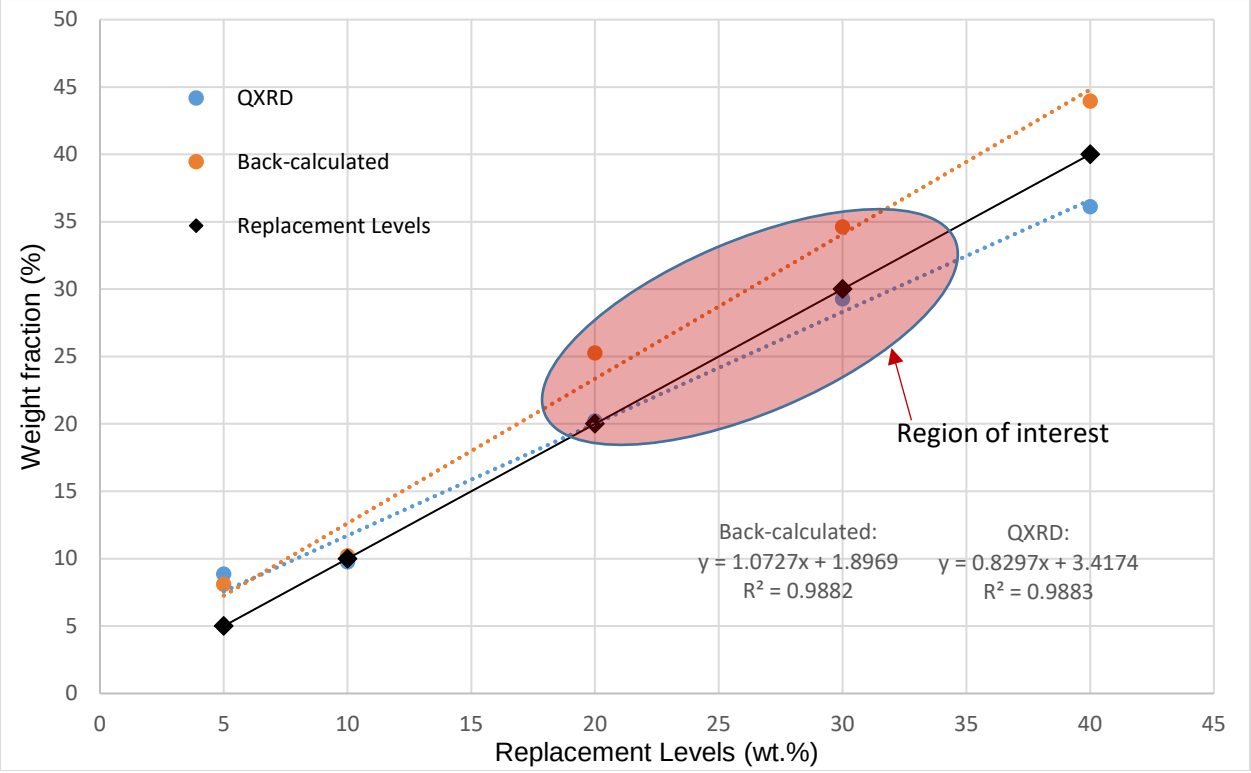

Figure 5. Comparison between the Added Fly Ash Determinations at Different Replacement Ratios Generated from QXRD and Back-Calculation from the Original Fly Ash and Cement QXRD Phase Quantification.

Identification and Quantification of Sulfate Polymorphs

The cement samples received from TxDOT were analyzed to establish the capability of QXRD to identify and quantify limestones and sulfates. Special focus was allotted for the sulfate polymorphs (gypsum, bassanite, and anhydrite) and the ability of QXRD to distinguish between them. A conventional powder QXRD of the bulk cements was able to clearly distinguish between the sulfate polymorphs. Table 3 illustrates the extent of success of QXRD in distinguishing between sulfate polymorphs to the nearest rounded number. Figure 6 represents an example QXRD analysis of sample I/II 208.

Table 3. Sulfate Polymorphs Identified Using QXRD for the Studied Cement Samples.

Sample notations	Sulfate polymorphs (approx. to the nearest 0.5 wt.%)
I/II 657	Bassanite only
II/V 751	1% Bassanite, 2% Anhydrite only
II/V 751 (2^{nd})	2% gypsum (2^{nd})
II/V 710 (Q)	1% bassanite, 2% anhydrite
II/V 180	1% gypsum, 2% anhydrite
I/II 651	No gypsum (Only anhydrite and basanite)
I/II 629	Bassanite only
IL 707	Only gypsum
IL 707 (2^{nd})	Similar to old
I/II 754	4% bassanite only
I/II 754 (2^{nd})	3% gypsum, 1% basanite (2^{nd})
IL 561 (Q)	Only gypsum
IP 668	Only gypsum
IL 589 (Q)	Only gypsum
IP 585	Only gypsum
I/II 148	4% gypsum, 1% bassanite
I/II 208 (Q)	2% gypsum, 1.3% bassanite
III 008 (Q)	Bassanite only
III 099 (Q)	2% gypsum, 1 % bassanite
III 056 (Q)	Only gypsum
I 063 (Q)	Only gypsum
II/V 148	1% bassanite, 1.5% anhydrite
II/V 019 (Q)	2.5% bassanite, 1% gypsum
II/V 002	Only gypsum
II/V 058 (Q)	Only gypsum

Anhydrite was observed in a few cases, which refers to a situation of excessive finish grinding when the calcium sulfate dihydrate (gypsum) phase converts to calcium sulfate anhydrite. Current protocols using the Bogue method cannot discern this effect, and extra tests

(isothermal calorimetry or setting time tests) are required. Making concrete with such a cement can lead to the well-known problem of flash setting. Similarly, the conversion of gypsum to bassanite can cause the false setting problem. Unlike flash setting, the latter can be recovered by re-tempering or aggressive mixing, so it is not considered a major issue. In both cases, direct application of QXRD to quantify cement phases will be very useful to predict such issues in quality control stage itself. More information on the reasoning behind the flash setting problem and its implications on site can be found from the isothermal calorimetry results in Chapter 5.

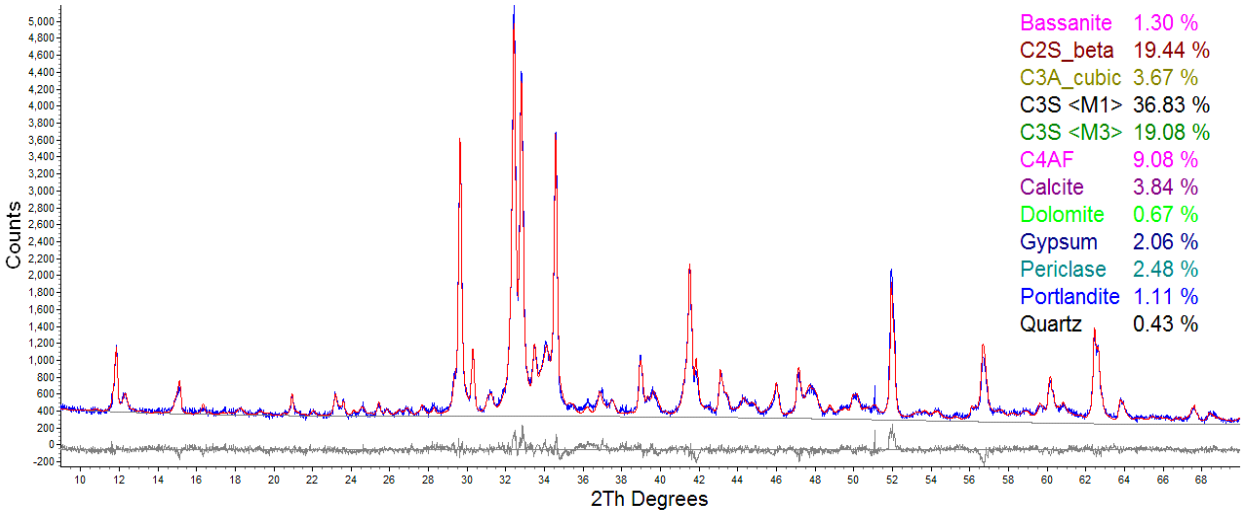

Figure 6. An Example of the QXRD Analysis Using Sample I/II 208.

INVESTIGATIONS INTO PRESSED PELLET QXRD

The XRD experiment to improve precision involves the utilization of a consistent sample format, such as a pellet, that can be prepared using hydraulic pressing. The optimum pressure and sample quantity were narrowed down based on the height of the pellet required (around 8 mm). Several pellet iterations with differences in applied pressure, dwell time, and sample quantity were evaluated before the exact parameters were narrowed down. Other factors related to XRD measurement (such as scan time, scan range, refinement parameters) were embellished by deciding on the quality of the XRD pattern. Depending on the extent of preferred orientation, the demand for the preferred orientation correction shall be ascertained. The alite phase in the pellet is supposed to present an increased preferred orientation, which can be corrected using the March-Dollase orientation correction and correlated with the accurate alite quantification through microscopy.

Preparation of Pellets

Cement pellets were made (as in Figure 7) by pressing the specimen to an optimized force of 130 kN, with a dwell time of 15 seconds. No grinding was performed on the commercial cements and the pellets were pressed without the use of a binder. The pelletization methodology (outlined in Table 4) was identical for both the clinker powder and the cement, with the bulk clinker ground to around 30 μm (passing through 400 mesh and retained on 625 mesh US sieve).

The particle sizes of the cements were around 10–20 μm. The clinker was obtained from Lehigh Hanson cement plant in Union Bridge, Maryland, and was of the Type I/II variety. The cement samples were provided by the Texas Department of Transportation (TxDOT) and comprised of the most common North American cement types (Type I/II, III, II/V, and IL). X-ray diffraction measurements were performed on a Bruker D2 instrument operating at 30 kV and 10 mA (300 W), a Bruker D8 instrument operating at 40 kV and 25 mA (1000 W), and a PANalytical X'Pert MPD operating at 40 kV and 40 mA (1600 W).

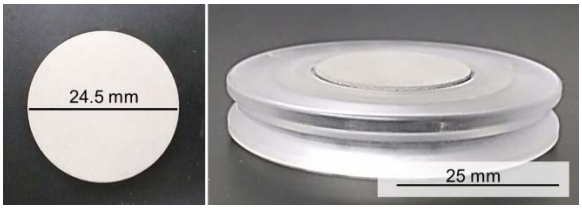

Figure 7. Top View of a Cement Pellet (Left) and the Pellet in a PMMA Specimen Holder (Right).

Table 4. Manual XRD Pellet Preparation Procedure.

Pour the sample into a die with a diameter 0.5 mm less than the sample holder opening.
Press the sample at 280 MPa at a dwell time of 15 seconds. The dwell time, pressing force, and, sample quantity can be varied depending on the pelletizing equipment and the sample fineness.
A smooth surfaced pellet is essential for XRD. The pellet will be very fragile immediately after preparation. Place the pellet in an ambient atmosphere for at least 15 minutes before testing for stability.
The pellet should be dropped from a height of at least 1 feet as a test of stability. If the pellet breaks down, it should be discarded. At least one side of the pellet should be perfect. In case of imperfections (cracks, ridges, pores, etc.), the side that has no imperfection should be exposed to X-rays.
Clean the whole die set using ethanol before every pressing iteration.

In the Bruker instruments (D2 and D8), the bulk powder samples were loaded onto a 51.5 mm diameter PMMA holder with a height of 8.5 mm, and a specimen well diameter of 25 mm. In the PANalytical instrument (MPD), a similar loading scheme was followed except that the specimen well diameter was around 30 mm. However, for the pellets a customized loading technique was followed. In the D2 and D8, the pellet was held tightly in a backloading holder and then height adjusted by pressing the underlying PMMA backing till the pellet was flat with the holder surface. Since the diameter of the pellet (24.5 mm) was equivalent to the well diameter (25 mm), movement of the pellet inside the well was precluded. This movement can cause unwanted signals arising from the empty space in the well to be detected. In the MPD, the pellet was rigidly clamped in the backloading holder and was held without movement.

Data Collection and Rietveld Refinement

Parameters involving data collection and Rietveld refinement are instrument and user dependent and do not have a large influence on the QXRD. However, the optimum parameters for data collection (XRD scan time, scan range, dwell time, etc.) and the Rietveld refinement (structure parameters, atomic positions, polymorphic variations, etc.) were obtained through the experience of working with several test samples. Rietveld refinement was performed using

DIFFRAC.TOPAS 5.0 (Bruker), X'Pert Highscore Plus (PANalytical) and GSAS following similar refinement procedures. Table 5 highlights the important instrumentation parameters that must be minimally satisfied before a QXRD analysis is to be performed. Table 6 lists the procedures to be followed for a good Rietveld refinement. The Rietveld refinement process in TOPAS is explained here as a single-step process where the refinement parameters are selected first and the program refines all parameters together. Although the protocols for refinement in X'Pert HighScore Plus were explained as a step-by-step process (Table 6), it can also be performed as a single-step process by selecting and refining all parameters together, similar to TOPAS.

Owing to the low power operation of the Bruker D2, the resolution power and the intensity of the X-rays is reduced compared to the other two instruments. Hence, the optics of the Bruker D2 were optimized in such a way that increased intensity and a better signal to noise ratio could be obtained with the power fixed at 300 W. The incidence slit of the D2 was increased to allow for more X-rays to be incident on the sample. This meant that for a fixed power a larger number of X-ray reflections from the sample can be collected in the detector. To reduce the background contribution, an anti-air scatter slit (AAS) of 2 mm was suspended above the sample. This greatly filtered the background noise observed at smaller angles and improved the overall signal to noise ratio of the pattern.

Table 5. Instrumental Settings Necessary for a Good X-ray Diffraction Pattern Generation.

Settings	Bruker D2	Bruker D8	PANalytical MPD
Current (mA)	10	25	40
Voltage (kV)	30	40	45
Power (W)	300	1000	1800
Detector Assembly	LynxEye Position Sensitive Detector (PSD)		X'Celerator PSD
Bragg-Brentano geometry	Y-goniometer	θ-2θ	θ-2θ
Source to Detector length (mm)	282	560	560
Soller slits (°)	4	2.5	2.3
Divergence slit (mm)	0.6 (Fixed)	0.3 (Fixed)	1 (Variable)
Anti-air scattering (AAS) module (mm)	2	3	No AAS
PSD opening width (°)	5.8	3	2.2
Scan Range	7 to 70° 2θ		
Step size	0.02° 2θ	0.018° 2θ	0.015° 2θ
Scan time (minutes)	20	20	20
Spin rate (rpm)	15	15	15

Table 6. Rietveld Refinement Protocols that Can Be Followed for an Acceptable QXRD Results.

	TOPAS 5.0 (and later versions)	**HighScore Plus 4.5 (and later versions)**
1	Chebyshev background function (3rd order), refinement of (1/X) function for blended cements.	Chebyshev background function (3rd order), refinement of (1/X) function for blended cements.
2	Specimen displacement (mm): refinement limits at ±0.5. For pellet QXRD, refinement limits at ±2.	Zero position error or specimen displacement: refine any one of the two. Specimen displacement has similar refinement limits to TOPAS.
3	Lorentz - Polarization factor: set at 0.	Fix or uncheck all other parameters. Refine only the background function till a good fit is obtained (increase the polynomials for fit improvement). Fix the fitted background and if used, the (1/X) function.
4	Absorption correction (1/cm): refine between 95 and 105 (optimal value for cement is around 100).	Now refine all lattice parameters (a, b, c), unit cell angles, and other structure parameters. Refinement limits: same as TOPAS.
5	Lattice parameters: refinement limits at ±0.1.	Peak shape function: Fix the Pseudo-Voight (PV) mixing parameter, η at 0.6 or refine it if better fitting is desired.
6	Unit cell angles (α, β, γ): refinement limits at ±1°.	Cagliotti parameters: select u, w, and v; for Pawley or LeBail fitting of amorphous hump in blended cements select PV components $\eta_1 + \eta_2 (2\theta) + \eta_3 (2\theta)^2$.
7	Scale factor: refinement without limits.	Simultaneously refine the lattice parameter a and peak shape parameter w.
8	Crystallite size L (nm): refinement limits at 50 to 1000 nm.	Refine v along with a and w. Perform similar additive refinements with u, and if necessary η_1, η_2 and η_3.
9	Atomic positions and displacement parameters: no refinement.	Scale factor, crystallite size, preferred orientation: Refinement limits similar to TOPAS.
10	Preferred orientation (March-Dollase correction): refinement for alite, gypsum, anhydrite, calcite, dolomite, and portlandite between 0.5 to 1 (reflections that need this correction are listed in Appendix A).	
Refinement		
	I. Refinement format: Fundamental Parameters (automatically selected in TOPAS) II. Single step refinement process: the refinement parameters are selected first and the program refines all parameters together. III. No. of cycles for a good fit: 1–2 cycles.	I. Refinement format: Hierarchical. II. Step-by-step refinement is followed, if not results will differ. III. No. of steps for a good fit: 20–30 steps.

Repeatability and Reproducibility Experiments

A recent analysis of a set of anhydrous cements was carried out by 29 different labs around the world to calculate the precision and bias of the QXRD method [57]. However, the successful evaluation of both the precision and bias of the results was based on the assumption

that the resulting consensus means would be almost equal to the actual cement composition. The proficiency test served a good purpose to designate the consistency (precision) of QXRD protocols to within a select range (example, ±3 wt.% for alite). But the test shall be fully effective only if the actual phase composition of the cement or clinker is known, for accuracy evaluation of the consensus means. Moreover, a degree of freedom was provided to the sample preparation stage where the sample preparation protocols of the different labs were not restricted or stabilized.

Here, the QXRD precision was evaluated after making the clinker sample preparation consistent across all instrumentation. The improved precision is apparent from the restriction of the quantification variability to within ±1 wt.% for alite. During pelletization, the alite crystallites can get oriented preferentially and this can cause a slight overestimation in its quantification. Apart from the alite overestimation and corresponding belite underestimation, a slight ferrite underestimation due to absorption contrast effect was the only other anomaly observed from pellet quantification. The mass absorption coefficient of ferrite is very high compared to the other cement phases, which leads to an increased X-ray absorption by the ferrite relatively. The total quantity of sample used for making the pellet (4 g) is several times higher than the powder (0.5 g). A combination of these two effects (i.e., higher quantity of sample and high absorption coefficient of ferrite phase along with crystallite size) lead to an increased X-ray absorption behavior by the ferrite phase in the pellet than the powder, hence the corresponding underestimation. Figure 8 shows the repeatability and reproducibility of powder and pellet QXRD.

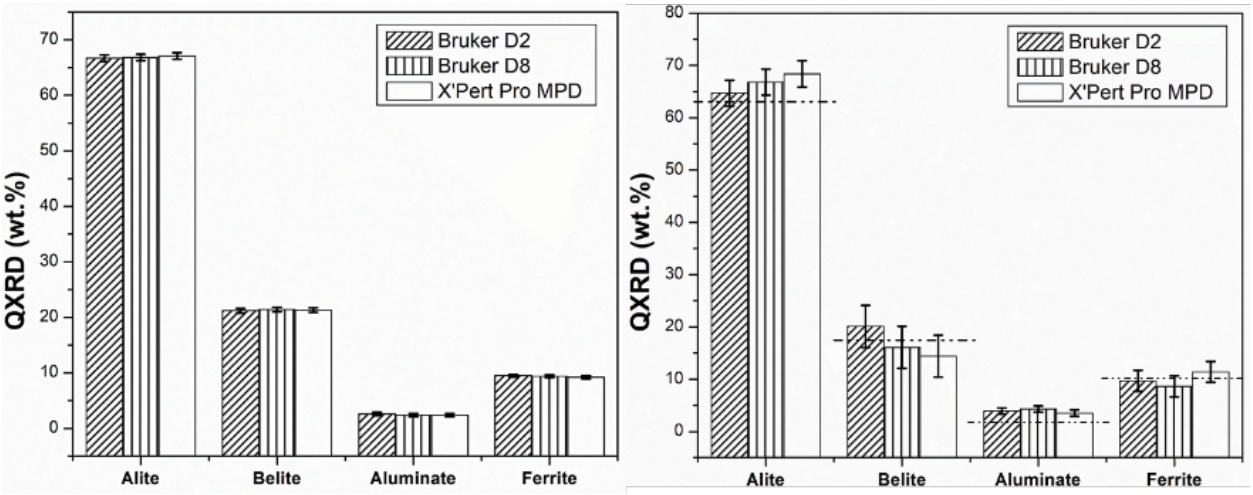

The powder sample used here was the NIST SRM 2686a and for the pellet a Type I clinker was used. The dotted lines on the right image indicate the NIST reference values. The black vertical lines represent the repeatability variable (sr) in accordance with ASTM E177 and are used throughout the text.

Figure 8. Comparison between Pellet (Left) and Powder (Right) Quantification for the Major Clinker Phases across Instrumentation.

Notwithstanding the aforementioned effects, the precision of pellet QXRD was significantly improved from powder QXRD. This observation was extended to cement by the rigorous testing of nine commercial cement pellets, with varying mineralogy, representing different ASTM C150 cement types. QXRD results of the major cement phases illustrated the

overwhelming improvement to the precision in all nine cements. Figure 9 denotes the precision sacrificed during the performance of powder QXRD by comparing the quantification of the powder and the pellet in two different instruments (Bruker D2 Phaser and D8 Advance). The instruments differed heavily in their peak resolution characterization and in the operating power and were at wide variance in the quality of the produced pattern. The precision error (%) is an index of the deviation of the results when the same protocol is reproduced in cements of varying composition in both the instruments. It was calculated by multiplying the percent standard deviation of the quantification performed in different machines by 2.8, as per ASTM E177. Figure 10 illustrates the improved precision through pellet QXRD against other methods.

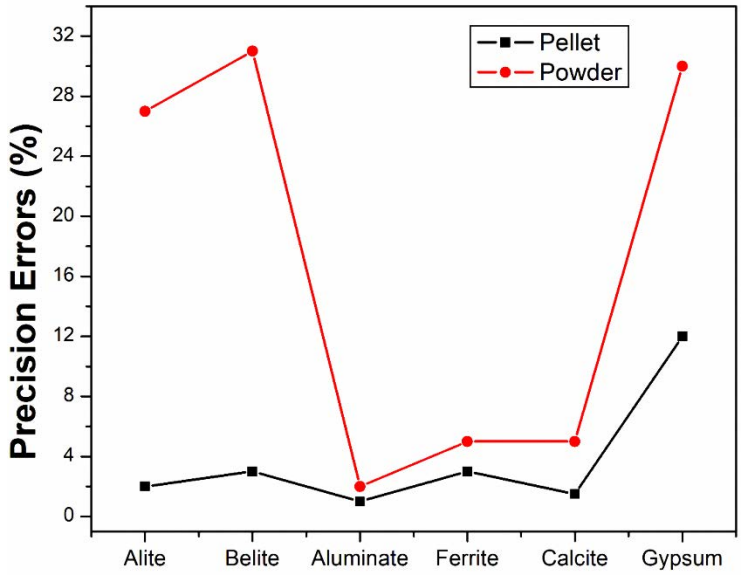

Figure 9. Plot Showing Cumulative Precision Errors in Different Cement Phases in the Nine Cements between Pellet and Powder.

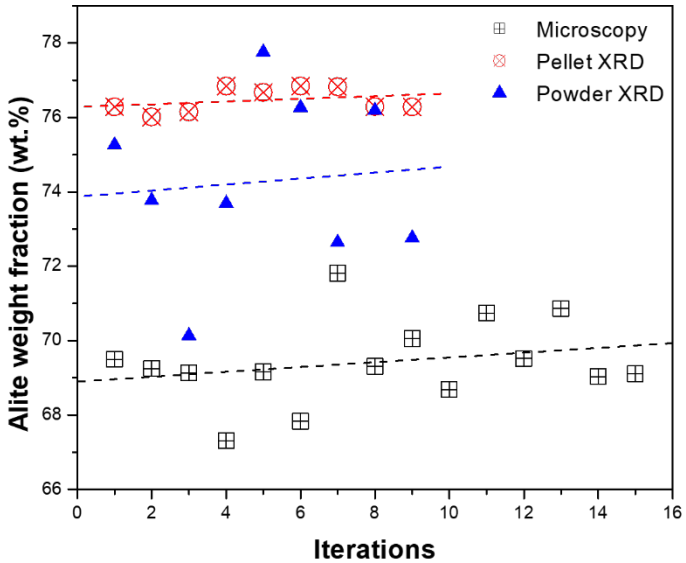

Figure 10. Graph Showcasing the Precision and Accuracy Differences of All the Investigated Quantification Techniques for the Alite Phase in the Type I/II Clinker.

Figure 10 shows that pellet XRD generates the most precise results in the clinker between all techniques. The effect of preferred orientation is evident in the alite overestimation after pelletization and in a few powder samples. The dotted lines represent linear regression curves, which reveal the difference in precision between the methods as a function of their increasing slopes (slopes of, pellet XRD = 0.06, powder XRD = 0.4, microscopy = 0.15). The lower the slope, the better the precision.

ACCURACY EXPERIMENTS

Comparison of the QXRD accuracy was proceeded with the help of quantification using microscopic methods: scanning electron microscopy and optical microscopy.

Powder and Pellet QXRD

Four clinker nodules of varying phase proportions were obtained from a Lehigh Hanson cement plant in Maryland. The clinker nodules were fine ground to size fractions around 30 µm initially for QXRD analysis. After initial size reduction, the clinker powders were pelletized and analyzed using X-ray diffraction at conditions explained previously.

For the analysis of the powder QXRD, the clinker powders at 30 µm were micronized with ethanol. The common practice is to add 5 mL of ethanol per gram of the clinker to minimize heat and maximize powder mobility. Micronizing was performed for 5 minutes after which the 30 µm average-sized clinker particles were reduced to below 10 µm. The wet, finely divided clinker powders were dried in an oven at 60°C for 2 hours to completely remove the ethanol. The dried clinker powders can be broken up by grinding at a very light pressure inducement using a mortar and pestle for 30 seconds. Powder QXRD of the micronized and dried clinkers was proceeded by backloading over a well-sanitized, frosted, or stained surface to prevent preferred orientation. Figure 11 represents the increased preferred orientation in pellet QXRD, and Table 7 illustrates the powder and pellet QXRD comparison between four clinkers.

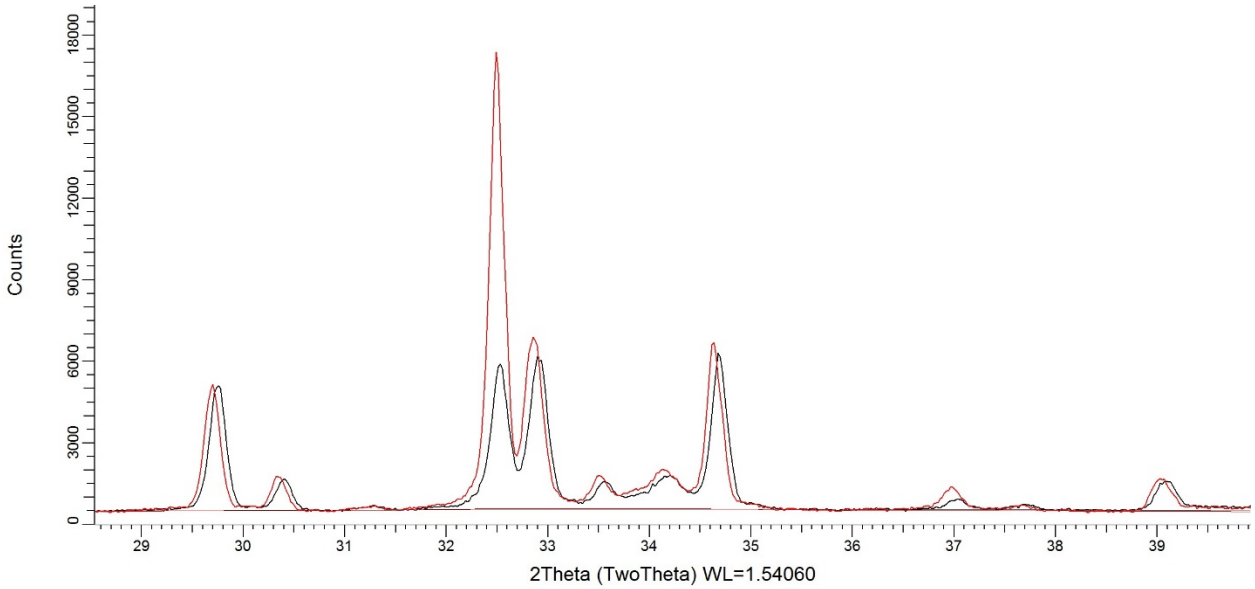

The reduction in preferred orientation is clearly evident in the wet ground, backloaded powder XRD at the peak range 32–33° 2θ. Pellet XRD is mildly shifted to the left due to the specimen displacement effect.

Figure 11. XRD Patterns of the Powder (Black) and Pellet (Red).

Table 7. Powder and Pellet QXRD of the Clinkers.

Phases	Clinker 1		Clinker 2		Clinker 3		Clinker 4	
	Powder	Pellet	Powder	Pellet	Powder	Pellet	Powder	Pellet
Alite	71.58	73.19	71.6	71.8	70.44	71.12	61.16	64.85
Belite	9.91	9.23	9.92	9.79	11.33	11.12	16.42	14.8
Interstitial	16.64	14.36	15.135	14.215	16.09	15.295	19.62	17.65

Comparison of Powder and Pellet QXRD with PC and MSIA

From Table 7, it is clear that there is a minor distinction between the pellet and powder QXRD results. Accuracy evaluation requires comparison with results that are considered to be highly accurate with the current form of the sample used. Although NIST 2686a provides reference values for the standard sample in powder form, the comparison of its results cannot be made with the pellet of the same sample. Hence, instead of making an NIST 2686a pellet, researchers resorted to alternative direct determination techniques for accuracy evaluation. The significant direct determination techniques for clinker and cement analysis are the optical microscopy-point counting method (PC) and the BSE-EDS image analysis method (MSIA).

Comparison of all four direct determination techniques (as in Table 8) revealed an acceptable degree of variation between them in the quantification of the major cement phases. Discrepancy between pellet and powder QXRD was around 2 percent for the alite phase, and 12 percent for the interstitial phases. The influence of preferred orientation on alite overestimation in pellet and absorption contrast in underestimating ferrite quantification in

QXRD were prominent over both pellet and powder QXRD. However, such effects were not found to affect the accuracy of the quantification in comparison with PC and MSIA. Hence, the average of the PC-MSIA results was considered as the consensus accuracy for these samples.

Table 8. Clinker Quantification from Powder QXRD, Pellet QXRD, Point-Counting, and Multispectral Image Analysis Methods.

Phases	Powder	Pellet	MSIA	PC
Clinker 1				
Alite	71.58	73.19	69.4	70.06
Belite	9.91	9.23	11.39	11.24
Interstitial	16.64	14.36	19.21	18.7
Clinker 2				
Alite	71.6	71.8	71.36	71
Belite	9.92	9.79	10.41	11.3
Interstitial	15.135	14.215	18.24	17.6
Clinker 3				
Alite	70.44	71.12	71	70.43
Belite	11.33	11.12	10.31	11.17
Interstitial	16.09	15.295	18.69	18.39
Clinker 4				
Alite	61.16	64.85	61.55	61.6
Belite	16.42	14.80	18.05	18.50
Interstitial	19.62	17.65	20.4	20

Table 9 and Table 10 illustrate the standard deviation differences between consensus accuracy results and QXRD of the clinkers, considering the individual repeatabilities into the calculation. The variation of pressed pellet QXRD from consensus accuracy is reasonably close to the powder QXRD variation. Although the accuracy of a meticulously prepared powder QXRD is excellent, the accuracy of the pressed pellet QXRD does not fall far behind. In case of a wider accuracy deviation (for instance, >5 wt.%), calibration correction can be performed using consensus accuracy results from a larger data set or by using standard reference results if applicable. One can infer that accuracy calibration might not be needed for pressed pellet QXRD if the results are not largely different from the consensus accuracy. The variation is illustrated as column charts in Figure 12–Figure 14.

Table 9. Variation of Pellet QXRD against the Accurate Values of the Cementitious Phases in the Four Clinkers.

Clinkers	Pellet vs. PC-MSIA SD (±wt.%)		
	Alite	Belite	Interstitial
1	1.95	1.21	2.43
2	0.33	1.31	2.04
3	0.37	0.93	1.71
4	1.89	2.02	1.49

Table 10. Variation of Powder QXRD against Accurate Values of the Cementitious Phases in the Four Clinkers.

Clinkers	Powder vs. PC-MSIA SD (±wt.%)		
	Alite	Belite	Interstitial
1	1.42	0.81	1.47
2	0.32	1.26	1.67
3	0.33	0.93	1.30
4	0.24	1.09	0.39

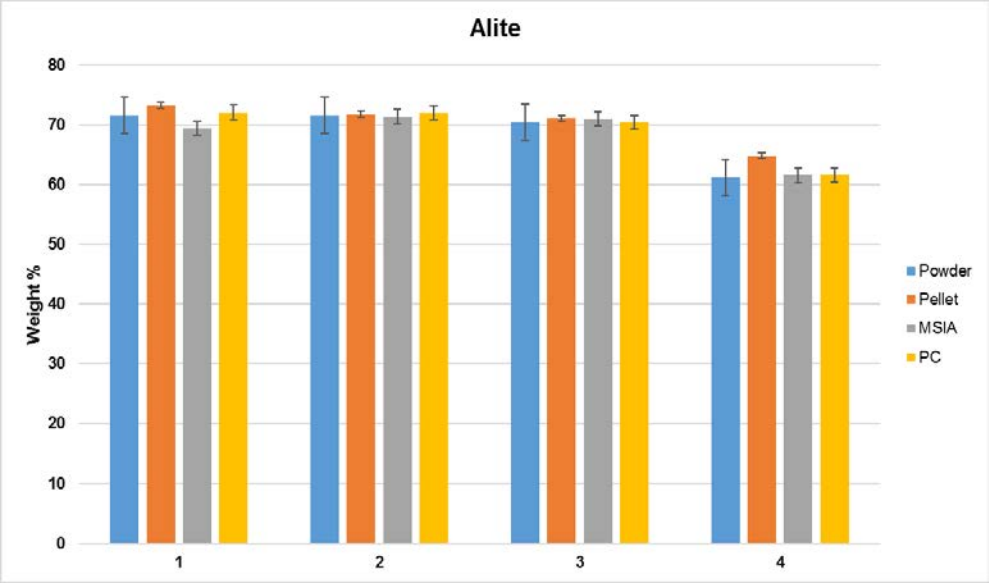

Figure 12. Alite Accuracy Variation between the Different Direct Quantification Techniques Used in This Study.

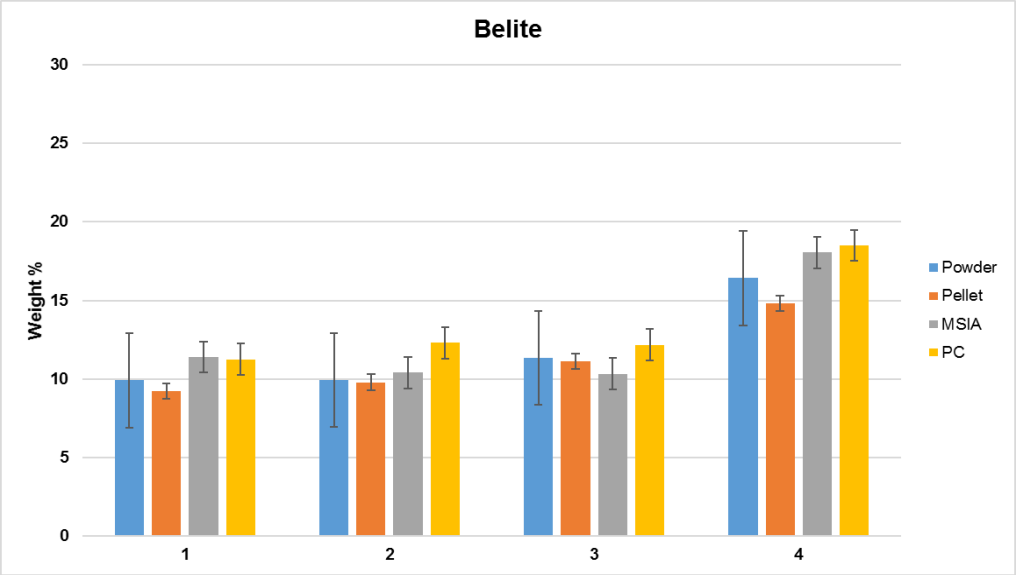

Figure 13. Belite Accuracy Variation between the Different Direct Quantification Techniques Used in This Study.

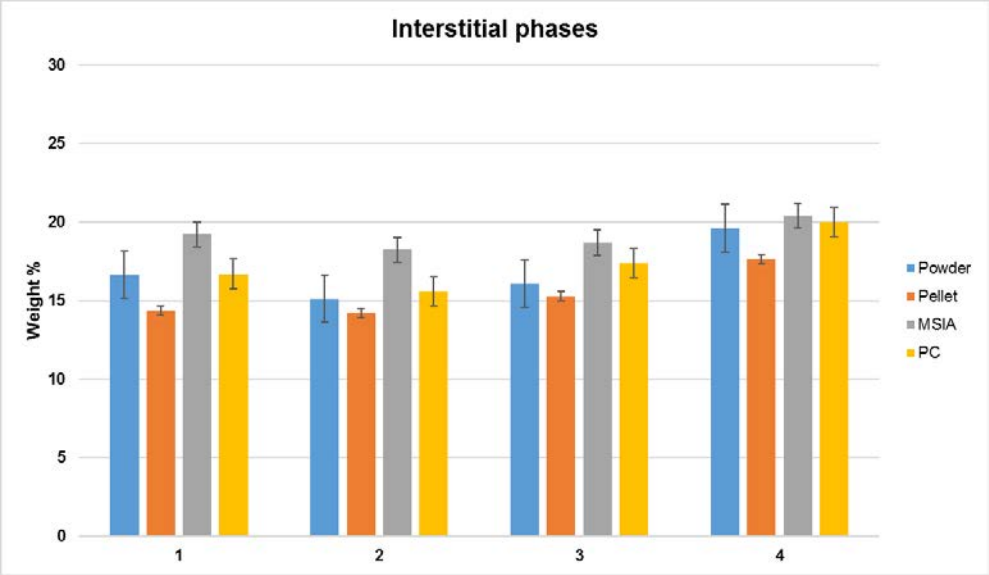

Figure 14. Interstitial Phase Accuracy Variation between the Different Direct Quantification Techniques Used in This Study.

PRECISION COMPARISON

The reproducibility in pressed pellet QXRD was improved significantly from powder QXRD without significantly sacrificing the accuracy. ASTM E177 calculates the reproducibility limit as a multiplier of the standard deviation ($1.96 \times \sqrt{2} \times$ standard deviation). The round robin analysis conducted by NIST in 2004 dealt the global repeatability and reproducibility of QXRD to compare against the Bogue method. This was used as a foundation to generate the first ASTM QXRD standard, the C1365.

Comparison of the ASTM reproducibility limits between the powder and pellet QXRD techniques (Table 11–Table 13) reveals that the pellet QXRD method improves on both aspects

of precision: repeatability and reproducibility. An almost negligible variation between different instruments, the Bruker D2, Bruker D8, and the PANalytical MPD using different Rietveld refinement programs were observed. Hence, the improvement in precision of pellet QXRD was established here.

Table 11. Historical Reproducibility Limit Comparison against Powder QXRD and Bogue.

With 95% coverage factor	**Alite (wt.%)**	**Belite (wt.%)**	**Aluminate (wt.%)**	**Ferrite (wt.%)**
QXRD Repeatability[55]	2.9	3.1	2.1	1.7
QXRD Reproducibility[55]	6.3	3.8	4.8	4
QXRD accuracy errors[4]	2.4	2	1	1
Bogue accuracy errors [4]	9.6	9.6	2.2	1.4

Table 12. Repeatability Limit Comparison between Pellet and Powder QXRD.

QXRD Repeatability#	**Alite (wt.%)**	**Belite (wt.%)**	**Aluminate (wt.%)**	**Ferrite (wt.%)**
Powder	1	1	1	3
Pellet	0.3	0.5	0.8	1.3

Table 13. Reproducibility Limit Comparison between Pellet and Powder QXRD.

QXRD Reproducibility#	**Alite (wt.%)**	**Belite (wt.%)**	**Aluminate (wt.%)**	**Ferrite (wt.%)**
Powder	5.1	8.1	1.2	4
Pellet	1.2	0.9	0.6	0.5

ACCURACY CALIBRATION

A linear regression correlation of the interstitial phase (Figure 15) and alite (Figure 16) from pellet QXRD was plotted against the corresponding point-counting determinations. The extent of the deviation between the point-counting and multispectral image analysis from the pellet (x-axis) was quantified as the root mean square error between the axes. Since the interstitial phases were naturally better separated in the etched clinker than the color-coded clinker image field from MSIA, the point-counting can be considered to be directly representative of the actual clinker contents. The utilization of the MSIA method for accuracy calibration does not provide extremely divergent results as is apparent from the extent of variation from the pellet QXRD (Figure 15). The variation parameter represents the coefficient of variation between the dataset. Alternatively, if the MSIA method were only to be used for accuracy calibration then the variation from point-counting would be only 4 percent for the interstitial phases and 0.2 percent for the alite phase.

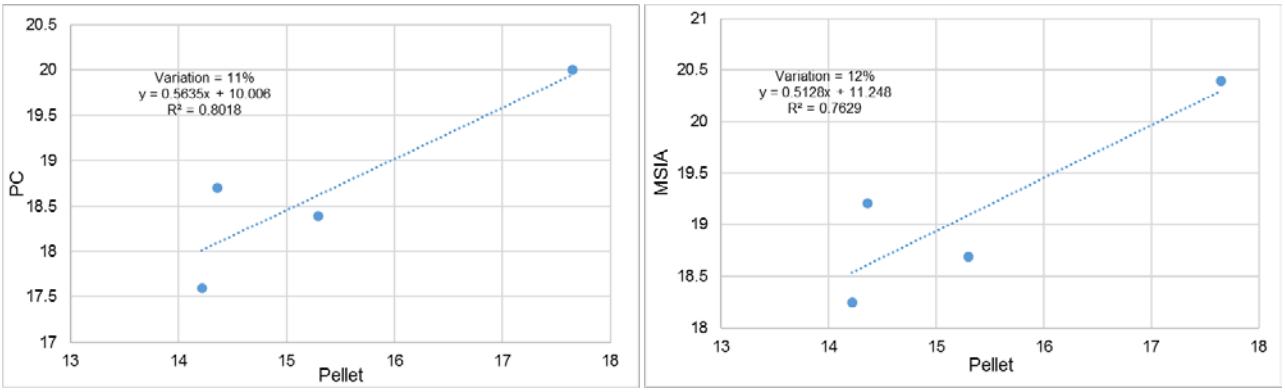

Figure 15. Regression Plot between Interstitial Phase Quantification of Pellet QXRD and Point-Counting (Left) and Multispectral Image Analysis (Right).

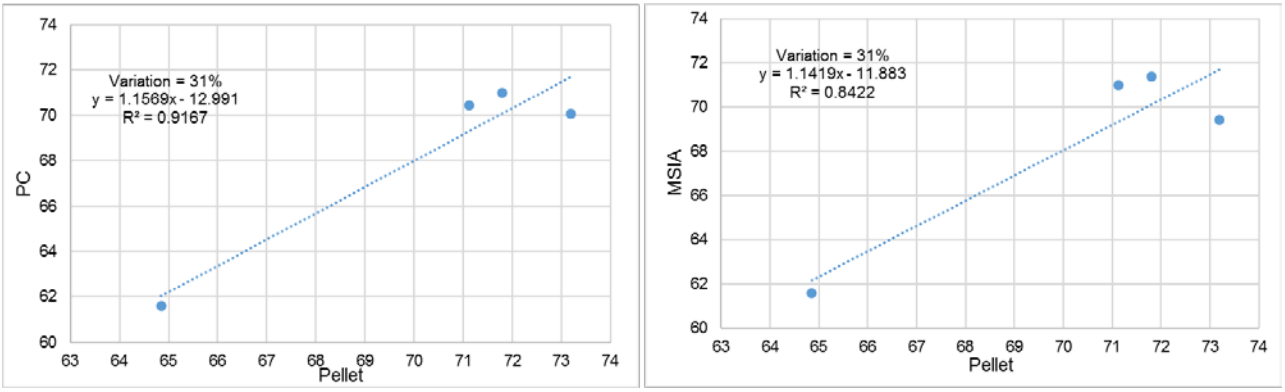

Figure 16. Regression Plot between Alite Phase Quantification of Pellet QXRD and Point-Counting (Left) and Multispectral Image Analysis (Right).

PROTOCOLS FOR THE QXRD OF ASTM C150 AND C595 CEMENTS

For powder QXRD:

1. Create a clean table space for placing the sample holder. Place the backloading sample holder over a frosted glass surface. Wash hands and put on the gloves.
2. Fine-ground the cement samples under ethanol using a mortar and pestle or a micronizing equipment to a fineness of 10–15 µm. Use 5 mL of ethanol per gram of the cement.
   Note 1—Usually, the cement samples from a finish mill are at a fineness of around 10–15 µm. In that case, there will be no need to fine ground the cement.
   Note 2—It is encouraged to calculate the fineness using a laser diffraction particle size analyzer instrument or sieves of US standard mesh sizes (sieve between 15 and 5 µm mesh sizes).
3. Weigh a sufficient quantity of the cement powder to just overfill the sample holder. Gently tap the holder to evenly distribute the sample inside the holder. If the sample does not fill the holder, repeat the process adding more sample. Close the filling side and flip the holder to expose the other side taking care not to spill any sample. If the holder is too overfilled, get the sample out and start Step 3 again.
4. Place the sample holder in the XRD instrument and run measurement. Table 5 describes the general measurement parameters to get a good XRD pattern. You can observe from

the table that the proper measurement parameters vary between instruments and are at the discretion of the user.

5. Cement phase quantification to be performed through Rietveld refinement. For quantifying the amorphous content in Type IP cements, follow the procedure as detailed in ASTM C150.
   Note 3—See Table 6 for the general Rietveld refinement protocols. Refinement can lead to different results depending on the order of refinement. The user is encouraged to use the refinement protocols from practice and those that better suit the sample.
6. For replicate measurements, follow procedures as in ASTM C1365. The precision and accuracy of results should be expressed according to the procedures outlined in ASTM E177 [50].

For pellet QXRD:

1. Follow steps 1 and 2. To make a pellet, weigh 4 g of the cement and use an automated QXRD pelletization equipment or use a manual pellet press. Only a circular pellet should be tested as it properly fills the dimension of the hole of the sample holder.
   Note 4—For a manual pellet preparation, see Table 5.
2. Place the pellet in the XRD sample holder. Care should be taken that the pellet surface is in line with the surface of the sample holder. No space should be left at the circumference of the circular pellet and hole of the sample holder.
3. Perform XRD measurement as described in Step 4.
   Note 5—The user is encouraged to use pellet QXRD only if there is a need to perform routine analysis, like for instance in quality control application. The results from powder and pellet QXRD can vary up to ±3 wt.% in alite and belite, and up to ±1 wt.% in ferrite based on user expertise with XRD pellets.
4. Pellet QXRD provides extremely better precision than powder QXRD and does not need to be repeated for a reliable result. To generate precision and accuracy values for pellet QXRD as per ASTM E177 terminology, please follow Step 6.

SUMMARY ON CHAPTER 3

The outlying issues in ASTM C1365 protocols such as optimum fineness, use of internal standard, preferred orientation minimization, absorption contrast reduction, and use of extraction techniques were debated for their relevance in online quality control with support from experimental investigations and literature. Recommendations were provided in the new QXRD protocols to optimize the particle fineness, preferred orientation mitigation, and amorphous quantification (internal standard method) while extraction methods and absorption contrast mitigation were not suggested for QXRD protocols.

In order to improve the repeatability and reproducibility of the QXRD process and to improve the efficiency of the protocols, a modified sample preparation regime using pressed pellets was investigated.

With information from cement industrial QXRD protocols and inspiration from XRF, pressed pellet QXRD was optimized to fit the requirements of XRD sample preparation. Although preferred orientation can increase in certain phases due to pressing, the improvement in repeatability and reproducibility is not affected due to preferred orientation, which was a similar outcome arrived at by a previous investigation [61].

The extent of deviation of pressed pellet QXRD from powder QXRD was ascertained by comparison with microscopic quantification techniques. The analysis revealed that pressed pellet QXRD is not highly variable from microscopic quantification and its accuracy is similar to powder QXRD.

CHAPTER 4. SPECIFICATION DEVELOPMENTS

Based on the information collected through literature and extensive testing from the previous chapters, QXRD protocols were generated with the aim to improve the efficiency of the procedures outlined in ASTM C1365. The developed protocols, described in the following sections, were used to generate the QXRD specifications based on the data from the cements provided by TxDOT and the clinkers sourced from Lehigh Hanson cement plant, Union Bridge, Maryland. In this chapter, the developed protocols are described first followed by the specifications where the models for generating the specifications were explained.

SPECIFICATIONS

A comparative assessment between Bogue and QXRD can be used to derive QXRD based criteria for cement specification. A pilot study of establishing the Bogue vs. QXRD relationship was conducted by Stutzman [76]. In this method, QXRD results obtained by different researchers using various methods, such as single-peak fitting, internal standard, Reference-Intensity-Ratio (RIR) method, and the Rietveld method, were compiled to establish this relationship. QXRD specifications were then developed by the direct interpolation of Bogue specifications for portland cements (ASTM C 150) using the established linear regression equation between Bogue vs. QXRD. As QXRD data generated by different methods (not restricted to Rietveld method alone) were used to develop this regression equation, the estimated QXRD results from a given Bogue data showed large deviations from the measured QXRD values in the lab.

In the current study, efforts were made to address such shortcomings. Direct comparisons between Bogue and Rietveld quantification for a clinker data set repository numbering above 300 was performed. The samples were predominantly Type I clinkers, and their quantification was sourced from the Lehigh Hanson cement plant in Maryland. A linear regression model was generated to derive estimated QXRD information from a given Bogue data. Simultaneous confidence limits using Working-Hotelling-Scheffe (WHS) bands were used to draw lower and upper limits for the specification.

Primary effort to apply simultaneous confidence limits for deriving the chemical composition of cements was made by Sieber et al. [77] to create a framework for the assignment of 1σ uncertainty ranges. This was extended by Stutzman in [76] with the use of WHS simultaneous confidence intervals based on statistical tests of significance [78]. Applying WHS processing creates wider confidence limits around a linear regression correlation and drastically reduces outlier data. It also extends the validity of correlation especially at lower Bogue quantification ranges.

The following information details the groundwork made in obtaining the QXRD specifications through the process described above.

QXRD Estimation Using Bogue Data

Table 1 of ASTM C150 has several specification criteria based on a historical relationship between performance behavior of cement and the phase quantities. Extensive research is necessary to renegotiate the terminology of ASTM C150 into QXRD terms. Hence, a linear regression of the 320 cements received from Lehigh Hanson yielded a general Bogue to QXRD correlation. This correlation was tested on 10 random TxDOT cements belonging to

various ASTM C150 cement types. These ten cements are marked with letter Q in Table 3. Mean QXRD quantification of the cements was observed to be within acceptable deviation (within ±1 wt.%) from the estimated QXRD. The Bogue to QXRD correlation, aided by WHS bands, covers the commercial range of phase quantities for the alite, belite, aluminate, and ferrite phases. Hence, its application over the gamut of the ASTM C150 types yielded highly accurate estimations.

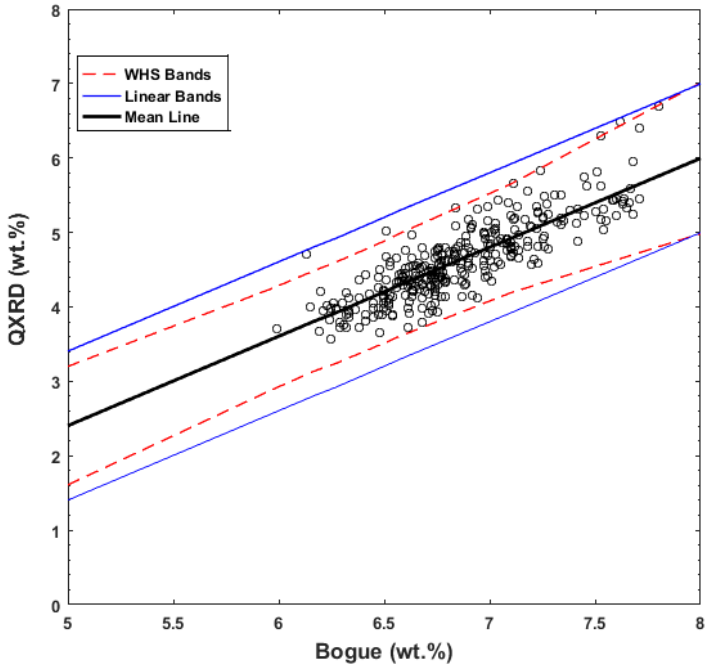

Figure 17. C3A Correlation between Bogue and QXRD for 320 Cements.

In Figure 17, the mean line represents the linear regression correlation, the solid blue lines represent ±1 wt.% linear confidence limits, and the dashed red lines represent the WHS confidence limits. WHS confidence limits consider the distribution of the data set, unlike the standard ±1 wt.% linear confidence limits. This is represented in the widening of the WHS confidence bands toward greater Bogue values and constriction at smaller Bogue values.

The WHS confidence bands condense the prediction to about 13 percent near the center of the data set. Stutzman [76] described that in the comparison of the Bogue technique to any direct quantification method, the bias contributed by the Bogue method is carried over in the correlation. It means that although both techniques calculate the same quantity parameters (phase fractions), the bias incorporated by the Bogue method can lead to the result not being equal to zero in the absence of a particular phase. This is apparent when the Bogue quantity is made zero. The corresponding absolute value of QXRD estimation (3.6 wt.%) was found to be equivalent to the distance from the centroid of the data set and the center of the hyperbola.

Figure 18 and Figure 19 represent the bias in quantification between estimated and quantified QXRD. The current model represents the estimations done using the model generated for this project and the literature model represents the model generated by Stutzman [76] used to calculate the ASTM C1365 phase limits albeit with a minor correction. Stutzman's model was fine-tuned by only considering Rietveld refinement data, whereas in its original form the literature model consisted of QXRD data from different techniques: RIR method, single peak

fitting, internal standard method, etc. This fine-tuned model, called the modified literature model, is in Table 14 where its effectiveness is compared with the current model.

Stutzman's model is used as is in the ASTM C1365 estimations for converting XRF/Bogue quantification to QXRD quantification. The ASTM C1365 estimations were derived from data that range over widely varying XRD quantification techniques such as single-peak fitting, RIR method, Pawley fitting, internal standard method, etc. collected since the 1940s. The QXRD phase estimations based on this earlier literature model are closer to the Bogue derived ASTM C150 phase limits, although the overestimation of aluminate and underestimation of alite in the Bogue is well understood. This identified as the inherent limitations of the previous model. Contrarily, the data considered in our investigations (represented as current model) were gleaned from a cement plant lab that used the same XRD and XRF instruments, following the same Rietveld based quantification methodologies, to generate the data. This ensured consistency in quantification methodology, which leads to reliable estimation. However, this model is derived from the data generated from only one cement plant, and a collection of similar data from several different cement plants can generate a very reliable master curve and lead to an improved and accurate QXRD estimation from Bogue values.

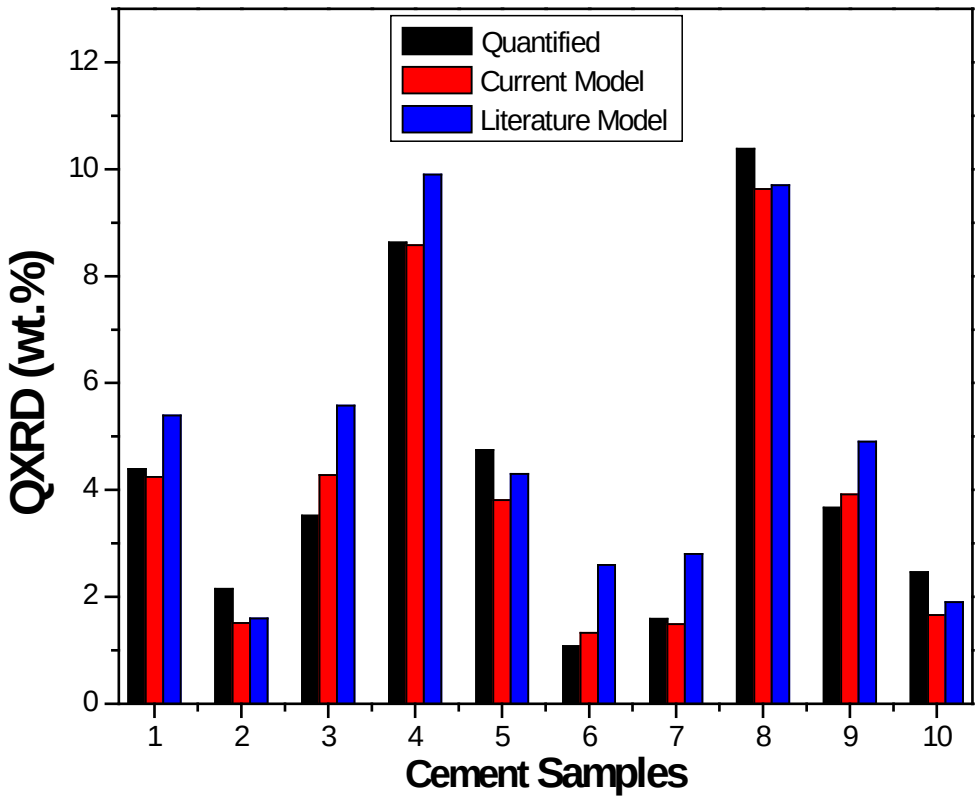

Figure 18. Bar Plot Tracing the Differences between QXRD Estimated and QXRD Quantified C3A for 10 Random Cements.

Bias in Estimated QXRD

Differences between estimated and quantified QXRD were represented in the form of the bias between the estimated and quantified results. The accuracy of the estimations was reinforced by the negligible bias in the quantification between estimated and actual QXRD. Nine out of the 10 cement samples (range of C3A estimations = 1.7 to 8.9 wt.%) passed the C3A correlation when the standard XRD variation of ±0.8 wt.% was imposed (this model will hereby be mentioned as current model). In comparison, the modified literature model only passed 4 out of 10 estimations. Factors such as the type of the cement, the quantity of Bogue estimations, or the errors incorporated in Bogue did not play a significant role in affecting the estimations. Figure 19 illustrates this observation.

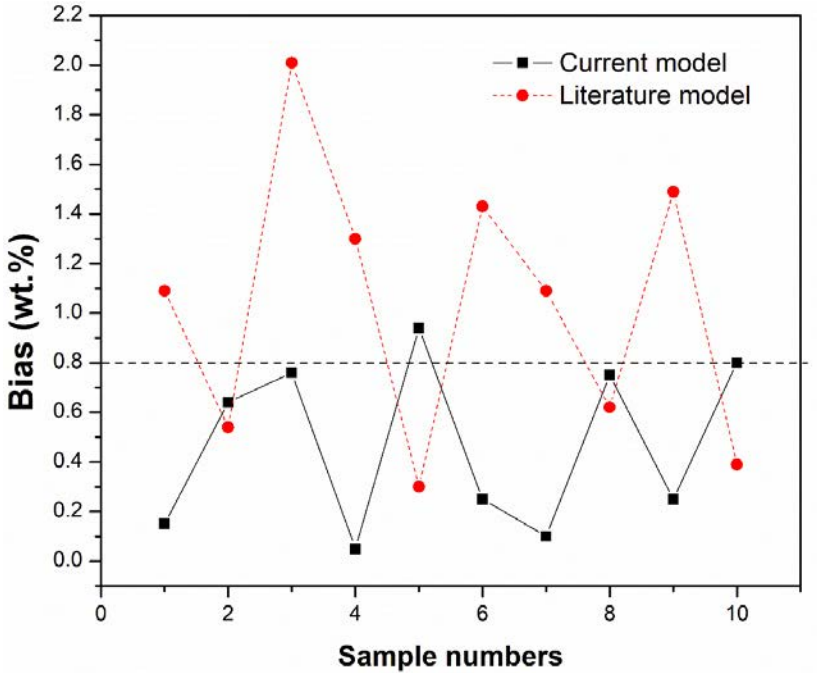

The literature model was reproduced from Stutzman [76].

Figure 19. Plot Showing Controlled Bias between the Means of the Estimated and Quantified QXRD for the C3A Phase in the Current Model against the Wide Bias Variations in the Modified Literature Model.

For the C3A, the correlation ceased to be valid below 3.5 wt.% in Bogue (corresponding QXRD estimation = 0 wt.%) without the application of the WHS limits. The validity of the estimated QXRD correlation extended till above 1 wt.% (where upper limit of estimated C3A = 0 wt.%) after using WHS confidence bands. In contrast, the application of linear bands restricted the correlation to 2.7 wt.% below which the QXRD estimation turned zero. The Bogue quantification can sometimes churn out C3A estimations lower than 2 wt.% especially in IL cements. WHS correlations are advantageous in such cases since they incorporate the distribution of the data set into their processing.

Extension to Significant Phases and Relationships

When the correlation was extended to alite using the current model, the variation between the estimated and quantified QXRD increased owing to the higher abundance of alite in cement. Hence, the acceptance limit was extended to ±4 wt.% for alite. The validation was encouraging for all alite fractions except for a few cases where the correlation was slightly incompatible. Since the C3S is the more abundant phase, it is logical to infer that the errors in determination or estimation increase as the occurrence of the phase increases. Figure 20 and Figure 21 represent the C3S WHS correlation of 320 cements and the bias in the correlation, respectively.

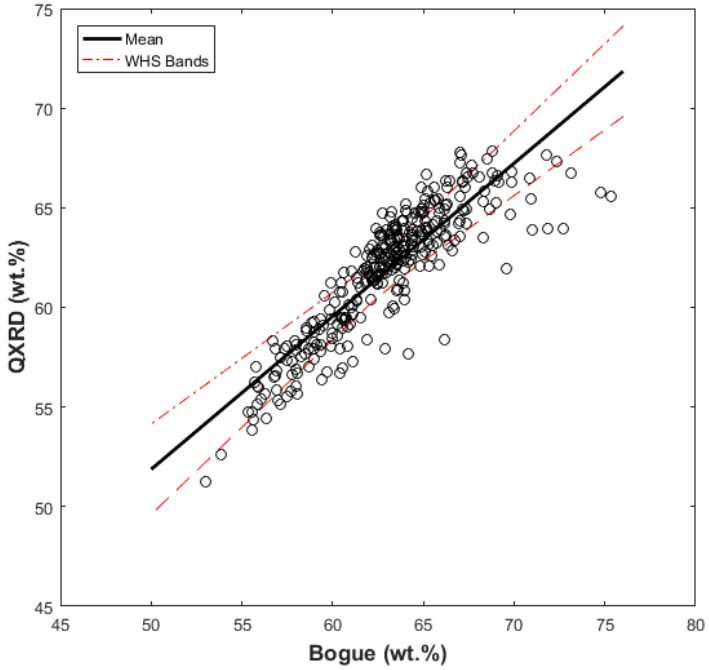

Figure 20. Plot of the C3S Bogue to QXRD Correlation of 320 Cements with WHS Confidence Limits.

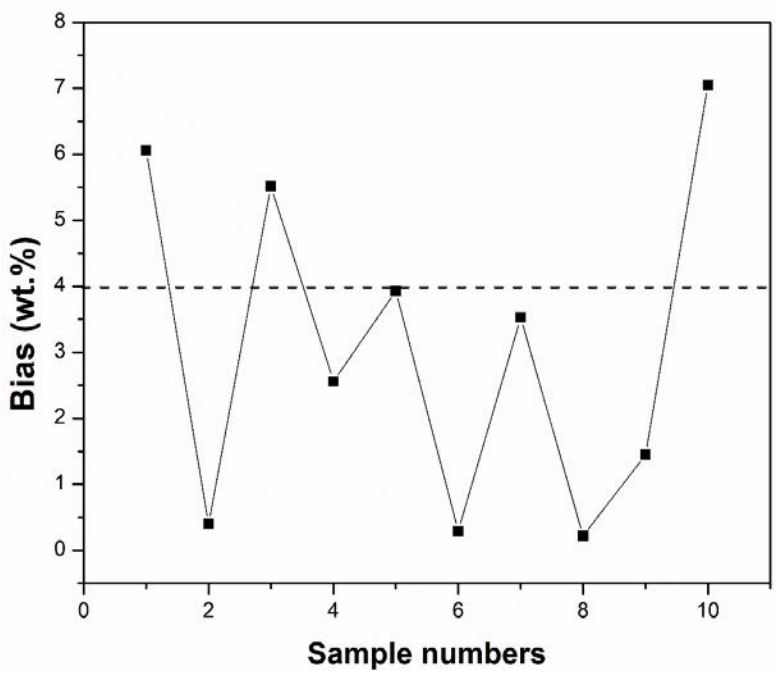

Figure 21. Bias Estimates of C3S Bogue to QXRD Correlation (Acceptance Range for the Relationship Was Fixed at ±4 wt.%).

The special relationships (C3S + 4.75.C3A) and (C4AF+2.C3A) were calibrated next where the Bogue quantification specification should be closer to 100 and 25, respectively. These combinations are used as practical markers for heat of hydration and sulfate resistance phase quantity limits, respectively. Detection of the corresponding QXRD phase limits was performed to understand these long-standing relationships from a QXRD perspective. Figure 22 and Figure 23 illustrate special correlations elucidated in ASTM C150.

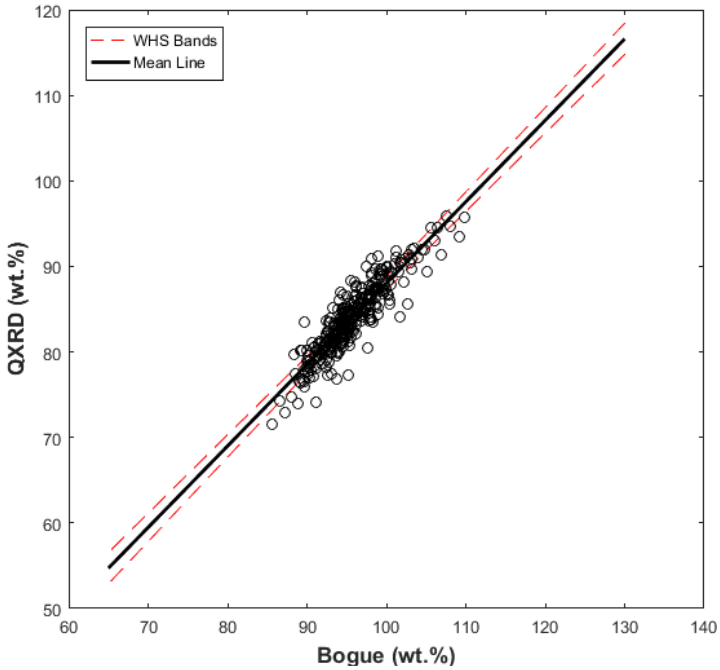

Figure 22. Plot of C3S + 4.75.C3A Correlation.

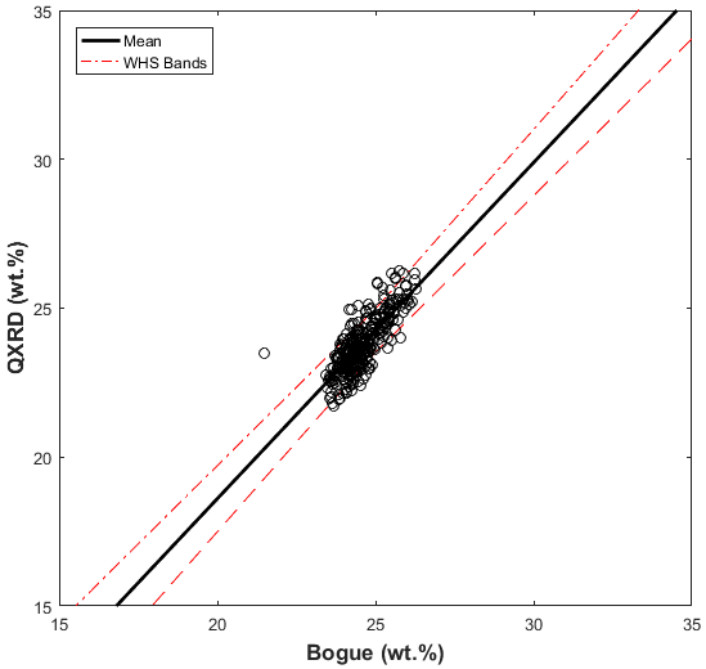

Figure 23. Plot of C4AF + 2.C3A Correlation.

Specification Limits and Discussion

The correlation technique was then applied to obtain the QXRD phase specification limits and resulted in the following estimates as in Table 14. This extrapolation was performed on the Bogue method specific ASTM C150 specifications limits. In general, the Bogue quantification overestimates phases at lower quantities (example, aluminate) and underestimates phases at

higher quantities (example, alite) relative to direct determination methods. The same pattern was observed here in alite and aluminate correlations, which are significant in affecting the performance of the cement.

Table 14. QXRD Specification Ranges for the Important Phases in Cement (Includes Tables 1 and 2 of ASTM C150).

Phase	Significant cement type	ASTM C150 limits (max. Bogue wt.%)	Current Model estimations (wt.%)			Modified literature model estimations (wt.%)		
			Lower limit	Mean	Upper limit	Lower limit	Mean	Upper limit
Alite	Type IV	35	33.4	40.3	**45.3**	31.4	34.9	**38.4**
Belite	Type IV	40	**28.6**	37.3	53	**39.8**	43	46.2
Aluminate	Type II	8	5.1	6	**6.9**	6.5	7.3	**8**
	Type III	15	12.5	14.4	**16.3**	16.2	18.8	**21.5**
	Type IV	7	4	4.8	**5.5**	4.9	5.6	**6.4**
	Type V	5	1.7	2.4	**3.2**	1.2	2.3	**3.5**
C3S + (4.75 x C3A)	Type II	100	87.5	88	**88.6**	98.1	102.6	**108.1**
C4AF + (2 x C3A)	Type IV	25	23.3	24.3	**25.2**	22.6	24	**25**

Stutzman [76] designed a similar table for the Bogue to QXRD conversion through statistical processing, which is mentioned in ASTM C1365. His correlation was modified here by considering only the Rietveld refinement data out of the data from several QXRD methods (modified literature model). The bolded numbers in Table 14 represent the comparison of the important parameters as seen in ASTM C1365.

Comparison of the modified literature model and the current model (Table 14) illustrates that the limits of the QXRD estimations for alite and belite are wider in the current estimations than the one from modified literature model. However, the limits for aluminate are relatively wider in the modified literature model than the current model. Significantly though, the mean value of the estimated QXRD based on the current model is closer to the actual QXRD than the corresponding mean derived from the modified literature model. This was made apparent in Figure 18 and Figure 19.

The ASTM C1365 estimations were derived from data that range over widely varying XRD quantification techniques such as single-peak fitting, RIR method, Pawley fitting, internal standard method, etc. collected since the 1940s. Furthermore, this lack of homogeneity in the quantification of samples and the age of certain data meant that a part of the data is unusable for direct comparison with current investigations. As a result, the QXRD phase estimations from ASTM C1365 are closer to the Bogue derived ASTM C150 phase limits although the overestimation of aluminate and underestimation of alite in the Bogue is well understood. Contrarily, the data considered in this study were gleaned from a cement lab that used the same XRD and XRF instruments, following the same methodologies, to generate the data. This lack of variation in quantification methodology makes the QXRD estimation more stable, and consequentially, more reliable. However, this model is derived from the data generated from only one cement plant, and a collection of similar data from several different cement plants can generate a very reliable master curve and lead to an improved and accurate Bogue equation.

SUMMARY OF CHAPTER 4

The knowledge gained from the previous chapter was experimentally applied for Rietveld refinement of cement, with a view to develop a practical testing procedure. In this context, focus was allotted to the potential errors associated with QXRD and to generate a procedure that can mitigate the effect of such errors. Based on the information obtained from literature and personal communications, the protocols can be adjusted to incorporate parameters specific to the industrial setup and to most instrument models. In view of this, two independent protocols were developed to cover the most popular XRD vendors.

Repetitive testing on different ASTM C150 and C595 samples with the developed protocols indicated consistent results over different machines. The issue of repeatability was negated by averaging the powder diffraction results. In order to tackle the extent of reproducibility between varying instruments, pressed pellets were employed as QXRD samples. This methodology provided a much-improved reproducibility variation for the specimens. The tested samples also helped to provide the optimum quantification ranges for specific phases as outlined in ASTM C150 for Bogue dependent cement analysis.

CHAPTER 5. SPECIFIC VALIDATION OF QXRD USING SUPPORTIVE CHARACTERIZATION TOOLS

The developed protocols and the resulting outcomes from the previous chapters were leveraged to perform parallel investigations to improve the QXRD process in a holistic manner. Limestone quantification from QXRD was supported through TGA quantification of select cements. Similarly, researchers performed isothermal calorimetry tests to gain understanding about the XRD sulfate to aluminate ratio and the influence of the sulfate polymorphs on the performance properties.

DIFFERENTIATING THE EFFECT OF SULFATE POLYMORPHS USING ISOTHERMAL CALORIMETRY

Flash and false setting are the commonly observed problems with cement-concrete on the job site [58]. Although false setting can be countered by mixing or tempering, flash setting cannot be as it is a result of the polymorphic transition of the calcium sulfate dihydrate (gypsum) phase present in the cement into calcium sulfate anhydrite [40]. ASTM C150 protocols do not prescribe a method to detect this problem before the batch mix is performed on the job site. In this study, the potential of the QXRD to identify the issue of anhydrite presence is highlighted by describing the performance behavior of the cement paste, with gypsum and anhydrite, using isothermal calorimetry.

A mixture of clinkers, with known mineralogy (Table 15), was mixed individually at a ratio of 0.95 clinker to 0.05 gypsum or anhydrite. The sample and reference cells were filled with 4.18 ± 0.5 wt.% of the prepared cement and 2.85 ± 0.5 wt.% of sand (specific heat = 0.75 J/K), respectively. The method B in ASTM C1702 [79] was followed to record the hydration behavior. Water addition to the cement (ratio of water:cement = 0.5:1) was performed with the help of syringes after making sure that heat flow between both cells was minimal. The experiment was logged for 72 hours at a step of 0.3 s per recording. The difference between the anhydrite cement and gypsum cement can be apparent from the following figures (Figure 24 and Figure 25).

Table 15. Powder and Pellet QXRD of the Clinkers.

Phases	Clinker 1		Clinker 2		Clinker 3		Clinker 4	
	Powder	Pellet	Powder	Pellet	Powder	Pellet	Powder	Pellet
Alite	71.58	73.19	71.6	71.8	70.44	71.12	61.16	64.85
Belite	9.91	9.23	9.92	9.79	11.33	11.12	16.42	14.8
Aluminate	3.08	3.17	3.77	3.87	3.75	3.79	4.82	4.3
Ferrite	13.56	11.19	11.37	10.35	12.34	11.51	14.81	13.35

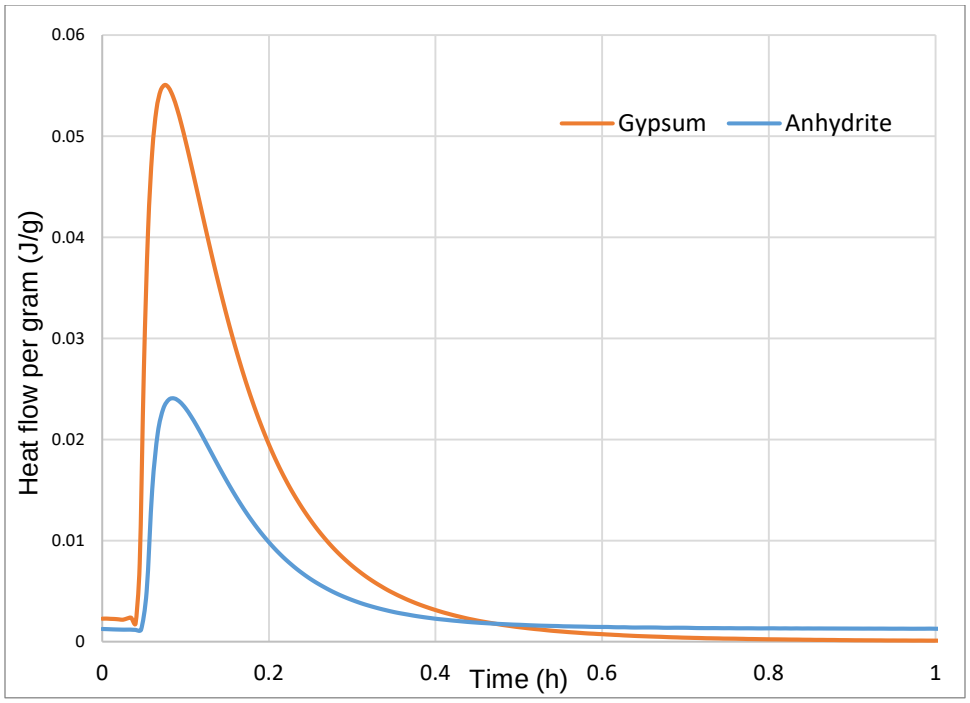

Figure 24. Initial Heat of Hydration Peak of Clinker Mixture with Gypsum and Anhydrite.

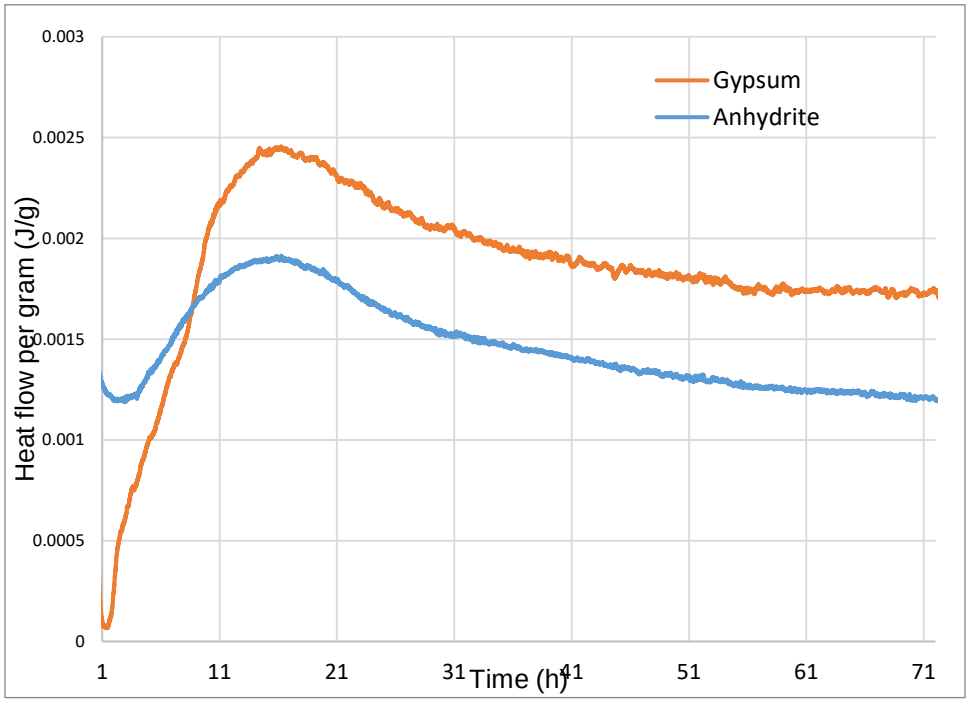

Figure 25. Hydration Peak of Clinker Mixture with Gypsum and Anhydrite.

The amount of heat produced in the first stage of the gypsum reaction with clinker was greater than the same produced by the anhydrite reaction. Due to anhydrite's lower solubility, the gypsum contains more readily dissolvable sulfate ions than the anhydrite. The ions are released immediately on dissolution, which produces a higher first peak than the anhydrite [80].

Moreover, the observed total hydration heat produced due to gypsum reaction was higher than the anhydrite reaction. Anhydrite does not dissolve as readily as gypsum, which can lead to the slow formation of longer needles of ettringite [81]. This reaction proceeds slowly and merges along with the CH and CSH formation reactions. Hence in anhydrite, there is a delayed conversion to monosulfate.

Winnefeld [42] observed that some anhydrite remains in the solution even after three full days of hydration. It was also suggested that the heat of hydration of gypsum-containing cement will be greater than 4–6 times the similar parameter with an anhydrite-based cement depending on the anhydrite to gypsum ratio. In this work, the heat of hydration of clinker with pure gypsum was almost 25 times greater than the heat of hydration of clinker with pure anhydrite at working or substitution levels indicating deferral of the calcium sulfate reaction by the anhydrite.

The experiment reveals that the presence of calcium sulfate as anhydrite will result in hydration delay as explained in the above discussion. This delay can be significant when predominantly anhydrite-rich calcium sulfate is present in cement hydrated on the field. Particularly, it can lead to the concrete not reaching maturity by a calculated period which can lead to huge losses in construction. Figure 24 illustrates this effect.

VALIDATION OF QXRD LIMESTONE QUANTIFICATION

The loss on ignition method is the current standard prescribed by ASTM C150 for calcite quantification. However, Mertens et al. in their hydration study of limes observed that the TGA and QXRD methods were more accurate than the Loss on Ignition (LOI) method in quantifying calcite and portlandite [82]. Calcite quantification can be used as a measure of limestone content in IL cement provided the limestone does not contain any dolomite. The CO_2 contribution from dolomite (if dolomite present in limestone) and moisture loss from organic impurities (may get incorporated in the cement during handling and transport) can be a part of the measured LOI. Because of these additional contributions in LOI, the estimated amount of calcite based on LOI can be erroneous sometimes. This conclusion was justified by several researchers who proclaimed that TGA and QXRD provide the closest and the most consistent results for limestone quantification [32, 33, 36, 38]. Hence, the TGA method was used to test the capability of the recommended QXRD protocols to quantify the limestone content in cement.

Cements with varying calcite fractions, calculated from powder QXRD done in D2 Phaser, were analyzed using thermal gravimetric analysis (TGA) from 400 to 1000°C. The amount of TGA calcium carbonate can be calculated by quantifying the gradual weight loss due to CO_2 expulsion from 500 to 900°C. The CO_2 loss is converted to the amount of calcite lost (in mg) by multiplying with the molecular weight of calcite divided by the molecular weight of CO_2. Now the TGA calcite wt.% can be calculated based on the original quantity of sample (about 30mg).

The TGA instrument was calibrated, and the standard deviation of 15 percent was applied. This standard deviation of 15 percent is an effect of the extreme sensitivity of the weight balance in the TGA equipment to weight percentages as low as 1 mg. The QXRD standard deviation was obtained by testing three powder replications per each sample measurement. The standard deviation for LOI measurements was calculated from the data provided for the three most recent measurements performed by TxDOT.

Table 16 shows that the TGA and QXRD quantification are highly comparable considering the uncertainties of the QXRD and the TGA. Moreover, the calcite quantity calculated from LOI observations is a bit overestimated in comparison with the direct

determination techniques, TGA and QXRD. QXRD phase quantification below 2 wt.% is generally not very reliable as they are close to the value of the standard deviation. As a result, Sample 4 shows the largest divergence between QXRD and TGA results of calcite quantification (Table 16). But in the rest of the cases (especially in IL cements), QXRD can be a good indicator of the actual calcite quantification in the cement. Figure 26 is a representation of all peaks of calcite that were obtained from TGA.

Table 16. Comparison of Calcite Quantification from TGA, QXRD, and LOI Techniques.

Samples	TGA	SD	QXRD	1σ Uncertainty	From LOI	SD
Sample 1 – IL 589	7.95	±1.2	7.3	±0.8	10	±2
Sample 2 – I/II 208	4	±0.6	3.8	±0.2	6.8	±0.1
Sample 3 – IL 707 (second Batch)	9.89	±1.5	12.5	±1	14.7	±0.7
Sample 4 – II/V 710	2	±0.3	0.5	±0.7	2.3	±0.9

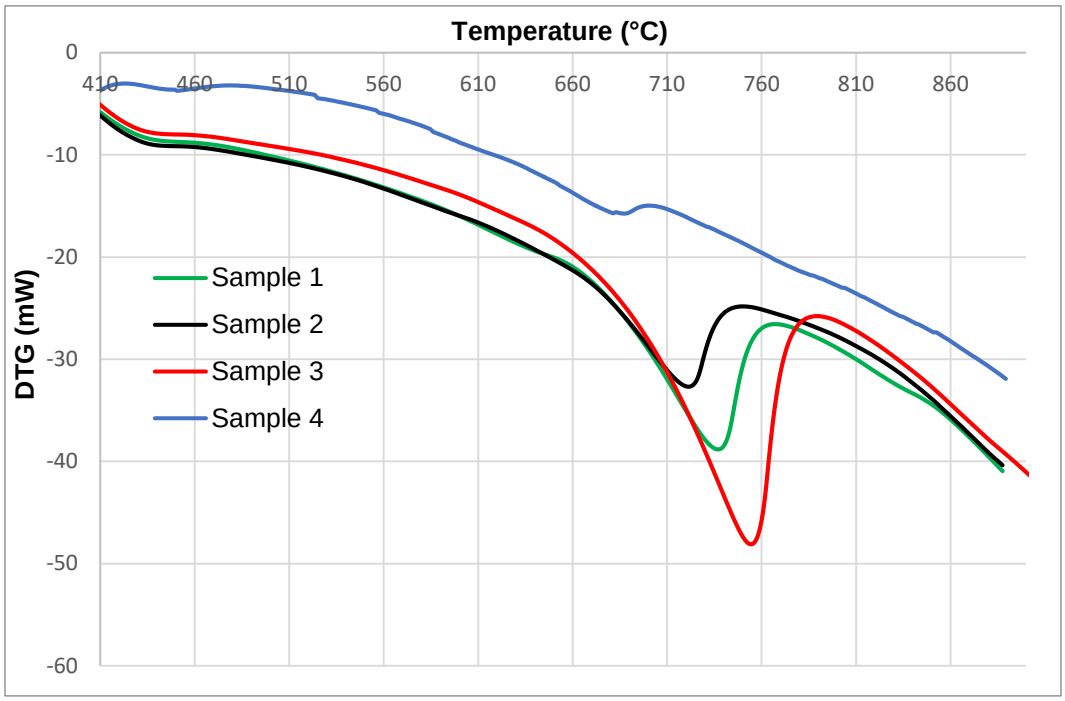

Figure 26. Representations of the Calcite Quantities by the TGA Peak Profile.

SUMMARY OF CHAPTER 5

The recommended protocols were validated for their physical reasonability with the help of supportive characterization tools: isothermal calorimetry and TGA.

Furthermore, the validation of QXRD limestone quantification against a compatriot high-accuracy method, the TGA, was performed to provide an outline of the accuracy of QXRD limestone quantification. Good compatibility of the QXRD results with the TGA results of limestone was obtained within the working range of limestone from 3–15 wt.% in commercial

cements. In contrast, the current method of limestone quantification (from LOI) showed poor correlation with the TGA results underlying the high inaccuracy in limestone quantification by the LOI method.

The effect of sulfate polymorphs in impacting cement paste properties was explained through isothermal calorimetry, further underscoring the need for QXRD based characterization for commercial cements. The anhydride reaction was indicatively slower than the gypsum reaction and hence is unfavorable for use in commercial cements. This situation can only be detected by the QXRD as the Bogue method is incapable of identifying between gypsum and anhydride. However, more work is required to completely define the influence of anhydride on concrete setting considering the inclusion of fly ash, slag, and other chemical admixtures, all of which can control setting.

CHAPTER 6. DETERMINATION OF EFFECTS ON CEMENT PROCESS CONTROL

Although QXRD can perform accurate phase quantification than the Bogue method, the areas where the employment of QXRD can make an impact on process valorization is not fully understood. The following sections contain qualitative and quantitative information on cement production domains where QXRD adoption in online process control can lead to significant advantages.

EFFECT OF ALITE POLYMORPHIC INFORMATION ON CEMENT PERFORMANCE

Alite phase in industrial clinker undergoes polymorphic transformations through the process of clinkerization at different temperatures. Bigare et al. in 1967 [83] established the presence of six polymorphs, the rhombohedral R polymorph (above 1050°C), three monoclinic M polymorphs (950–1000°C), and three triclinic T polymorphs (600–900°C). The polymorph that is stabilized at the highest temperature of formation at above 1050°C is the R polymorph. Incidentally, this polymorph is the most stable of all alite polymorphs. However, due to impurity considerations in the substitutional lattice spaces, the alite is sometimes stabilized in the form of M or the T polymorph. Following the pioneering research, Maki et al. established the prevalence of only three polymorphs in commercial alites in successive papers [84, 85] with a conjunctive microscopy-XRD study. Depending on the SO_3 and MgO composition in the hot meal, the alite phase can stabilize in the form of the monoclinic M1 and M3 polymorphs, or in rare cases, the T3 polymorph. The pseudo-hexagonal phases of M1a (the R polymorph) and M1b polymorphs were re-designated as the M1 and M3 polymorphs, which extended the count of polymorphic transforms to 7. Further, Maki et al. generated a precursor method to identify the difference between the two polymorphs through their X-ray diffraction profiles. The M3 polymorph displayed characteristic doublet peaks between 32–33° 2θ and 51–52° 2θ.

A more realistic method of differentiating between M3 and M1 was succinctly outlined in a recent paper by Li et al. [86], depending on the MgO and SO_3 ratio, which extended on Maki's observations. Two important observations were reported: 1) stabilization of the M3 polymorph of C_3S with increasing MgO content, and 2) stabilization of the M1 polymorph of C_3S along with increasing belite content under SO_3-rich kiln atmosphere. However, in a commercial clinker both the M1 and M3 polymorphs are often seen in a defined ratio based on the SO_3/MgO ratio in the kiln. Figure 27 and Figure 28 represent the relationship between MgO/SO_3 ratio and the formation of the M3 or the M1 polymorph.

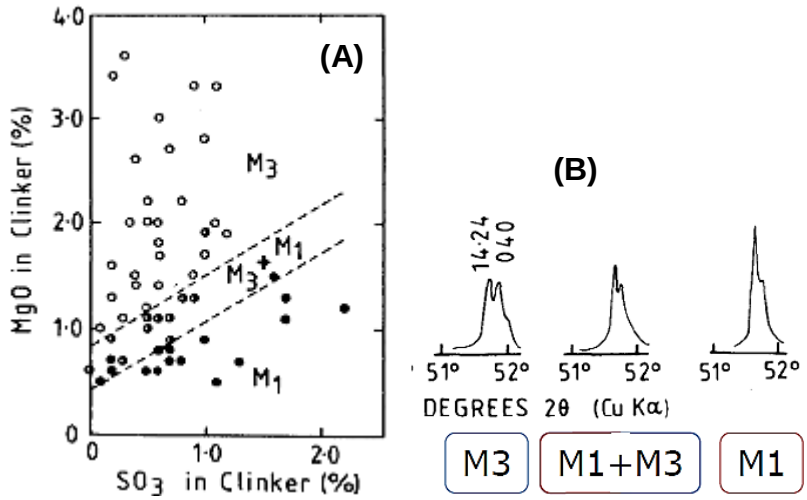

Figure 27. (A) Regions of Formation of the Two Proliferous Alite Polymorphs Based on Kiln Chemistry, and (B) Difference between M3 and M1 Polymorphic Variations Found in Commercial Clinkers (Reprinted from [84]).

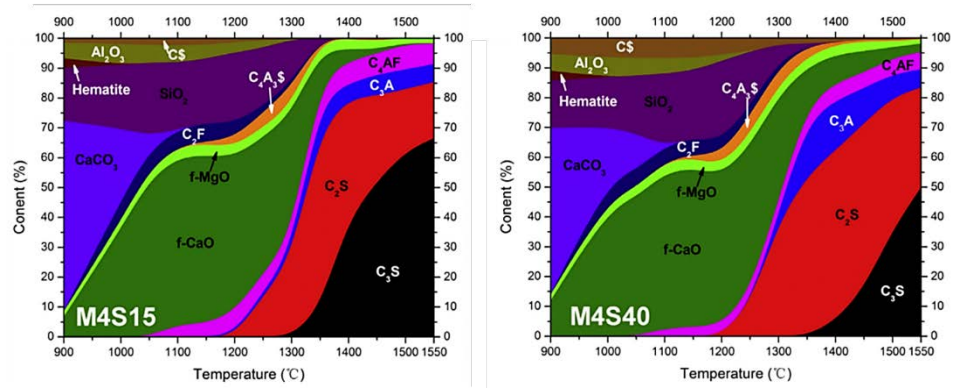

Figure 28. Images Illustrating the Increase in C2S and Reduction in C3S with SO3 Addition (Reprinted from [86]).

The above findings generated by the previous researchers [84-86] were extremely useful in advancing the cement chemistry understanding in an industrial kiln atmosphere. There needs to be a cap on the ratio of the M3 polymorph to the M1 polymorph to promote better control over cement strength development behavior. Kiln burning temperature and MgO/SO3 ratio are the major variables that can control the stabilization of the M3 polymorph within a required limit. It allowed cement plants to perform case studies to clearly delineate the extent of the accuracy of our current understanding of cement chemistry. Preliminary work on this regard was performed by Supreme Cemento (Brazil) (Figure 29), where the advantageous characteristics of the M1 polymorph was clearly seen. Subsequent research by Dyckerhoff (Switzerland) (Figure 30) showed a slight increase in the 3-day strength of the cements with increasing M1 ratio in the alite. The compositional accuracy was realized by reducing the particle size of the raw meal so that increased M1 can be obtained. Another method of producing M1-rich alites is to use a fuel combination of natural coal and petroleum coke, which can give rise to an increased SO_3 environment than other conventional fuels [87].

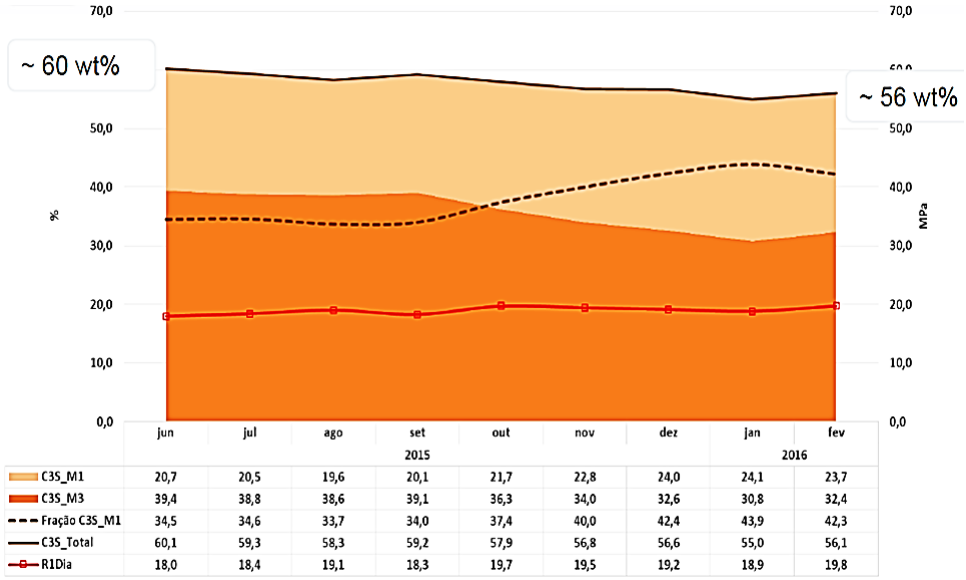

Figure 29. Case Study Performed by Supreme Cemento (Brazil) Describing the Increase in M1 Polymorph with SO_3 Content in Clinkers Most Closely Representing the Types I/II and V.

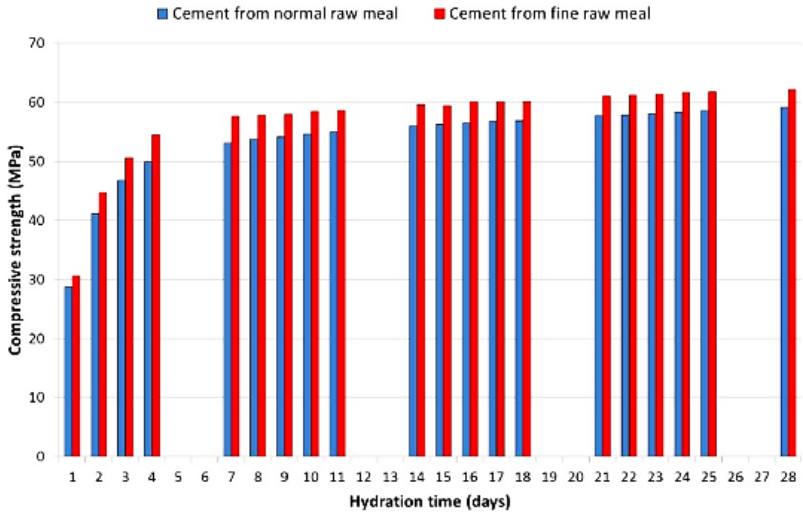

Figure 30. Case Study Performed by Dyckerhoff Cement Illustrating the Observance of Increased Strength with Increased M1 Polymorph Brought about by Using a Finer Raw Meal.

Figure 31 represents the QXRD of one of the TxDOT samples (III 056) where the ability of QXRD to clearly distinguish between M3 and M1 polymorphs of tricalcium silicate can be clearly seen. QXRD can quickly and efficiently identify between M3 and M1 and is perfectly suited to routine quality control. Similar results for other TxDOT samples can be found in the Appendix B. The QXRD results for the remaining cements are presented in the Appendix B (Figure 41–Figure 65).

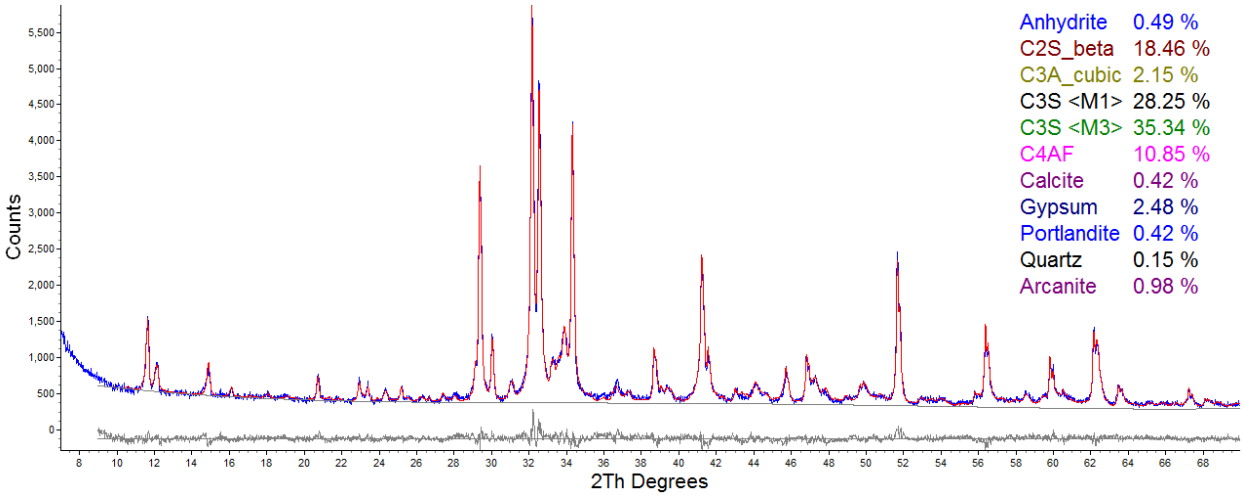

Figure 31. Different Contents of M3 and M1 C3S in III 056 Cement.

EFFECT OF SULFATE AND ALUMINATE POLYMORPHS

C3A is a very important phase in cement as its dissolution in water is rapid and proceeds through initial precipitation to C3AH6 (hydrogarnet) and calcium hydroaluminate (AFm phases) [88-91]. C3A stabilizes as different polymorphs depending on the prevailing conditions in the kiln. During the cooling stage in the kiln, the C3A is present in the form M_{3x} Ca_{3-x} Al_2O_3, where the M represents the type of the prevalent alkali ion in the kiln, and x can be anywhere between 0 to 0.25 [3, 92]. If the alkali-ion content (usually Na) is quite low, x will be between 0–0.1 and leads to the formation of the cubic aluminate polymorph. If the alkali content is higher, orthorhombic aluminate will be stabilized with the x between 0.1–0.2 [3, 93-95]. Often, the alkali-ion concentration in a kiln is not highly enriched beyond the limit x = 0.1 (cubic), which makes the monoclinic polymorph of C3A (x = 0.2–0.25) extremely rare. Furthermore, alkali enrichment in the kiln is often an indicator of poorly maintained furnace conditions, so is the monoclinic polymorph.

Alkali or orthorhombic aluminate dissolves faster in water saturated with gypsum than the cubic aluminate owing to a fundamental difference in the morphology, which is apparent on their reactivities [8]. As a result, cubic aluminate is most preferred owing to the control it offers in deciding the quantity of sulfate addition. Hence, the control of the alkali-ion rich atmosphere in the kiln is very important to obtain a cubic aluminate ratio greater than 95 percent of the orthorhombic aluminate [87] to better predict of hydration behavior.

In order to prevent the rapid reaction of C3A phase with water, calcium sulfate phases are added to the clinker at varying compositions based on the dissolution chemistry of sulfate and aluminate phases. In addition to the C3A polymorphs, the reactivity of the different polymorphs of the sulfates play a crucial role in the hydration behavior of C3A and the formation of ettringite. Benstead in 1982 [9] proposed that hemihydrate has a higher solubility than gypsum, which promotes faster supersaturation of the pore solution with sulfate ions, thereby increasing the early strength by quicker reaction with aluminate to form ettringite. This behavior is valid provided the gypsum and/or hemihydrate quantity remains within 30 percent of the total C3A in the sample. The trend was found to be reversed with values above that limit. Hemihydrate increases the rate of precipitation of the ettringite (67 percent greater than gypsum) since the reaction is disposed of the precipitation of the transitional AFm phases, thereby favoring strength

development during the first 2 hours. However, the presence of anhydrite will destabilize the aluminate-sulfate reaction, owing to its significantly low solubility, and is not favored in the cement.

Prominent work performed by Pourchet et al. [6] on C3A-gypsum reactivity by a combinatorial analysis of Minard's procedure and calorimetry analysis describes the exact difference between the reactivities of gypsum-hemihydrate (illustrated in Figure 32). In commercial cements, 30 percent of the added aluminate reacts with pure gypsum instantaneously to provide the AFm phases while the rest of the aluminate converts to ettringite gradually. When hemihydrate is added, no AFm production takes place which in fact offers better control over the reaction as the ettringite reaction can be monitored more effectively. Although hemihydrate has a reactivity advantage over gypsum and anhydrite, the presence of hemihydrate leads to rapid setting, which is undesirable in field conditions.

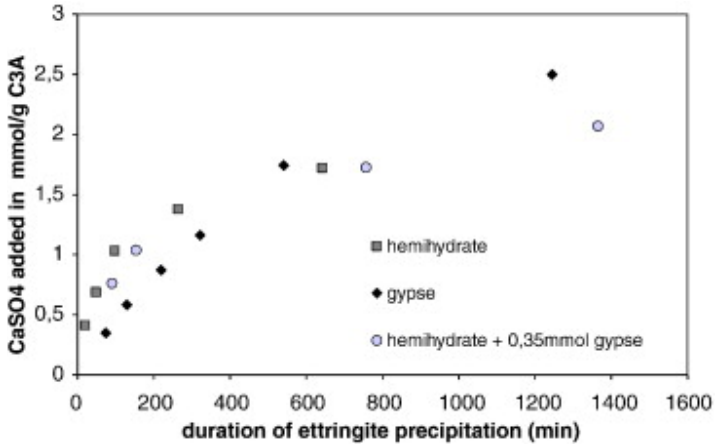

Figure 32. Difference in Reactivities between Aluminate-Hemihydrate and Aluminate-Gypsum in Presence of Water (Reprinted from [6]).

QXRD was successfully used to identify and quantify aluminate polymorphs (Appendix B) and sulfate phases (Table 3) using cement samples received from TxDOT.

PHASES INTRODUCED DUE TO ALTERNATIVE FUEL SUBSTITUTION

Increasing usage of secondary/alternative fuels is employed in the clinkerization and grinding processes to reduce the carbon footprint. With the prospect of modifications to the burnability with increasing substitution of conventional fuels, distinct phases emerge during clinker production. Ferruginous materials in alternative fuels such as glauconite, chlorite, etc. can lead to ferrous iron formation in the clinker, while also providing mineralizing effects [96]. Generally, combustible organic wastes contain a lot of energy and increase the atmosphere of major oxides such as CaO, Al_2O_3, MgO, etc. Especially, increasing alumina environment can increase the generation of tricalcium aluminate in the clinker and the introduction of the amorphous aluminate phase, which is more reactive than the crystalline form [8]. Alternative fuel utilization can also manipulate the clinker phase chemistry of alite and belite. As seen in Figure 33 with the substitution of sewage sludge to increase belite formation [97], the introduction of various alternative fuels can cause a marked shift in the performance characteristics. It is highly important to track such and similar changes in clinker process control using QXRD to improve the predictability of the final cement performance.

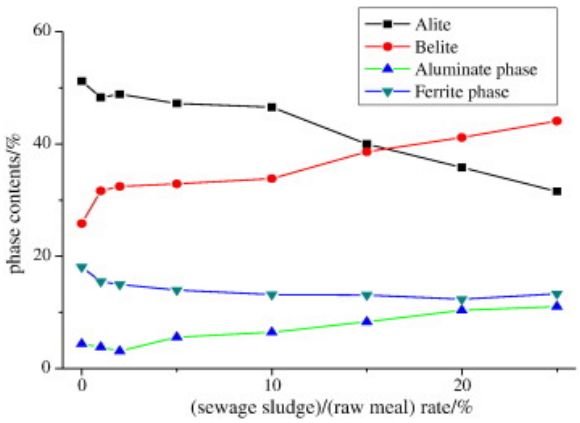

Figure 33. Change in the Clinker Phase Constituents with Increasing (Sewage Sludge)/(Raw Meal) Ratio (Reprinted from [98]).

Here, online QXRD can play a leading role in tracking the modifications to the clinker chemistry from the well-known cement chemistry perspectives. For instance, standalone analysis by Dyckerhoff Cement showed that online QXRD analyses of rubber tires (a cheap alternative to coal) imparts phases as divergent as metallic iron, wax, and sucrose to the cement. Using an online QXRD setup, the dehydration of gypsum after grinding can be monitored and the quality of gypsum added before grinding [99]. However as the organic content in the sewage sludge increases, the viscosity of the molten meal can decrease, thereby increasing the size of the alite crystals owing to increased ion mobility [100]. This can lead to the stabilization of the M1 morphology (as seen in Figure 34 [right]) as the predominant alite polymorph since M1 alite forms larger crystals than M3 alite [86]. Similar grain growth behavior for alite was observed with increased phosphorus content found in most bio-fuels [97, 100-102]. It can be inferred that sewage sludge with a rich organic content shall be preferred for substitution; however, the general increase in sewage sludge above a threshold can reduce the alite phase formation as shown in Figure 33.

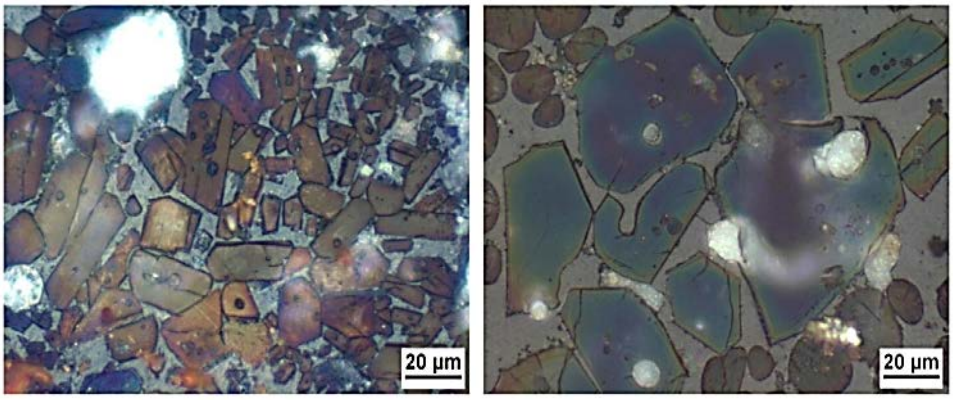

Figure 34. Increase in Alite Crystal Size due to Alternative Fuel Usage (Reprinted from [100]).

Apart from bio fuels, alternative fuel usage can also impart increased heavy metal ion fraction in the kiln, which can cause health hazards such as Zn, Sn, and Cu [103, 104]. Most importantly, heavy metals can isomorphically substitute the interstitial Al^{3+} and Fe^{2+} ions to

significant property alterations. When in abundance, the heavy metals can react with major clinker oxides to produce new phases. Sn^{2+} can react with lime to form calcium stannate ($CaSnO_4$) inhibiting carbonation reaction [105]. Moreover, increased Sn can promote the formation of Aft and Afm phases without impacting the performance of the hydrated paste [106]. In another case [107], the trapped Cu ions in the clinker phases can be detrimental to the formation of C3S since they favor decomposition of C3S to C2S and free lime. Increased Zn ion concentration can in turn affect the formation of the aluminate phase favoring ferrite [103]. Since the existing online quality control protocols cannot identify such markers of inferior performance, the current situation (without QXRD) poses as a handicap toward the increasing substitution of conventional fuels.

IMPURITIES IN LIMESTONE, POLYMORPHS, AND ASSOCIATED PHASES

Retrospective addition of limestone to Type I cement to promote the early strength is characterized as Type I-L cement [33, 108]. ASTM C595 allows the incorporation of 15 percent limestone by weight of the blended cement. Alternatively, limestone aggregates are added to concrete for high early strength as coarse or fine fractions. The positive aspects of the fine limestone aggregates impacting the concrete early strength have been investigated extensively by Bentz in [109, 110]. However, to predict the performance characteristics of I-L cements, the various polymorphs of limestone should be characterized. Calcite, aragonite, and vaterite are the three polymorphs commonly seen in conventional limestones. A multiscale investigation by Bentz et al. in 2013 [110] revealed that the trigonal calcite is preferred in concrete because: 1) it promotes nucleation and growth of calcium silicate hydrate gel at early ages, 2) it accelerates and amplifies silicate hydration, and 3) provides a source of carbonate ions to participate in reactions with the aluminate phases present in the cement (and fly ash). Conversely, the orthorhombic crystal structure of aragonite withdraws the hastening effect on silicate hydration at a similar particle size as calcite. However, because these two forms have similar solubilities in water, the aragonite does contribute to an enhancement in the reactivity of the aluminate phases in the investigated systems, chiefly via carboaluminate formation [111]. The carboaluminate makes for the reduction of sulfate addition and stabilizes the ettringite [112, 113]. Moreover, it is more voluminous [112, 114] and stiffer [115] than sulfoaluminates after hydration, thereby reducing porosity and increasing early strength. QXRD can help promote the formation of carboaluminate by clearly identifying between aragonite and calcite in the additive limestone.

The quantification of the purity of the added limestone as calcite is an important contributor to the desired performance enhancement. Online QXRD can help with the identification and quantification of the exact nature of the undesirable phases and their polymorphs, leading to their subsequent removal. Critical phases such as pyrite (usually found near limestone quarries), the different calcite polymorphs, dolomitic impurities in limestone, ankerite, siderite, etc. are the commonly observed impurities with natural limestone. A joint effort by Schwenk Zement KG (Germany) and Bruker AXS showed the presence of the aforementioned impurities (and a few more) in natural limestone that was considered to be highly pure. This is illustrated in Figure 35 with the observance of feldspathic, siliceous, and clayey impurities in limestone.

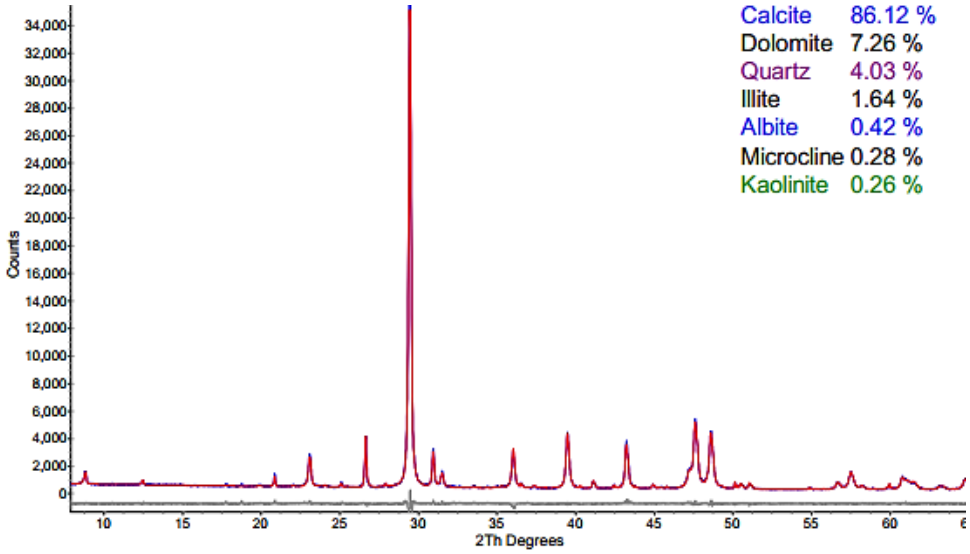

Figure 35. XRD Pattern from Bruker AXS Representing the Presence of Quartz, Feldspar, and Kaolinitic Impurities in Natural Limestone.

HOTMEAL AND RAW MEAL ANALYSES

The analysis of the feed raw meal sent into the kiln can be examined first before the manufacture process is initiated. In the raw meal, both favorable and unfavorable phases can co-exist depending on the quality and synthesis/extraction of the raw materials. Usual examples that pertain to the raw meal QXRD lie in analyzing the purity of gypsum and limestone added to the kiln, with the latter added either retrospectively or with the batch.

The raw meal after calcination undergoes de-carbonation and loss of bound water and is hauled out through the conveyor belt as the hot meal. In the hot meal, the degree of de-carbonation of limestone can be evaluated by the quantification of the free lime phase using QXRD. In another case, the presence of the alite phase at the intermediate stage of clinker processing is an indication of the excessive production of clinker dust in the kiln. Clinker kiln dust (CKD) is a mass of fine-grained materials rich in SiO_2 and can form a layer on the molten melt reducing the thermal efficiency of the kiln. The regular removal of the CKD is vital, which leads to their presence being unsolicited in the kiln. QXRD analysis of the hot meal can pinpoint this deviation from the process control routine to make timely adjustments.

In addition, the buildup of alkali sulfates or silicates in the kiln can lead to the blockage of preheaters or precalciners of raw materials, which can affect the overall thermal efficiency of the kiln. Case studies conducted by the Holcim plant at Siggenthal, Switzerland (Figure 36), revealed that the presence of alkali phases such as Spurrite and Langebeinite in the hot meal caused the obstruction of three preheater tubes leading to a monetary loss equivalent to around 36000 tons per year of cement as per 2009 inflation levels (equivalent to $1.6 million per year). The problem was resolved once the raw feed was adjusted to reduce the SO_3/Cl ratio such that crusting and lumping of the alkali phases was unseen afterward.

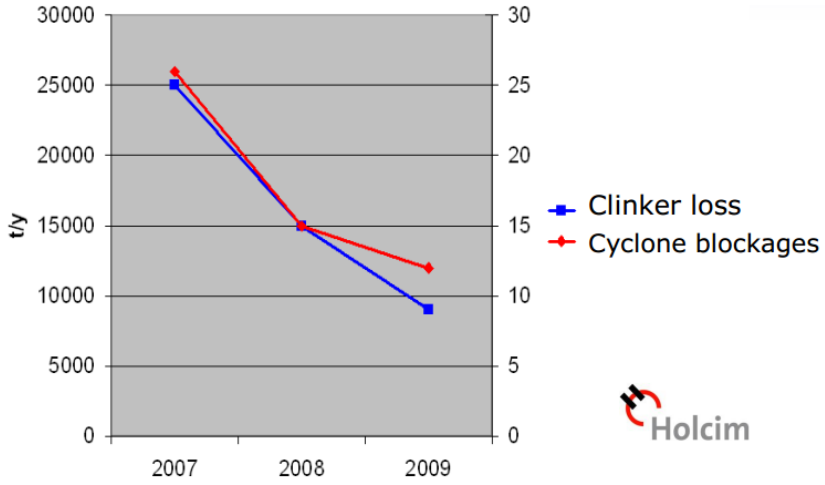

Figure 36. Graph from Holcim Cement Describing the Improvement on Financial Results after Addressing the Cyclone Blockages.

EFFECT OF ALKALI PHASES IN CEMENT

The presence of alkali sulfates in cement is often unstoppable owing to the prominence of alkali oxides in the raw meal. The alkali ions usually get substituted in the major cement phases, but a tiny fraction of the alkali ions can react with the sulfate or can get oxidized to form alkali oxides and sulfates. The existence of both compound groups is undesirable in cement, owing to the problems with excessive cement/mortar expansion on hydration. ASTM C191 specifies a test for the measurement of the expansion of cement using an autoclave apparatus, which are increasingly being relooked at due to safety concerns. Commonly seen phases that lead to such expansions include the periclase, free CaO, and various alkali sulfates (Arcanite, Spurrite, Aphthitalite, Langebeinite, Thenardite, etc.). The arcanite phase can lead to the formation of the syngenite phase whereas the MgO and CaO can lead to the formation of brucite and portlandite, respectively, leading to increased expansion. However, the presence of such phases below a universal fraction of 2 wt.% is acceptable provided that several such phases do not occur in the same clinker [49, 116]. Although the alkali oxide phases are limited to the expansion drawback, the alkali sulfate phases pre-hydrate the cement by just absorbing atmospheric moisture leading to clumping and encrustation in sample conveyors. The customary practice to counter clumping of cement is to add a small fraction of limestone to the cement such that it is workable for baggage and shipping. However, clumping due to alkali sulfate hydration cannot be solved that way as it is independent of limestone reaction. A workable solution would be to identify the alkali sulfate during the hot meal/sample batching analysis and retrospectively correct for the next batch. This solution is possible only with the use of the routine QXRD as the exact nature of the alkali sulfate can be identified through direct measurement.

SUMMARY OF CHAPTER 6

After the evolution of the standard protocols for QXRD, the areas related to production testing that may be affected by the employment of QXRD were gleaned. Some of the influenced areas where the improvements due to QXRD employment can be readily identified are the overgrinding problem with gypsum, the increase in alkali content in the raw meal with the

orthorhombic aluminate formation, the increase in the sulfur content in the raw meal, identified using the higher M1 ratio, etc.

Besides these, certain minor problems can further accrue costs such as the presence of syngenite in the final cement indicating premature hydration due to arcanite, the presence of minor alkali sulfates in raw meal affecting aluminate hydration, the difference between natural and artificial limestone, and gypsum incorporating with them certain unknown additive impurities.

Whereas other problems can have a long-term impact if left unattended, for example alite abundance in the hot meal can steadily increase energy losses. Such improvements due to QXRD employment in the performance of the process control operation, the quality of the clinker/cement, and its estimated monetary impact are recorded as outcomes of this phase using industrial case studies.

CHAPTER 7. COST BENEFITS ANALYSIS

Although the qualitative benefits of QXRD employment in holistic quality control was described in detail in Chapter 6, the quantification of those benefits is required before QXRD adoption. Assigning monetary values to the qualitative benefits listed in Chapter 6 requires extensive information on the cost of operation of every step of the clinkering process, in addition to the cost of sourcing and transporting the different raw materials. The benefits of increase in profit/year, increase in production, extension of the life of the system, and reducing maintenance costs through reducing conveyor stops by employing effective process flow streamlining were collected from literature and provided later. A specific example of incremental substitution of alternative fuels was analyzed to provide an illustration of the monetary advantages of employing QXRD.

The life-cycle cost analysis was performed using the Economic Input Output - Lifecycle Cost Assessment (EIO-LCA) [117], a financial prediction model devised by Wassily Leontief - Nobel Laureate in Economics. It uses real-time information on a specific sector such as steel industry, fishing industry, cement manufacturing, etc. and generates a fiscal prediction system that incorporates user-defined variables. Resultant outputs can belong to the economic or the sustainability aspects, while users can choose more in-depth variables within the major outputs (financial or sustainability). In this context, to predict the cost savings in cement manufacturing using alternative fuels the outputs were chosen accordingly as: total CO_2 emissions per annum, total costs savings per annum, and energy costs saved through incremental substitution.

SUBTASK 7.1. GENERATING REAL INPUTS FOR COST BENEFITS ANALYSIS

The life cycle cost analysis program was modeled based on the models derived from the EIO-LCA software. For deriving outputs based on direct economic activity (in billion dollars), the input of current total revenue is required. Being a producer-based model, the input was calculated from the total annual cement consumption in the United States, which was equal to $9.75 billion.

The cost-benefits model was generated based on the following steps:

1. Selecting the fuels used in each aspect of cement manufacturing—Selecting the indicators for CO_2 emissions and fuel expenditure.
2. Obtaining the total amount of CO_2 emissions by a particular fuel used in all cement manufacturing processes—Optimizing the emissions by trying combinations of fuels.
3. Calculating the total expenditure on a particular fuel—Optimizing the expenditure by trying combinations of fuels.
4. Deriving the emissions and economic fuel indices.

This model offers the advantage of entering customized inputs that can be obtained from other calculations. Examples in the fuel sphere include fuel procurement cost (influenced by current market trends), transportation/hauling costs (influenced by distance from coal mine or waste management plant [59]), etc. The CO_2 emissions for each fuel (Table 17) were calculated by incorporating the specific heat capacity (in kJ/(kg.K)) [118-121], extent of utilization (in kJ) [122], and the total CO_2 released by each fuel per year in cement manufacturing [122].

The normalized total CO_2 released per year (Table 18) metric indicates the amount of CO_2 released if only the particular fuel is used for cement manufacturing. One hundred percent

of coal usage for cement manufacturing will result in 0.5 million metric tons of CO_2 release in place of the current 0.48 million metric tons. Similarly, the normalized total expenditure recognizes the total cost expended on using the particular source as the only fuel for all aspects of cement manufacturing.

Table 17. Calculation of CO_2 Emissions per Fuel Type and the Associated Costs.

Fuel	Heat Capacity (kJ/kg.K)	Thermal Utilization per year = Total energy released by the fuel for cement manufacturing (in billion kJ)	Mass of fuel used = Thermal Utilization / Heat Capacity (in million metric tons)	Current Market Price per kg (includes hauling cost) (dollars)	Total expenditure on fuel ($billion per year)	Total CO_2 released per year (in million metric tons)
Coal	1.38	351	254.35	0.06 (0.016)	19.33	0.33
Pet Coke	1.5	123.7	82.47	0.13 (0.016)	12	0.13
Waste fuels	2.9	53.2	18.35	(0.016)	0.29	0.02

Table 18. Normalized Emissions and Costs Information.

Fuel	Percentage of utilization	Percentage Total CO_2 released per year	Normalized Total CO_2 released per year (in million metric tons)	Normalized Total expenditure (in billion dollars)
Coal	67	68.75	0.5	28.85
Pet coke	23	27	0.57	52.2
Waste fuels	10	4	0.2	2.9

SUBTASK 7.2. IMPLICATIONS ON THE ECONOMICS OF CEMENT PRODUCTION

Coal, petroleum coke (or pet coke), and municipal solid waste are the three commonly used fuels for cement manufacturing. The inputs were derived from the EIO-LCA software program on a cradle-to-gate scenario. Table 17 and Table 18 summarize the cost expended on a particular fuel, the CO_2 released by the fuel, and the calculations that lead to the outputs. Coal is the most popular fuel for cement manufacturing although the situation is inclining toward pet coke due to its high sulfur content. The other advantages of pet coke over coal for cement manufacturing such as better burnability, higher calorific value, lesser fire hazard than coal, etc. are explained in [68]. Municipal solid waste contains a high phosphoric and a healthy sulfate content, and its usage has numerous economic benefits arising out of international sustainability codes. In addition, solid waste fuel can be procured for free with only the hauling costs to be considered.

The hauling cost for the pet coke and coal were calculated from the coal freight transportation statistics released by the U.S. Department of Transportation [59], considering the nearest coal mine to be 75 miles away. In a similar manner, the hauling cost for solid waste was calculated by considering the nearest waste management plant to be 120 miles away from the cement plant.

Optimization of the fuel emissions and the expenditure was performed by increasing the substitution of the solid waste fuels from 0 percent till 100 percent for both pet coke and coal. Figure 37–Figure 40 illustrate this.

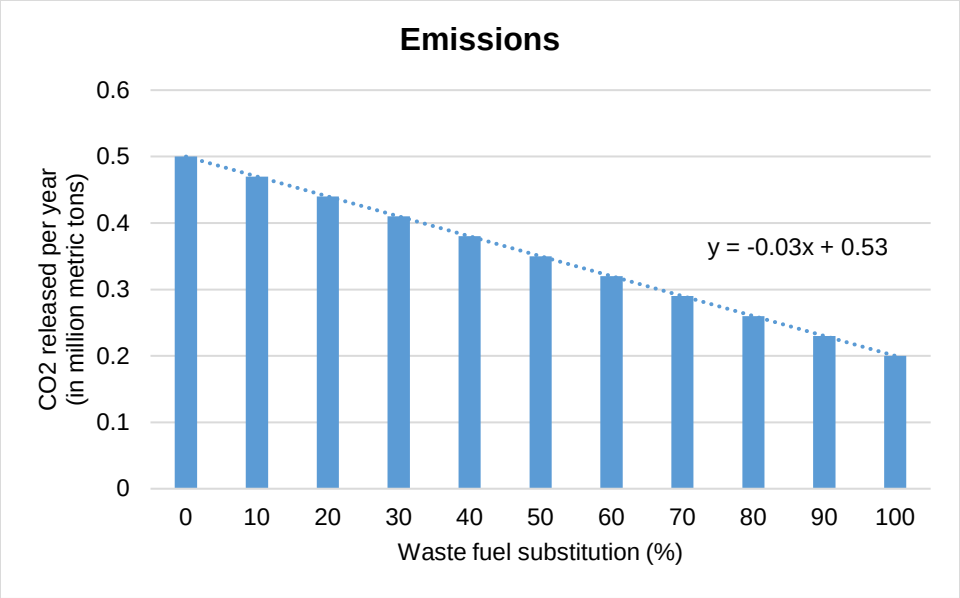

Figure 37. CO_2 Released per Year due to the Coal Substitution by Solid Waste Fuel.

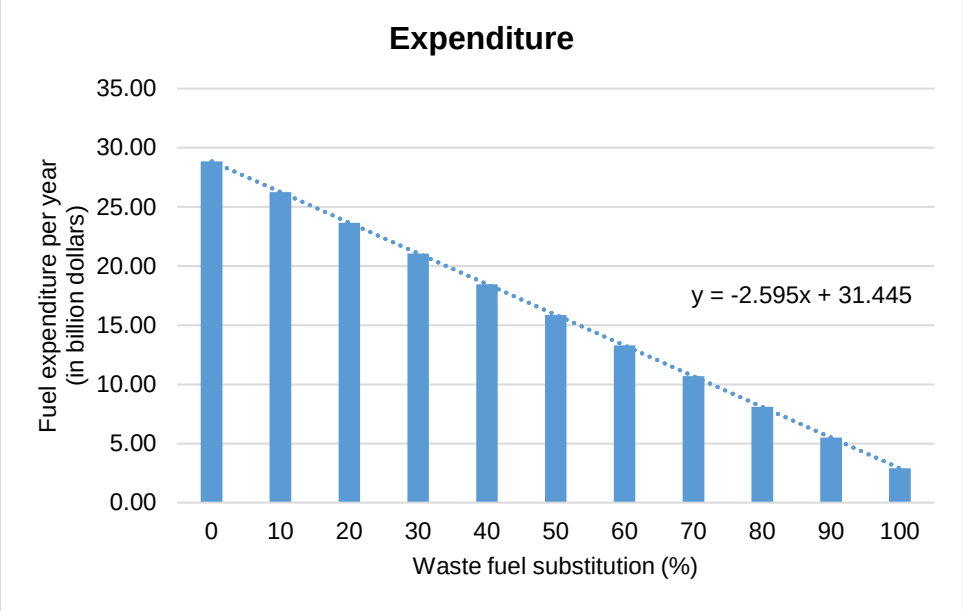

Figure 38. Cost Savings with Increasing Coal Substitution by Solid Waste Fuel.

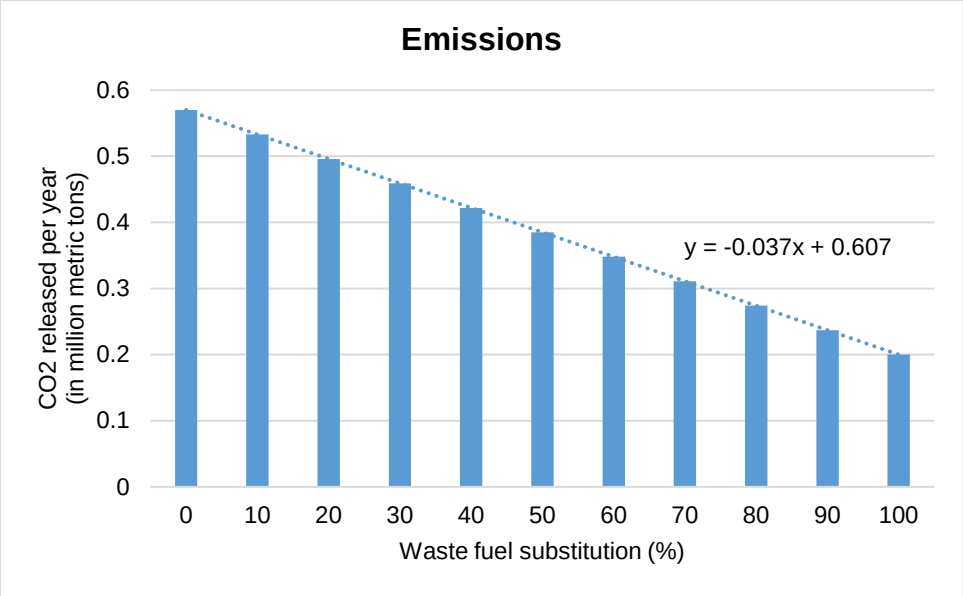

Figure 39. CO_2 Released per Year due to the Pet Coke Substitution by Solid Waste Fuel.

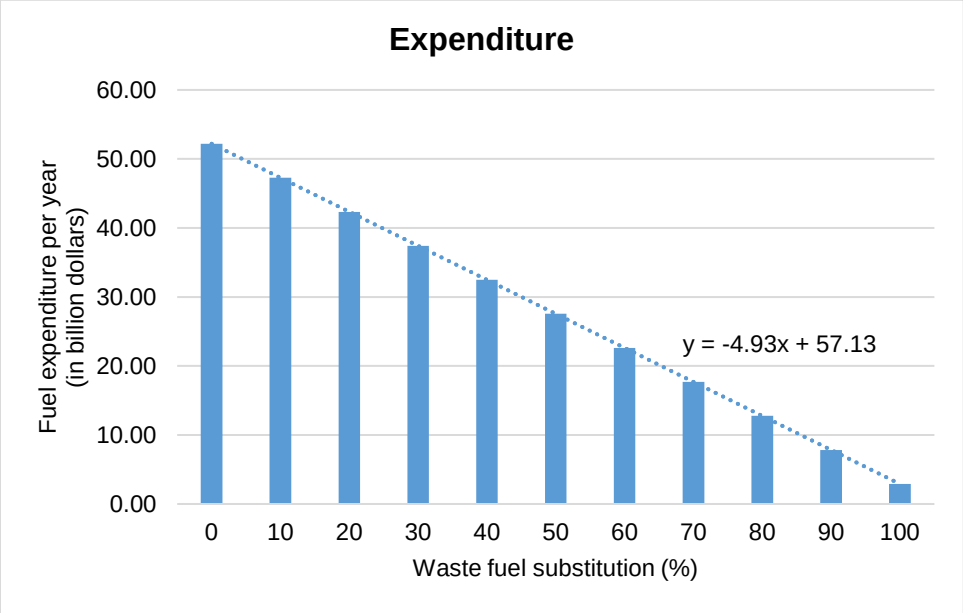

Figure 40. Cost Savings with Increasing Coal Substitution by Solid Waste Fuel.

In the United States, certain cement plants that employ online QXRD have increased substitution to typically about 30 percent, with some plants going even till up to 90 percent. It was estimated that the cumulative increase in profit over a single year in a single plant, just due to the changeover to an online QXRD system, was around $1.5 million in 2009 [123]. The increase in production was around 6,000 metric tons per year against a total production of 10,000 metric tons per year during the previous year. Process flow streamlining was made more efficient due to the use of the QXRD and the conveyor stops were reduced. Fewer stops extend the life of the system and reduce maintenance costs. Similar detailed information about the benefits of QXRD in specific industrial processes can be found in Chapter 6.

SUMMARY OF CHAPTER 7

This chapter is an extension of Chapter 6, which congregated the qualitative benefits of employing QXRD in holistic quality control. Employment of QXRD in routine production testing can help identify the impurities or deleterious phase properties in the incipient stages, which is not possible with the current protocols.

Extending this advantage of QXRD a manufacturer will be empowered to incrementally substitute alternative fuels in place of pet coke or coal during clinker production. The effects of such substitutions were elucidated in this chapter in terms of the emissions reduction gained and the corresponding savings in cost over 1 year using recently available process control data from various sources.

CHAPTER 8. SUMMARY

The specific issues outlined in the problem statement were distributed among different tasks to prioritize each problem. First, the barriers that prevented QXRD adoption for quality control were identified to understand the shortcomings of the procedure. Consequently, practical solutions were developed for each barrier and the problems were tackled by grouping them into QXRD stages: sample preparation, data collection, and accuracy of the analysis. The suggestions were incorporated into the QXRD protocols to generate universal protocols for cement analysis. In addition, improvements were suggested to the analysis to either enhance the generated protocols or to underscore the validity of the QXRD analysis. Furthermore, a technique was developed to engender cross-platform compatibility between the Bogue method and QXRD and vice versa.

CONCLUSIONS

The important conclusions from this research can be categorized as:

- Development of comprehensive QXRD protocols followed by validation using TxDOT sample cements.
- Documentation of universal Rietveld refinement protocols for clinker/cement quantification in Bruker TOPAS and PANalytical XpertHighScore Plus.
- Derivation of corresponding QXRD specifications for the important Bogue based specification limits listed in ASTM C150.
- Accurate derivation of QXRD phase quantification from the Bogue phase quantification to apply ASTM C150 specifications (Bogue to QXRD conversion).
- Validation of the accuracy of the QXRD limestone quantification using TGA.
- Experimental validation of the accuracy of the QXRD amorphous content quantification through PONKCS or pseudo-phase method.
- Experimental validation for the important cement chemistry aspects in QXRD through a combination of in-house performance testing and industrial collaboration.

FUTURE RECOMMENDATIONS

Although this project performed gap-filling research addressing some of the outstanding issues that plague the industrial QXRD process, the implementation of the derived solutions, and their effect on the performance of the cement is to be generated for a complete study. For instance:

1. Round robin analysis using pressed pellets can be promoted to establish pressed pellet QXRD for the implementation of the protocols developed in this project. A selection of labs from industrial quality control setups and research organizations along with TxDOT and TTI will establish the validity of the pressed pellet QXRD method following the recommended changes to ASTM C1365 identified in this project.
2. Actual performance and rehabilitation data of the concrete used for a rigid pavement with the gypsum versus anhydrite containing cement can be beneficial in highlighting the importance of QXRD in controlling setting. Consequently, the inter-dependent effects of other SCM additions such as fly ash or slag, along with chemical admixtures that

influence setting, should be investigated in greater detail by making several different mix designs. The characterization of the relationship between all contributing variables to concrete setting can clearly delineate the importance of the polymorphic influence on cement hydration. Therefore, further investigation to understand the effects of complex interactions between sulfate/C3A polymorphs of cement and commonly used admixtures (chemical and mineral) on concrete early age properties (e.g., setting time behavior, strength gain) is highly recommended to improve concrete performance prediction based on QXRD based C3A and sulfates data. Although, heat of hydration measurement is the best way to detect these incompatibilities, a cement paste rheology testing was found to be effective to detect these incompatibilities as an easy to use field testing method (past TxDOT project 0-5820).

3. Application of the fly ash characterization using PONKCS technique can be used to generate a new performance prediction system for alkali-silica reactivity. A combined approach of identification and quantification of crystalline phases and determination of amorphous contents of different types of fly ashes by the QXRD PONKCS method, pore solution measurements/estimation, ASTM C311 (available alkalis), and ASTM C618 was found to be effective by the authors to do performance prediction of different types of ashes (e.g., conventional, alternative SCMs, and off-spec ashes). The recently developed accelerated concrete cylinder test in project 0-6656-01 can effectively be used to validate these predictions and develop a performance-based approach to ensure effective utilization of these ashes along with determination of optimum contents.
4. Currently, there is an alarming situation of **zero** cement plants or industrial labs in Texas having a dedicated QXRD for offline/online analysis. Based on the outcomes of this project, a study can be performed to identify potential interest and bring in cement plants operating in Texas into the QXRD fold. This can also help in performing round robin analysis and create a valuable data sharing platform that can be used for future TxDOT projects. For instance, data from several plants can be collected to generate improved models for Bogue to QXRD correlation thereby circumventing the need for QXRD in quality control.

REFERENCES

[1] H.F.W. Taylor, Modification of the Bogue calculation, Adv. Cem. Res. 2(6) (1989) 73-77.

[2] L.P. Aldridge, Accuracy and precision of phase analysis in portland cement by Bogue, microscopic and X-ray diffraction methods, Cem. Concr. Res. 12(3) (1982) 381-398.

[3] H.F.W. Taylor, Cement Chemistry: 2nd Edition, Thomas Telford Publishing, London, UK, 1997.

[4] P. E. Stutzman, A. Heckert, A. Tebbe, S. Leigh, Uncertainty in Bogue-calculated phase composition of hydraulic cements, Cem. Concr. Res. 61-62 (2014) 40-48.

[5] A.A. Hanhan, Influence of the SO3 Content of Cement on the Durability and Strength of Concrete Exposed to Sodium Sulfate Environment, MS Thesis, University of South Florida, 2004, p. 112.

[6] S. Pourchet, L. Regnaud, J.P. Perez, A. Nonat, Early C3A hydration in the presence of different kinds of calcium sulfate, Cem. Concr. Res. 39 (2009) 989-996.

[7] L.P. Chaignat, F. Winnefeld, B. Lothenbach, G.L. Saout, C.J. Muller, C. Famy, Influence of the calcium sulphate source on the hydration mechanism of Portland cement–calcium sulphoaluminate clinker–calcium sulphate binders, Cem. Concr. Compos. 33 (2011) 551-561.

[8] R.J. Myers, G. Geng, E. Rodriguez, P.d. Rosa, A.P. Kirchheim, P.J.M. Monteiro, Solution chemistry of cubic and orthorhombic tricalcium aluminate hydration, Cem. Concr. Res. 100 (2017) 176-185.

[9] J. Benstead, Effect of clinker-gypsum grinding temperature upon early hydration of Portland cement, Cem. Concr. Res. 12 (1982) 341-348.

[10] R.H. Bogue, Calculation of the compounds in Portland Cement, Ind. Eng. Chem. 1(4) (1929) 192-197.

[11] ASTM C150M-17: Standard Specification for Portland Cement, ASTM International, West Conshohocken, PA, 2017.

[12] L. Hjorth, K.G. Lauren, "Belite in Portland Cement" Cem. Concr. Res. 1 (1971) 27-40.

[13] L. Aldridge, R.P. Eardley, Effects of Analytical Errors on the Bogue calculation of compound composition, Cem. Tech. 4 (1973) 177-183.

[14] W.A. Gutteridge, "On the dissolution of interstitial phases in Portland cement", Cem. Concr. Res. 9 (1979) 319-324.

[15] D.L. Bish, S.A. Howard, Quantitative Phase Analysis Using the Rietveld Method, J. Appl. Cryst. 21 (1987) 86-91.

[16] D.B. Wiles, R.A. Young, A new computer program for Rietveld analysis of X-ray powder diffraction patterns, J. Appl. Cryst. 14 (1981) 149-151.

[17] D.K. Smith, G.G.J. Jr., A. Schieble, A.M. Wims, J.L. Johnson, G. Ullmann, Quantitative X-ray powder diffraction methods using the full diffraction pattern, Powd. Diffr. 2 (1987) 73-77.

[18] P.E. Stutzman, Guide for X-ray powder diffraction analysis of Portland cement and clinker, NIST Intern. Rep. 5755 (1996) 1-38.

[19] H. Motzet, H. Poellmann, U. Koenig, J. Neubauer, Phase quantification and microstructure of a clinker series with lime saturation factors in the range of 100, 10th International Congress on the Chemistry of Cement, Gothenburg, 1997.

[20] T. Westphal, G. Walenta, M. Gimenez, E. Bermejo, T. Fuellmann, K. Scrivener, H. Poellmann, Characterization of cementitious materials, Inter. Cem. Rev., 2001.

[21] G. Walenta, T. Fuellmann, M. Gimenez, I. Leroy, R. Friedle, G. Schnedl, D. Hartung, G. Staupendahl, C. Lauzon, D. Decary, Quantitative Rietveld analysis of cement and clinker, Inter. Cem. Rev., 2001.
[22] G. Walenta, T. Fuellmann, Advances in quantitative XRD for clinkers, cements and cementitious additions, Adv. X-ray Anal. 47 (2004) 287-296.
[23] G.L. Saout, V. Kocaba, K. Scrivener, Application of the Rietveld method to the analysis of anhydrous cement, Cem. Concr. Res. 41 (2011) 133-148.
[24] K.L. Scrivener, T. Fuellaman, G. Walenta, E. Galucci, E. Bermejo, Quantitative study of Portland cement hydration by X-ray diffraction/Rietveld analysis and independent methods, Cem. Concr. Res. 34 (2004) 1541-1547.
[25] R. Snellings, K. Salze, K.L. Scrivener, Use of X-ray diffraction to quantify amorphous supplementary cementitious materials in anhydrous and hydrated blended cements, Cem. Concr. Res. 64 (2006) 89-98.
[26] A. G. de la Torre, M. G. Lopez-Olmo, C. Alvarez-Lua, S. Garcia-Granda, M.A.G. Aranda, Structure and microstructure of gypsum and its relevance to Rietveld quantitative phase analyses, Powd. Diffr. 19 (2004) 200-246.
[27] A.G. de la Torre, A. Cabeza, E. R. Losilla, M.A.G. Aranda, Quantitative Phase Analysis of ordinary Portland cement using synchrotron radiation powder diffraction, Z. Kristallogr. Suppl. 23 (2006) 587-592.
[28] ASTM C1365: Standard Test Method for Determination of the Proportion of Phases in Portland Cement and Portland-Cement Clinker Using X-Ray Powder Diffraction Analysis, ASTM International, West Conshohocken, PA (USA).
[29] L.D. Calvert, A.F. Sirianni, G.J. Gainsford, A Comparison of Methods for Reducing Preferred Orientation, Adv. X-ray Anal. 26 (1983) 105-110.
[30] W.A. Dollase, Correction of intensities for preferred orientation in powder diffractometry: application of the March model, J. Appl. Cryst. 19 (1986) 267-272.
[31] J. C. Taylor, C.E. Matulis, Absorption contrast effects in the quantitative XRD analysis of powders by full multiphase profile refinement, J. Appl. Cryst. 24 (1991) 14-17.
[32] A. Kumar, T. Oey, G.P. Falla, R. Henkensiefken, N. Neithalath, G. Sant, A comparison of intergrinding and blending limestone on reaction and strength evolution in cementitious materials, Construction and Building Materials 43 (2013) 428-435.
[33] W. Huang, H. Kazemi-Kamyab, W. Sun, K. Scrivener, Effect of cement substitution by limestone on the hydration and microstructural development of ultra-high performance concrete (UHPC), Cement and Concrete Composites 77 (2017) 86-101.
[34] A.V. Soin, L.J.J. Catalan, S.D. Kinrade, A combined QXRD/TG method to quantify the phase composition of hydrated Portland cements, Cement and Concrete Research 48 (2013) 17-24.
[35] A. Morandeau, M. Theiry, P. Dangla, Investigation of the carbonation mechanism of CH and C-S-H in terms of kinetics, microstructure changes and moisture properties, Cem. Concr. Res. 56 (2014) 153-170.
[36] Z. Tu, M. Guo, C.S. Poon, C. Shi, Effects of limestone powder on CaCO3 precipitation in CO2 cured cement pastes, Cem. Concr. Compos. 72 (2016) 9-16.
[37] J. Chang, Y. Fang, Quantitative analysis of accelerated carbonation products of the synthetic calcium silicate hydrate(C–S–H) by QXRD and TG/MS, Journal of Thermodynamic Analysis Calorimetry 119 (2014) 57-62.

[38] G. Ye, X.L.G.D. Schutter, A.M. Poppe, L. Taerwe, Influence of limestone powder used as filler in SCC on hydration and microstructure of cement pastes, Cem. Concr. Compos. 29 (2007) 94-102.
[39] F.J. Tang, E.M. Gartner, Influence of sulfate source on Portland cement hydration, Adv. Cem. Res. 1(2) (1988) 67-74.
[40] S. Mindess, J.F. Young, Concrete: 2nd Edition, Prentice Hall, Englewood Cliffs, New Jersey, USA, 2003.
[41] P. Lausser, Bruker AXS, Personal Communication.
[42] F. Winnefeld, B. Lothenbach, M. Plotze, The influence of different calcium sulfates on the hydration of Portland cement - A practical study, ZKG Int. 58(3) (2005) 62-70.
[43] P.S. Whitfield, L.D. Mitchell, The effects of particle statistics on Rietveld analysis of cement, Z. Kristallogr. Suppl. 30 (2009) 53-59.
[44] T. Moderl, Improved backloading for better results, Mat. Sci. Forum, Transtech Publications, Switzerland, 2001, pp. 240-247.
[45] B.A. Supernant, G. Papadopoulous, Selective Dissolution of Portland Fly Ash Cements, J. Mater. Civil. Eng. 3(1) (1991) 48-59.
[46] K. Luke, F.P. Glasser, Selective dissolution of hydrated blast furnace slag cements, Cem. Concr. Res. 17 (1986) 273-282.
[47] K.V.L.S. G. V. P. Bhagath Singh, Quantitative XRD study of amorphous phase in alkali activated low calcium siliceous fly ash, Constr. Build. Mater. 124 (2014) 139-147.
[48] Y. P. Stesko, N. Shanahan, H. Deford, A. Zayed, Quantification of supplementary cementitious content in blended Portland cement using an iterative Rietveld–PONKCS technique, J. Appl. Cryst. 50 (2017) 498-507.
[49] P.E. Stutzman, P. Feng, J.W. Bullard, Phase Analysis of Portland Cement by Combined Quantitative X-Ray Powder Diffraction and Scanning Electron Microscopy, J. Res. NIST 121 (2016) 47-107.
[50] ASTM E177: Standard Practice for Use of the Terms Precision and Bias in ASTM Test Methods, ASTM International, West Conshohocken, PA (USA), 1986.
[51] J.R. Crandall, R.L. Blaine, Statistical Evaluation of Interlaboratory Cement Tests, Proc. Am. Soc. Test. Mater. 59 (1959) 1129-1154.
[52] L.P. Aldridge, Accuracy and Precision of an X-ray diffraction method for analyzing Portland cements, Cem. Concr. Res. 12 (1982) 437-446.
[53] I. C. Madsen, N. V. Y. Scarlett, L. M. D. Cranswick, T. Lwin, Outcomes of the international union of crystallography commission on powder diffraction round robin on quantitative phase analysis: samples 1a to 1h, J. Appl. Cryst. 34 (2001) 409-426.
[54] L. Leon-Reina, A.G. de la Torre, J.M. Porras-Vasquez, M. Cruz, Alcobe, X., M. Ordonez, F. Gispert-Guirado, A. Larranage-Varga, M. Paul, T. Fuelman, R. Schmidt, M.A.G. Aranda, Round robin on Rietveld quantitative phase analysis of Portland cements, J. Appl. Cryst. 42 (2009) 906-916.
[55] P.E. Stutzman, Development of an ASTM standard test method on X-ray powder diffraction analysis of hydraulic cements, Adv. X-ray Anal. 47 (2004) 206-211.
[56] S.T. Petersen, B. Weber-Wisman, X-ray Powder Sample Preparation, World Cem. (5) (1997) 34-40.
[57] P.E. Stutzman, Quantitative X-ray Powder Diffraction of Portland Cements: Proficiency Tests for Laboratory Assessment, Adv. Civ. Eng. 3(1) (2014) 122-141.
[58] Jeff Hook, Lehigh Hanson North America, Personal Communication.

[59] Peter Lausser, Bruker AXS, Germany, Personal Communication.
[60] M. Enders, Sample preparation for quantitative X-ray diffraction in cement plants: sources of errors and solutions, ZKG Int. 58 (2005) 28-37.
[61] V. Kocaba, Development and Evaluation of Methods to Follow Microstructural Development of Cementitious Systems Including Slags, PhD Thesis, EPFL, Switzerland, 2009, p. 263.
[62] ASTM, E562: Standard test method for determining the volume fraction by systematic manual point counting, 2011.
[63] ASTM, C1356: Standard test method for quantitative determination of phases in Portland Cement clinker by microscopical point-count procedure, 2012.
[64] M. Mouret, E. Ringot, A. Bascoul, Image analysis: A tool for the characterisation of cement in concrete - metrological aspects of magnification, Cem. Concr. Compos. 23 (2001) 201-206.
[65] P.T. Durdzinski, C.F. Dunant, M.B. Haha, K.L. Scrivener, A new quantification method based on SEM-EDS to assess fly ash composition and study the reaction of its individual components in hydrating cement paste, Cem. Concr. Res. 73 (2015) 111-122.
[66] R.T. Chancey, P.E. Stutzman, M.C.G. Juenger, D.W. Fowler, Comprehensive phase characterization of crystalline and amorphous phases of a Class F fly ash, Cem. Concr. Res. 40 (2010) 146-156.
[67] P.E. Stutzman, J.W. Bullard, P. Feng, Quantitative Imaging of Clinker and Cement Microstructure, NIST Technical Note 1877, Gaithesburg, Maryland, 2015.
[68] Greg Barger, Ash Grove Cement, Personal Communication.
[69] M. Enders, Quantitative XRD analysis in automated cement laboratories: requirements for the sample preparation, ZKG Int. 56(5) (2003) 54-62.
[70] I.C. Madsen, N.V.Y. Scarlett, A. Kern, Description and survey of methodologies for the determination of amorphous content via X-ray powder diffraction, Z. Kristallogr. 226 (2011) 944-955.
[71] T. Westphal, T. Fullmann, H. Pollmann, Rietveld quantification of amorphous portions with an internal standard-mathematical consequences of the experimental approach, Powd. Diffr. 24 (2009) 239-243.
[72] D. Jansen, Ch. Stabler, F. Goetz-Neunhoeffer, S. Dittrich, J. Neubauer, Does Ordinary Portland Cement contain amorphous phase? A quantitative study using an external standard method, Powd. Diffr. 26(1) (2011) 31-38.
[73] P.M. Suherman, A.v. Riessen, B. O'Connor, D. Li, D. Bolton, H. Fairhurst, Determination of amorphous phase levels in Portland cement clinker, Powd. Diffr. 17(3) (2002) 178-186.
[74] D. Jansen, F. Goetz-Neunhoeffer, C. Stabler, J. Neubauer, A remastered external standard method applied to the quantification of early OPC hydration, Cement and Concrete Research 41(6) (2011) 602-608.
[75] A.B. R. Snellings, K. Scrivener, The existence of amorphous phase in Portland cements: Physical factors affecting Rietveld quantitative phase analysis, Cem. Concr. Res. 59 (2014) 139-146.
[76] P. Stutzman, Direct determination of phases in Portland cements by Quantitative X-ray Powder Diffraction, US Department of Commerce, Washington D.C, 2010.
[77] J. Sieber, D. Broton, C. Fales, S. Leigh, B. MacDonald, A. Marlow, S. Nettles, J. Yen, Standard reference materials for cements, Cem. Concr. Res. 32 (2002) 1899-1906.

[78] J. Mandel, Evaluation and Control of Measurements, Marcel Dekker, New York, 1991.
[79] ASTM C1702: Standard Test Method for Measurement of Heat of Hydration of Hydraulic Cementitious Materials Using Isothermal Conduction Calorimetry, ASTM International, West Conshohocken, PA (USA).
[80] A. Quennoz, K.L. Scrivener, Hydration of C3A-gypsum systems, Cem. Concr. Res. 42 (2012) 1032-1041.
[81] J.P. Bayoux, A. Bonin, S. Marcdargent, A. Mathieu, M. Verscaeve, Study of the hydration properties of aluminous cement and calcium sulphate mixes, in: R.J. Mangabhai (Ed.), Calcium aluminate cements, SPON Press, London, 1990.
[82] G. Mertens, P. Madau, D. Durnick, B. Blanpain, J. Elsen, Quantitative mineralogical analysis of hydraulic limes by X-ray diffraction, Cement and Concrete Research 37 (2007) 1524-1530.
[83] M. Bigare, A. Guinier, C. Maizieres, M. Regourd, N. Yannquis, W. Eysel, T.H. Hahn, E. Woermann, Polymorphism of Tricalcium Silicate and Its Solid Solutions, J. Am. Cer. Soc. 50(11) (1967) 609-619.
[84] I. Maki, K. Goto, Factors influencing the phase constitution of alite in Portland cement clinkers, Cem. Concr. Res. 12(3) (1982) 301-308.
[85] I. Maki, K. Kato, Phase Identification of Alite in Portland Cement Clinker, Cem. Concr. Res. 12 (1981) 93-100.
[86] X. Li, W. Zhou, S. Wang, M. Tang, X. Shen, Effect of SO3 and MgO on Portland cement clinker: Formation of clinker phases and alite polymorphism, Constr. Build. Mater. 58 (2014) 182-192.
[87] L. Gobbo, L. Sant' Agostino, L. Garcez, C3A polymorphs related to industrial clinker alkalies content, Cem. Concr. Res. 34 (2004) 657-664.
[88] A.C. Jupe, X. Turrillas, P. Barnes, S.L. Colston, C. Hall, D. Häusermann, M. Hanfland, Fast in situ X-ray-diffraction studies of chemical reactions: a synchrotron view of the hydration of tricalcium aluminate, Phys. Rev. B 53 (1996) R14697-R14700.
[89] L. Black, C. Breen, J. Yarwood, C.S. Deng, J. Philips, G. Maitland, Hydration of tricalcium aluminate (C3A) in the presence and absence of gypsum-studied by Raman spectroscopy and X-ray diffraction, J. Mater. Chem. 16 (2006) 1263-1272.
[90] A.N. Christensen, T.R. Jensen, N.V.Y. Scarlett, I.C. Madsen, J.C. Hanson, Hydrolysis of pure and sodium substituted calcium aluminates and cement clinker components investigated by in situ synchrotron X-ray powder diffraction, J. Am. Cer. Soc. 87 (2004) 1488-1493.
[91] L.G. Baquerizo, T. Matschei, K.L. Scrivener, M. Saiedpour, L. Wadso, Hydration states of AFm cement phases, Cem. Concr. Res. 73 (2015) 143-157.
[92] H.W.W. Pollitt, A.N. Brown, The Distribution of Alkalis in Portland Cement Clinker, Proceedings of the Proceedings of the 5th International Symposium on the Chemistry of Cement, Tokyo (Japan), 1968.
[93] I. Maki, Nature of the prismatic dark interstitial material in Portland cement clinker, Cem. Concr. Res. (1973) 295-313.
[94] M. Regourd, A. Guinier, The Crystal Chemistry of the Constituents of Portland Cement Clinker, Proceedings of the 6th International Congress on the Chemistry of Cement, Moscow (Russia), 1974.
[95] F.C. Lee, H.M. Banda, F.P. Glasser, Substitution of Na, Fe and Si in tricalcium aluminate and the polymorphism of solid solutions, Cem. Concr. Res. 12 (1982) 237-246.

[96] A.K. Chatterjee, Raw Materials Selection, in: F.M.M. J.I. Bhatty, S.H. Kosmatka (Ed.), Innovations in Portland Cement Manufacturing, Portland Cement Association, Skokie, Illinois (USA), 2004.
[97] D. Lechtenberg, Dried sewage sludge as an alternative fuel, Glob. Cem. Mag. (2011) 36-39.
[98] S. Puntke, Auswirkungen des Phosphateintrages in Drehofenanlagen der Zementindustrie auf Klinkermineralogie und Zementeigenschaften, TU ClausthalZellerfeld, 2005.
[99] P.S. D. Rapson, Improving control and quality, World Cem. (2006) 67-71.
[100] H. Moeller, Control of product quality during the use of secondary materials, VDZ Congress 2009: Process Technology of Cement Manufacturing, Verlag Bau + Technik GmbH Düsseldorf, Düsseldorf (Germany), 2009.
[101] Z. Wang, W. Wang, Influence of sewage sludge on the formation and microstructure of Portland cement clinker, 8th International Symposium on Cement & Concrete (ISCC2013), Nanjing (China), 2013.
[102] N. Husillos Rodríguez, S. Martínez-Ramírez, M.T. Blanco-Varela, S. Donatello, M. Guillem, J. Puig, C. Fos, E. Larrotcha, J. Flores, The effect of using thermally dried sewage sludge as an alternative fuel on Portland cement clinker production, J. Clean. Prod 52 (2013) 94-102.
[103] G.A. N. Gineys, F. Sorrentino, D. Damidot, Incorporation of trace elements in Portland cement clinker: thresholds limits for Cu, Ni, Sn or Zn, Cem. Concr. Res. 41 (2011) 1177-1184.
[104] G.A. N. Gineys, D. Damidot, Managing trace elements in Portland cement - Part II: Comparison of two methods to incorporate Zn in a cement, Cem. Concr. Compos. 33 (2011) 629-636.
[105] K.G. A. Stumm, G. Beuchle, L. Black, P. Stemmermann, R.Nüesch, Incorporation of zinc into calcium silicate hydrates, Part I: formation of C-S-H(I) with C/S = 2/3 and its isochemical counterpart gyrolite, Cem. Concr. Res. 35 (2005) 1665-1675.
[106] S.K. N. Saikia, T. Kojima, Influence of Sn on the hydration of tricalcium aluminate Ca3Al2O6, J. Therm. Anal. Calorim. 109 (2012) 273-286.
[107] J.-E.C. P.-H. Shih, H.-C. Lu, L.-C. Chiang, Reuse of heavy metal-containing sludges in cement production, Cem. Concr. Res. 35 (2005) 2110-2115.
[108] M. Zajac, A. Rossberg, G.L. Saout, B. Lothenbach, Influence of limestone and anhydrite on the hydration of Portland cements, Cem. Concr. Compos. 46 (2014) 99-108.
[109] D.P. Bentz, Activation energies of high-volume fly ash ternary blends: hydration and setting, Cem. Concr. Compos. 53 (2014) 214-223.
[110] J.T. D. P. Bentz, A. Ardani, Ternary blends for controlling cost and carbon content: high-volume fly ash mixtures can be enhanced with additions of limestone powder, Concr. Int. 35(8) (2013) 51-59.
[111] W.K. K. Song, J. Bang, S. Park, C. W. Jeon, Polymorphs of pure calcium carbonate prepared by the mineral carbonation of flue gas desulfurization gypsum, Mater. Des. 83 (2015) 308-313.
[112] T.M. V. T. Cost, J. Shannon, I. L. Howard, Extending the use of fly ash and slag cement in concrete through the use of Portland-limestone cement, Proceedings NRMCA international concrete sustainability conference, 2014.
[113] B.L. T. Matscehi, F. P. Glasser, The role of calcium carbonate in cement hydration, Cem. Concr. Res. 37 (2007) 551-558.

[114] M.B.H. K. De. waardt, G. Le Saout, K. O. Kjellsen, H. Justnes, B. Lothenbach, Hydration mechanisms of ternary Portland cements containing limestone powder and fly ash, Cem. Concr. Res. 41 (2011) 279-291.
[115] J.E.O. J. Moon, M. Balonis, F. P. Glasser, S. M. Clark, P. J. M. Monteiro, High pressure study of low compressibility tetracalcium aluminum carbonate hydrates 3CaO Al2O3 CaCO3 11H2O, Cem. Concr. Res. 42 (2012) 105-110.
[116] I. Dreizler, D. Knoefel, Effect of magnesium oxide on the properties of cement, ZKG B. 35(12) (1982) 293-301.
[117] C.F. Macrae, I.J. Bruno, J.A. Chisholm, P.R. Edgington, P. McCabe, E. Pidcock, L. Rodriguez-Monge, R. Taylor, J.v.d. Streek, P.A. Wood, Mercury CSD 2.0 - New Features for the Visualization and Investigation of Crystal Structures J. Appl. Cryst. 41 (2008) 466-470.
[118] J. Faitli, T. Magyar, E. A, A. Muranyi, Characterization of thermal properties of municipal solid waste landfills, Waste Management 36 (2015) 213-221.
[119] M. Long, J. Sheng, T. Liu, D. Chen, Y. Yang, S. Gong, C. Chen, Thermo-Physical Properties of Petroleum Coke during Calcining Graphitization Process, Drying, Roasting, and Calcining of Minerals, Springer, The Minerals, Metals & Materials Society, 2015.
[120] N. Sliusar, G. Armisheva, Energy resources recovery on municipal solid waste disposal, 2nd International Conference on Final Sinks, Finland, 2013.
[121] D.F. Varfolomeev, E.V. Artomonova, G.S. Degtyarev, Determination of heat capacities of petroleum cokes at elevated temperatures, Translated from Khimiya i TekhnoloEiya Topliv i Masel 6 (1986) 31-32.
[122] B.D. Hong, E.R. Slatick, Carbon dioxide emission factors for coal, Quarterly Coal Report. 7 (1994).
[123] Holcim LTD, Annual Report, Switzerland, (2009). Retrieved from http://www.annualreports.com/HostedData/AnnualReportArchive/h/OTC_HCMLF_2009.pdf

APPENDIX A. THE PHASES WITH CRYSTALLOGRAPHIC PLANES INFORMATION FOR PERFORMING MARCH-DOLLASE CORRECTION

The following table consists of the hkl planes information of specific phases (Table 6) to which the March-Dollase correction was applied.

Phase	hkl Plane
Alite - M3	1 0 1
Alite - M1	1 0 -1
Gypsum	0 1 0
Calcite	0 0 1
Bassanite	1 1 0
Anhydrite	0 0 1
Dolomite	1 0 4
Portlandite	0 0 1

APPENDIX B. QXRD RESULTS OF THE STUDIED CEMENTS

Figure 41–Figure 65 cover all the results of the cements that researchers received from TxDOT. Please refer to Table 3 for the list of all samples received from TxDOT.

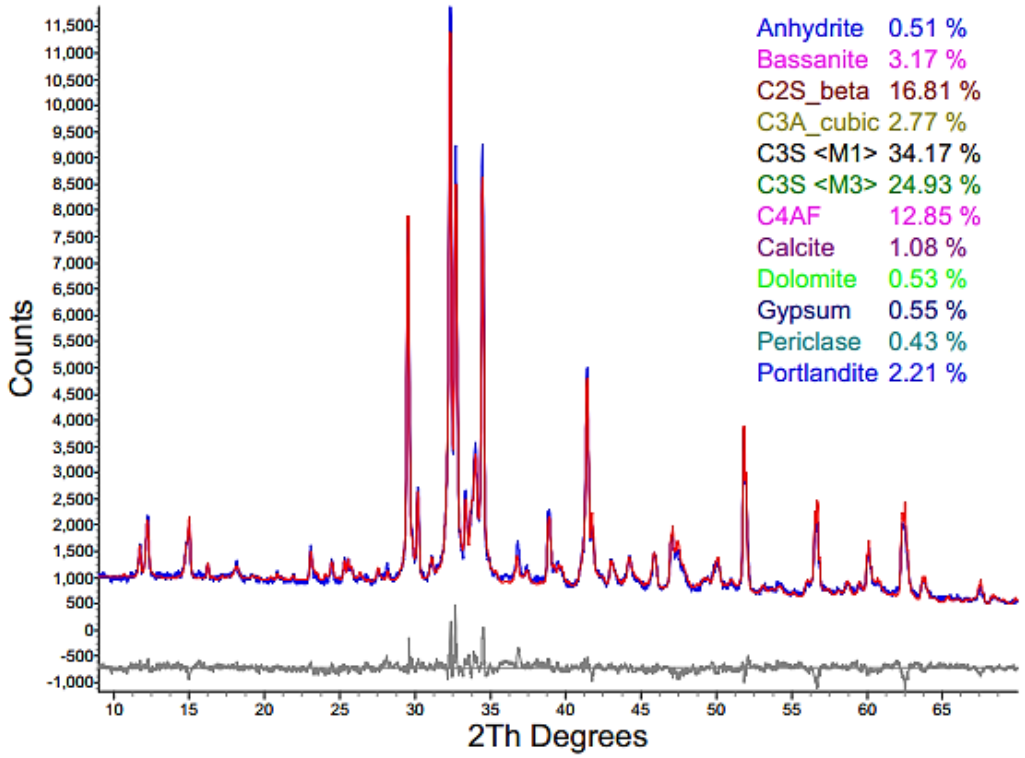

Figure 41. QXRD of Cement I/II 657.

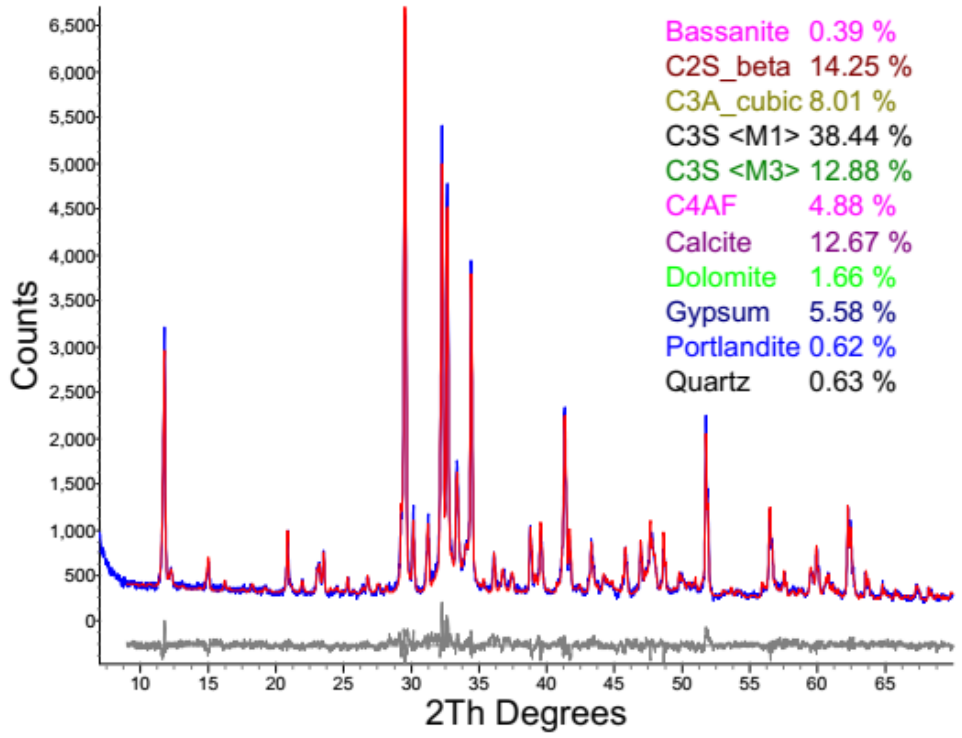

Figure 42. QXRD of Cement IL 561.

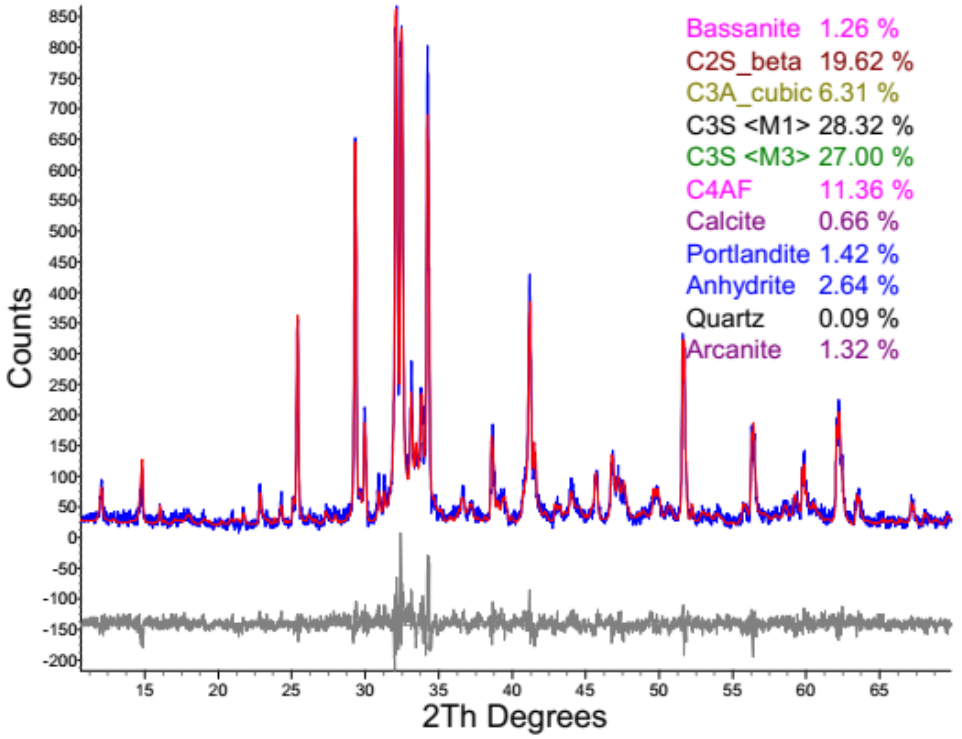

Figure 43. QXRD of Cement II/V 751.

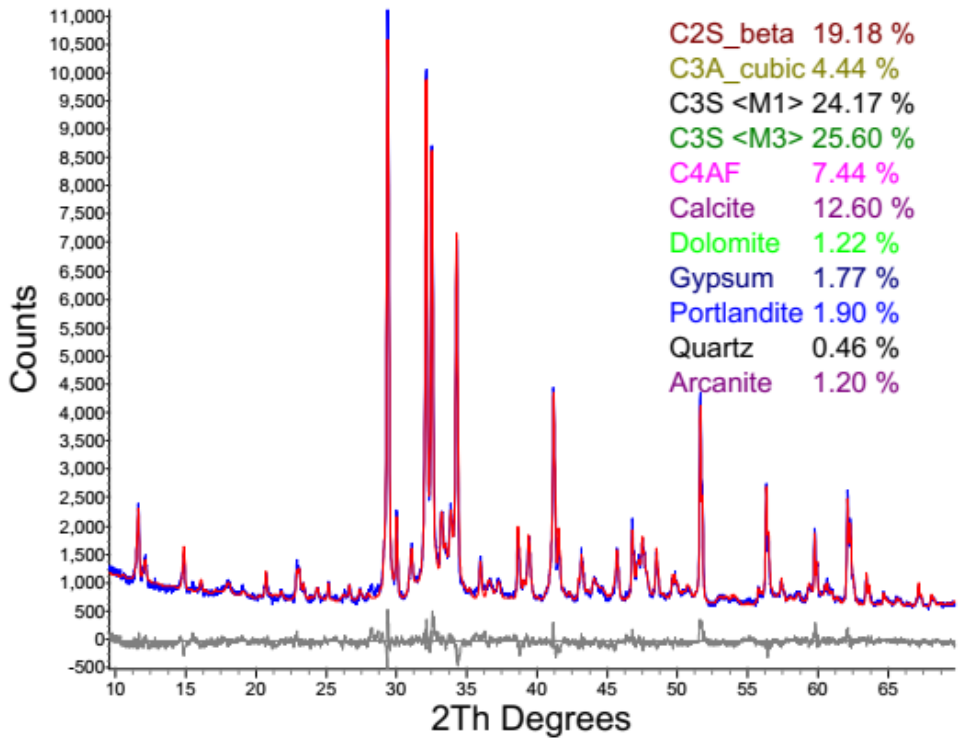

Figure 44. QXRD of Cement II/V 751 (Second Batch).

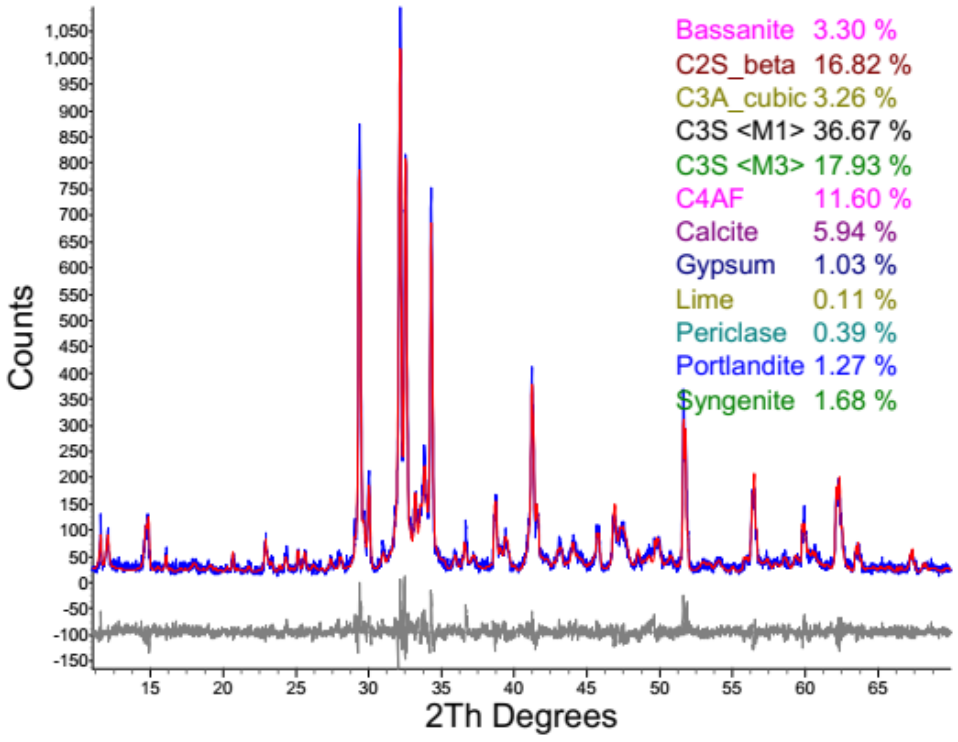

Figure 45. QXRD of Cement I/II 754 (First Batch).

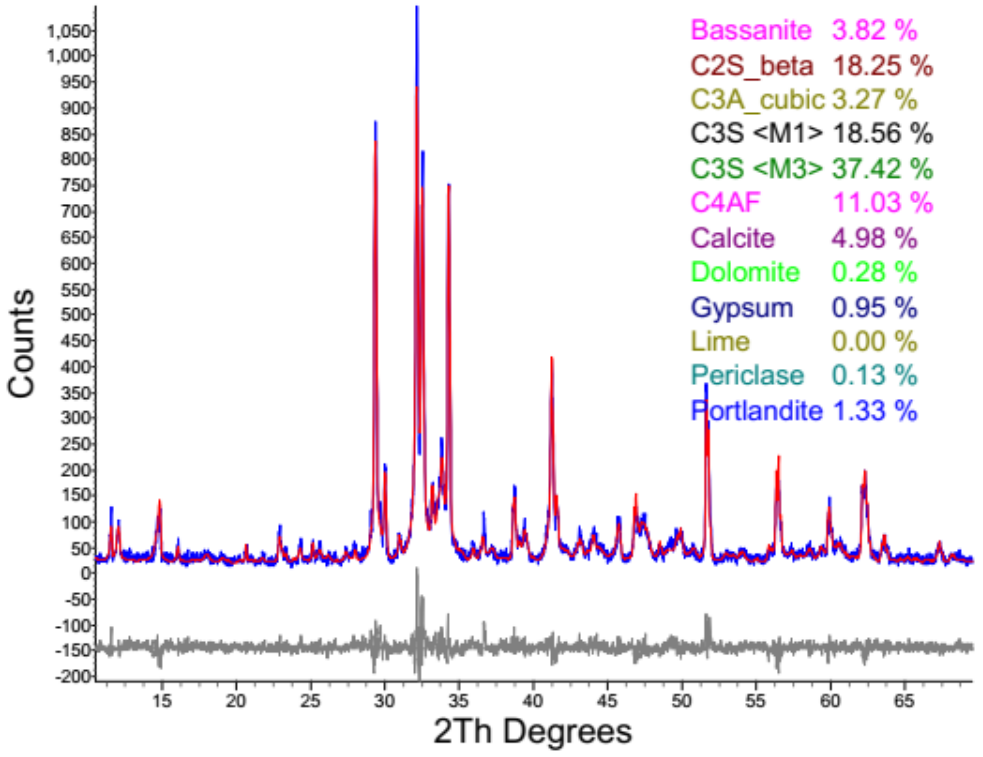

Figure 46. QXRD of Cement I/II 754 (Second Batch).

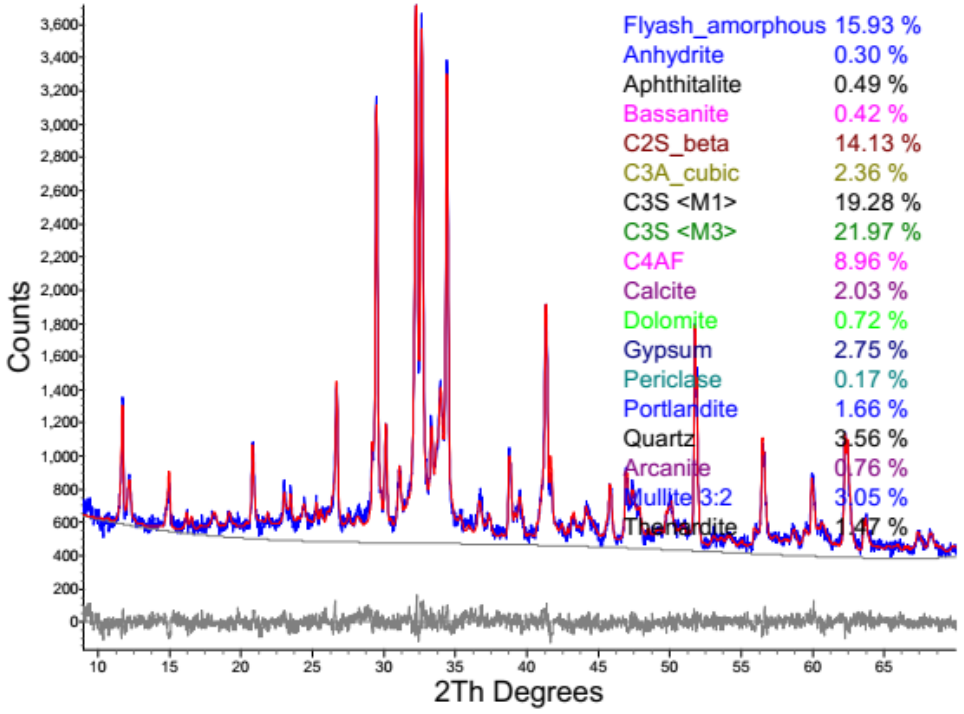

Figure 47. QXRD of Cement IP 585.

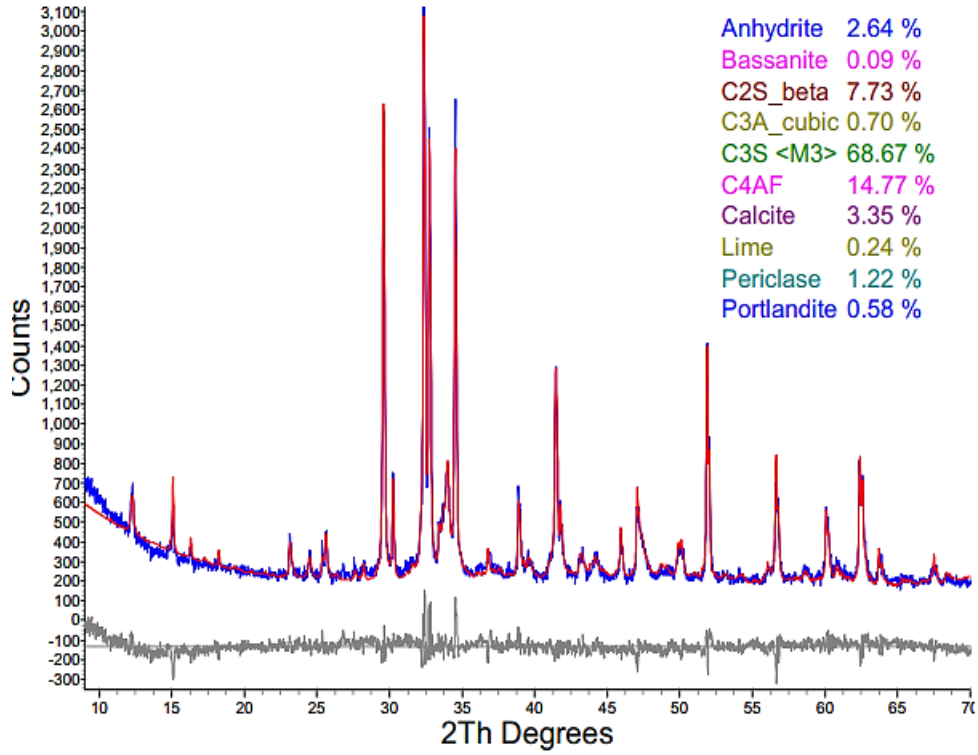

Figure 48. QXRD of Cement I/II 651.

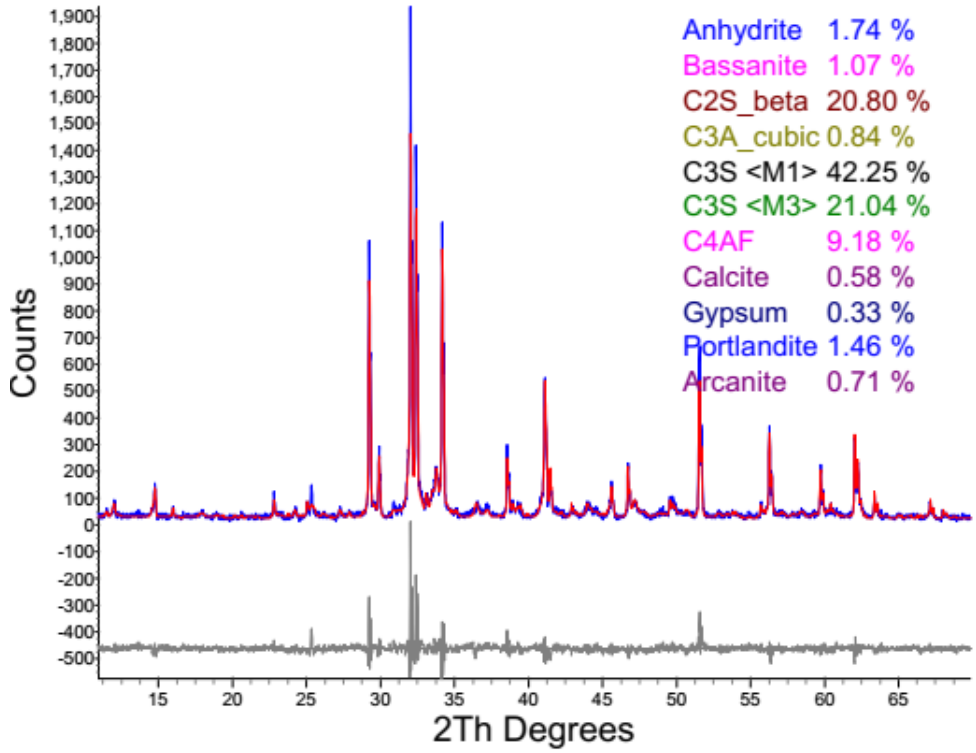

Figure 49. QXRD of Cement II/V 710.

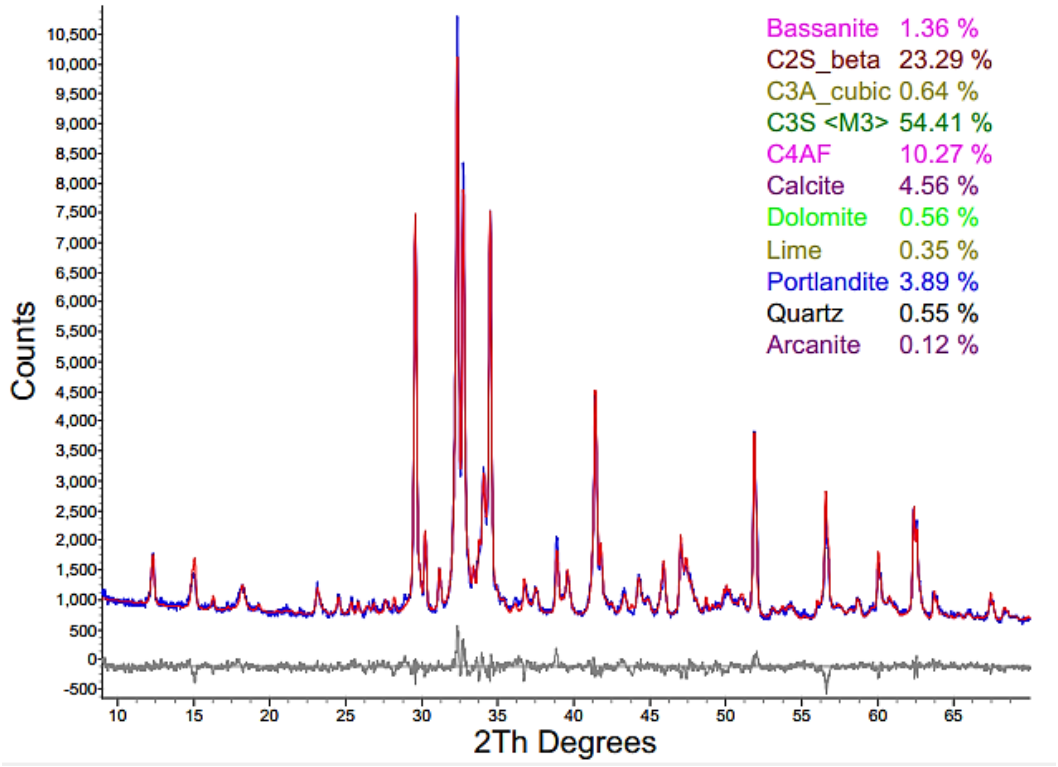

Figure 50. QXRD of Cement I/II 629.

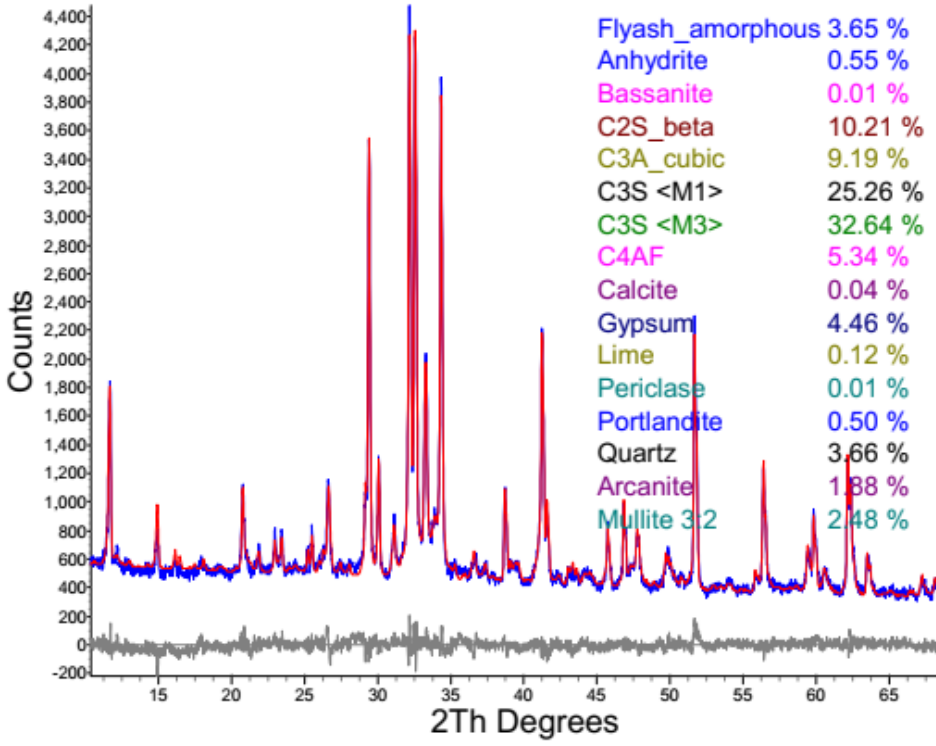

Figure 51. QXRD of Cement IP 668.

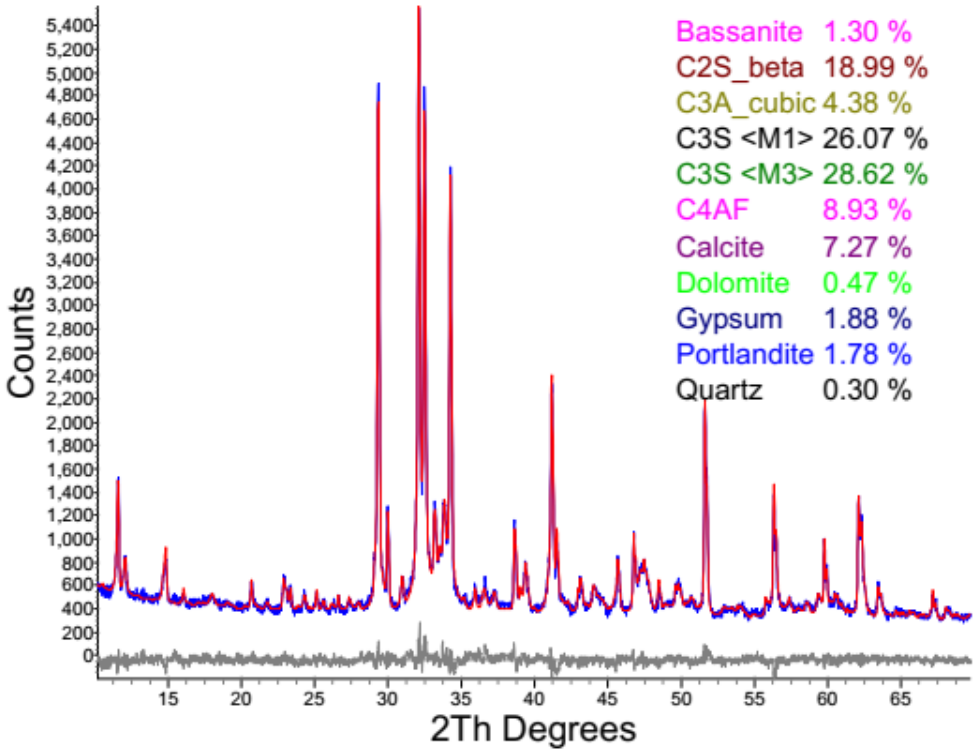

Figure 52. QXRD of Cement IL 589.

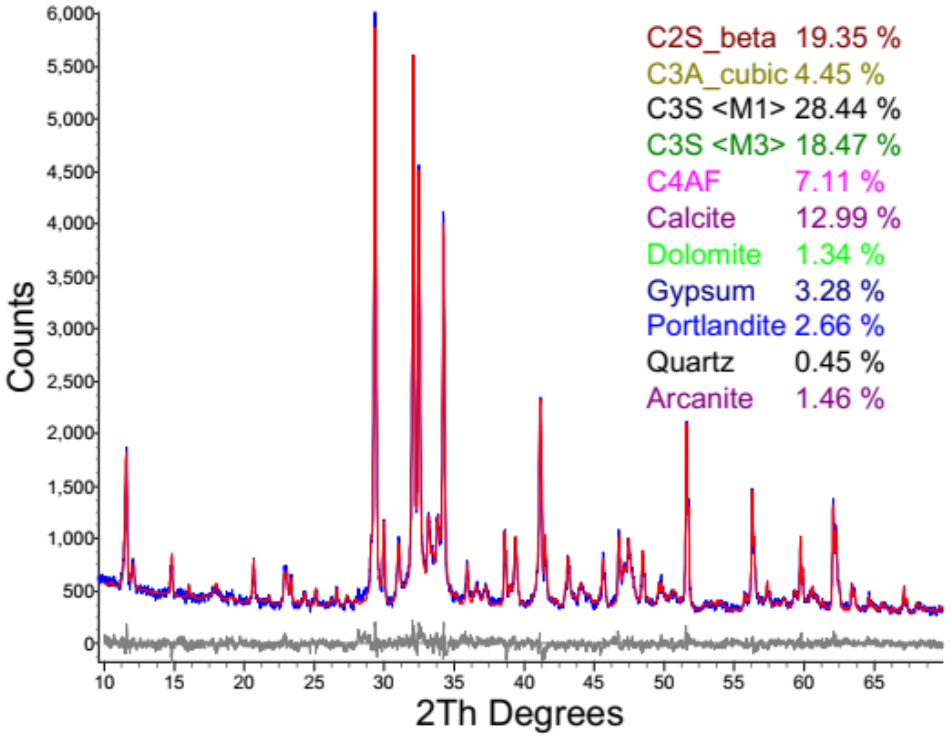

Figure 53. QXRD of Cement IL 707 (First Batch).

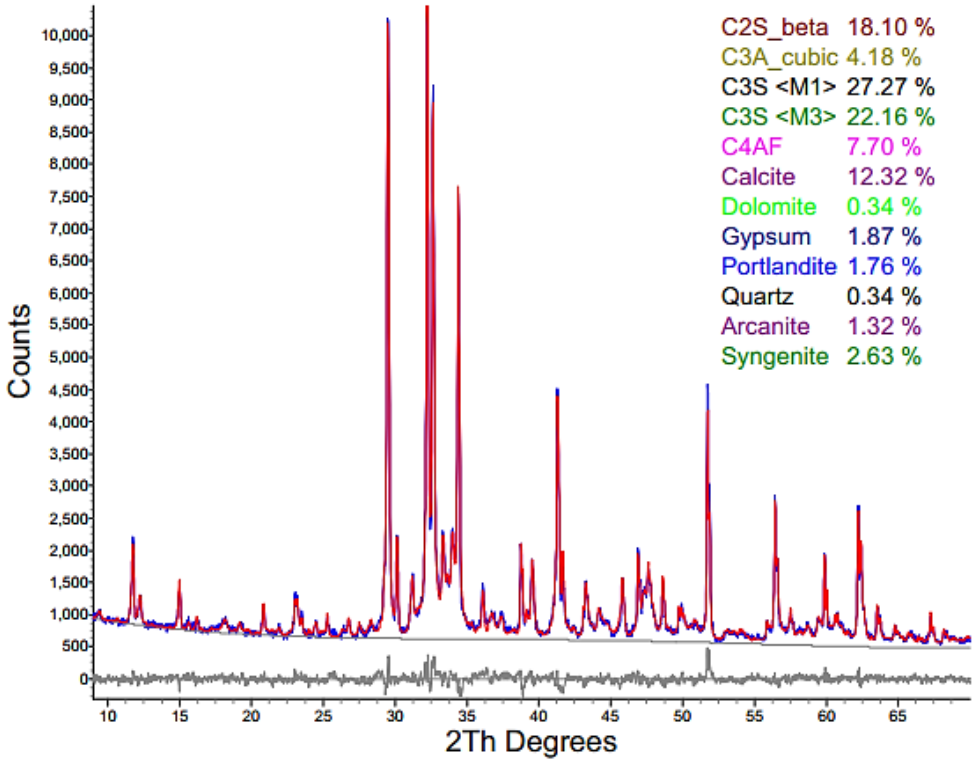

Figure 54. QXRD of Cement IL 707 (Second Batch).

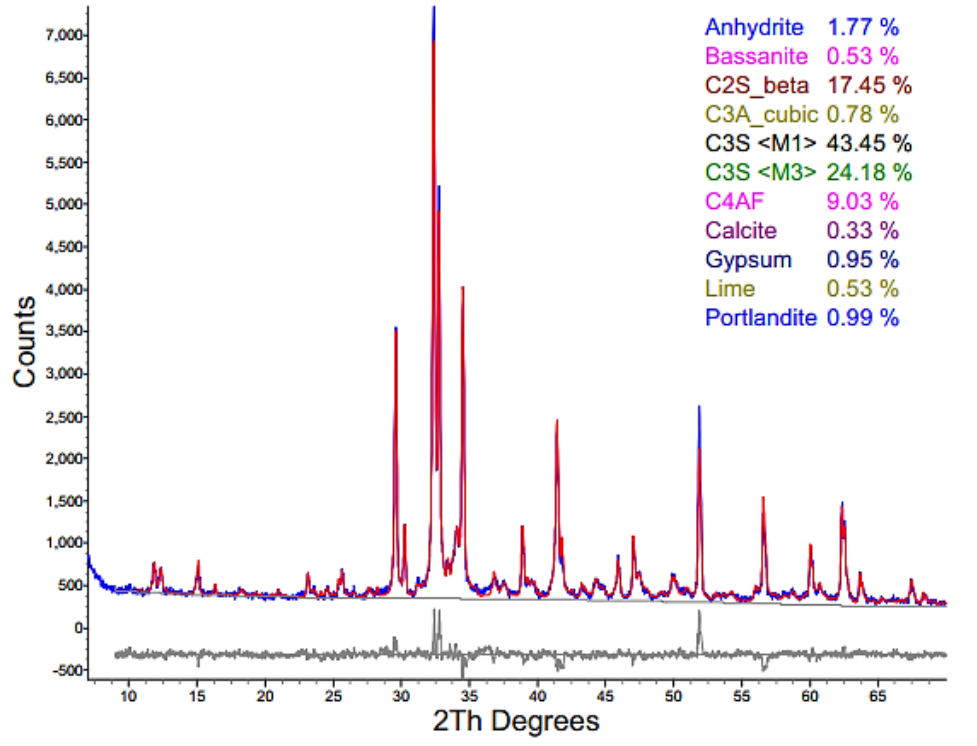

Figure 55. QXRD of Cement II/V 180.

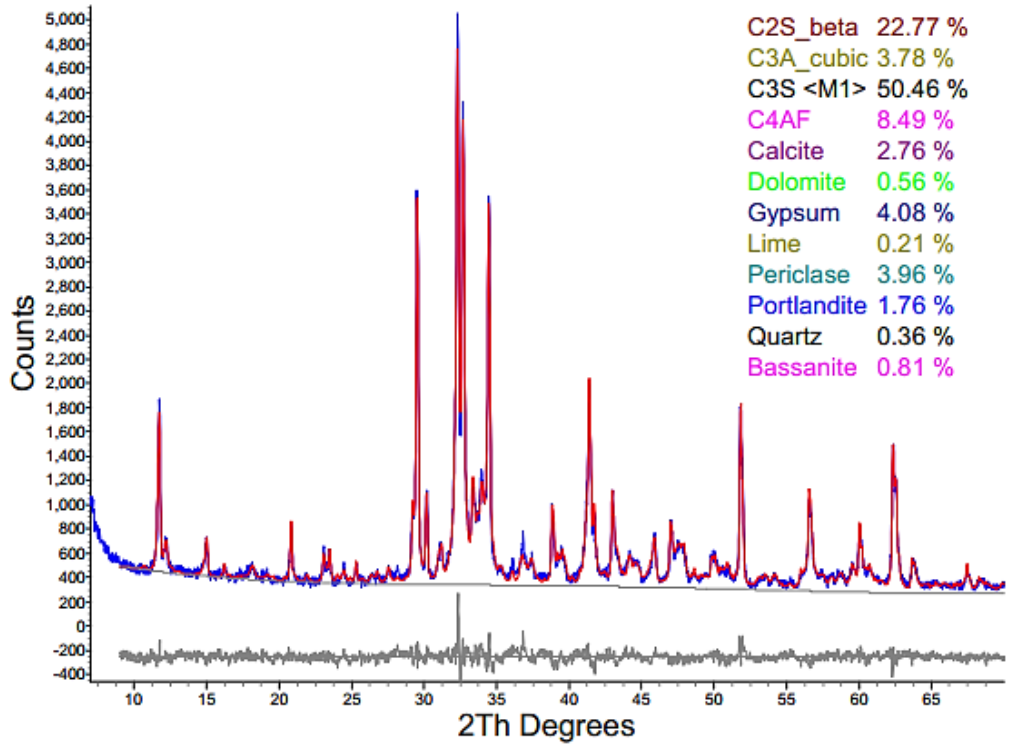

Figure 56. QXRD of Cement I/II 148.

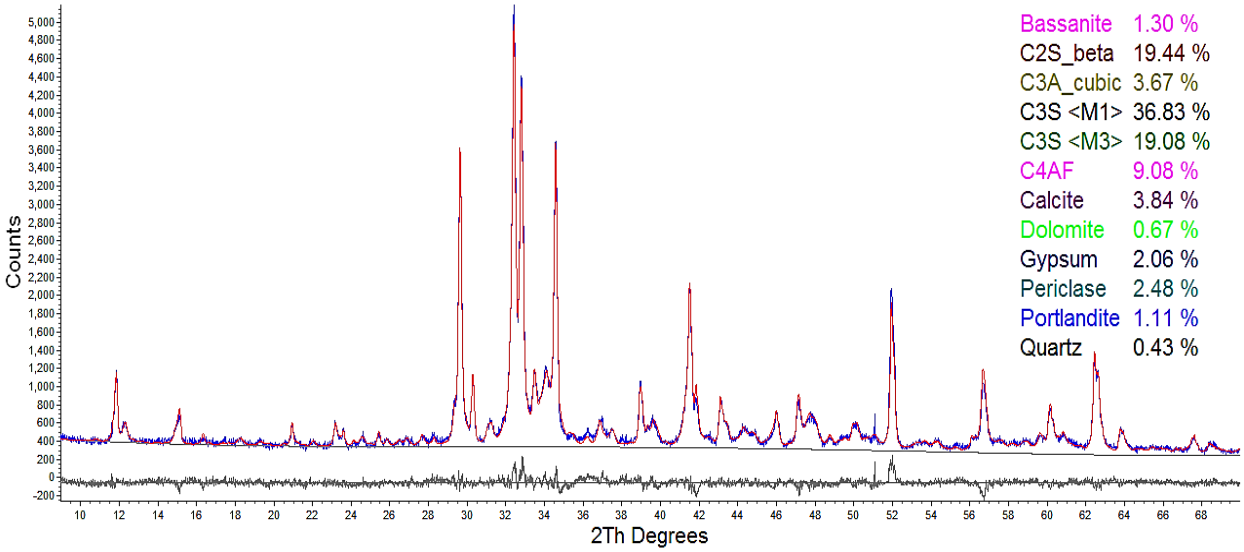

Figure 57. QXRD of Cement I/II 208.

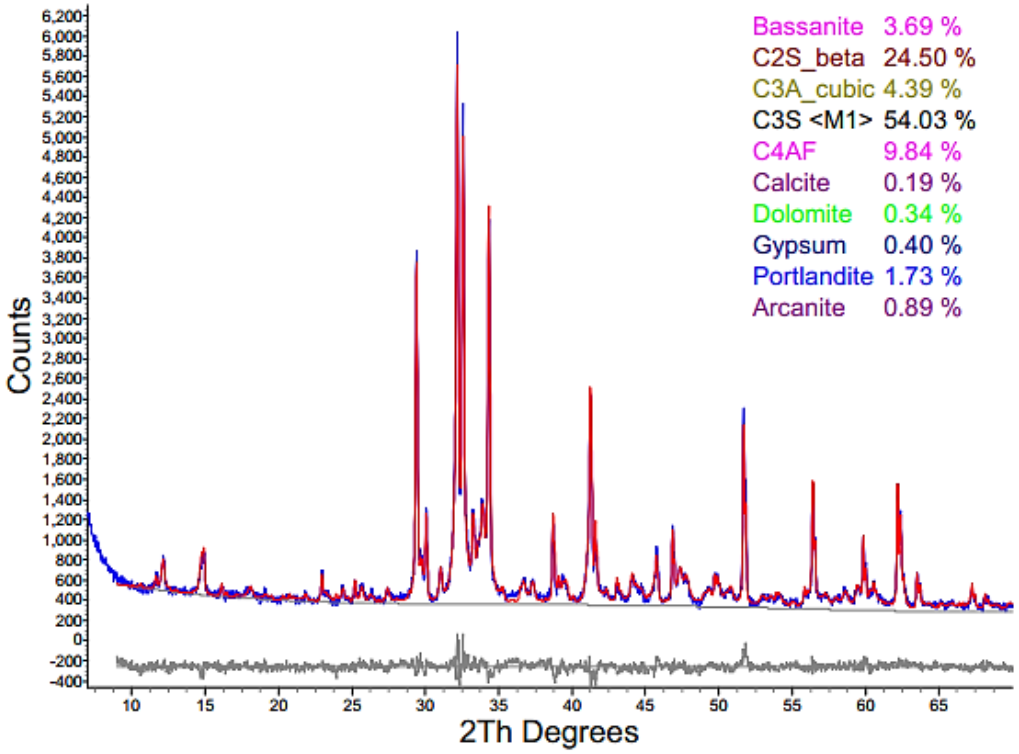

Figure 58. QXRD of Cement III 008.

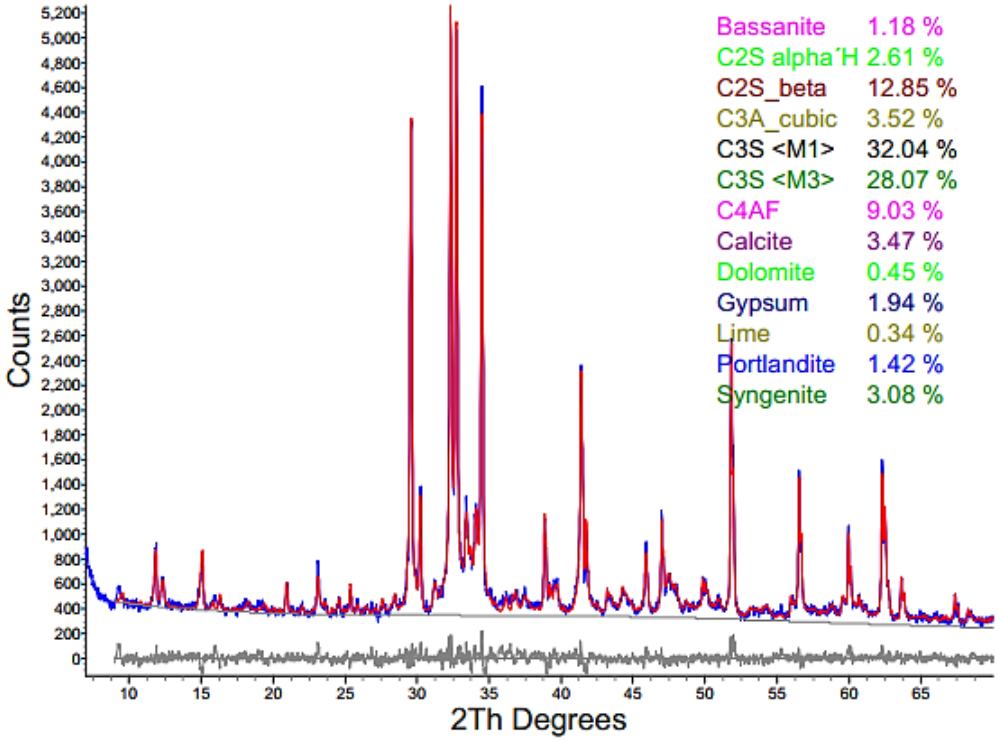

Figure 59. QXRD of Cement III 099.

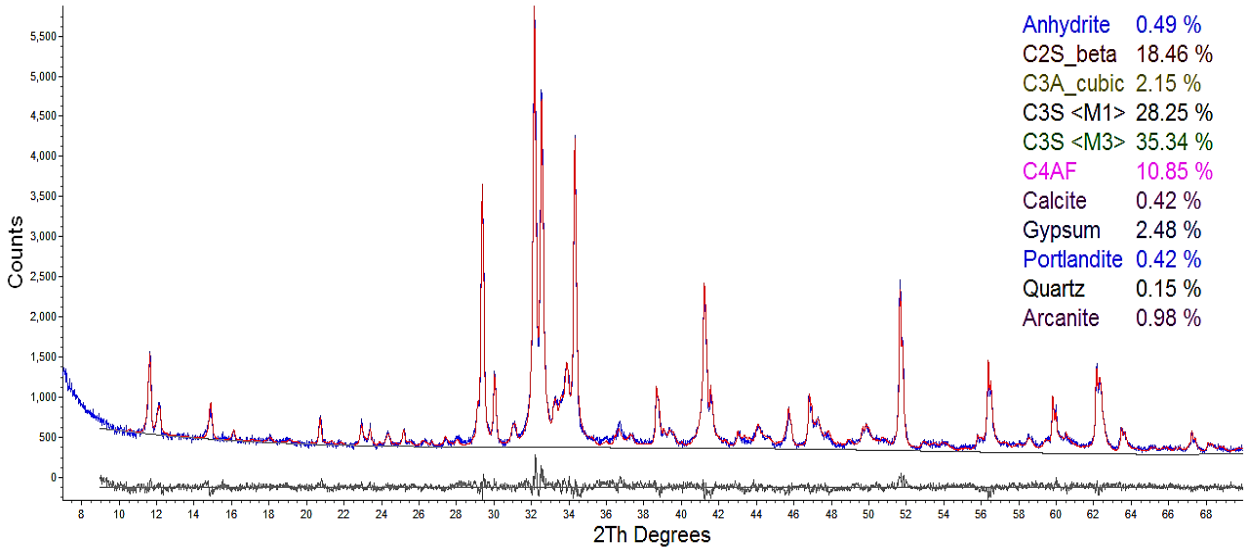

Figure 60. QXRD of Cement III 056.

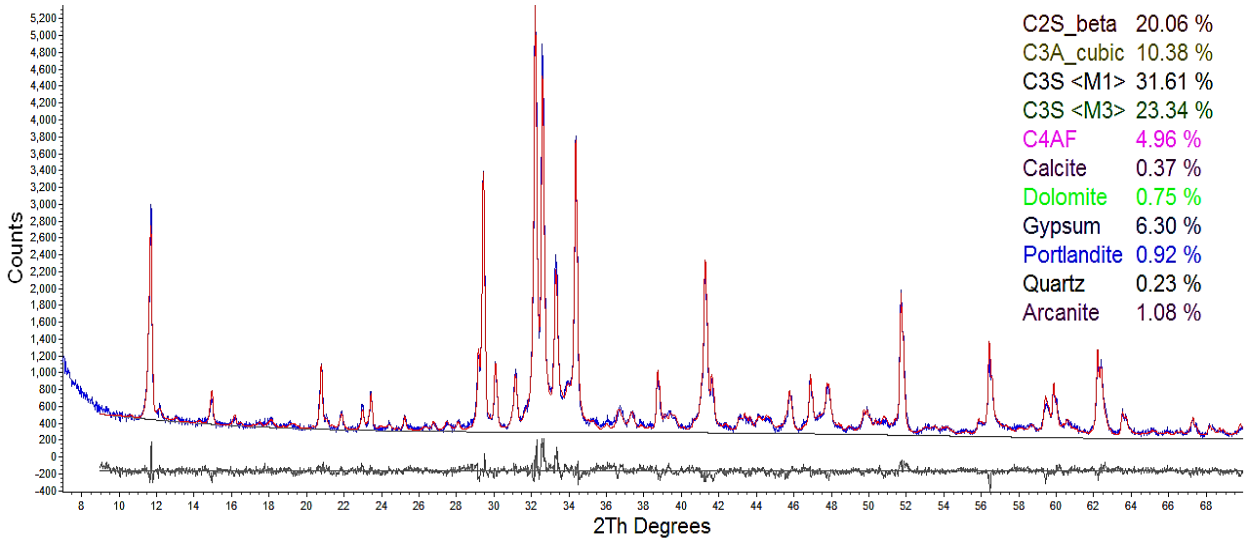

Figure 61. QXRD of Cement I 063.

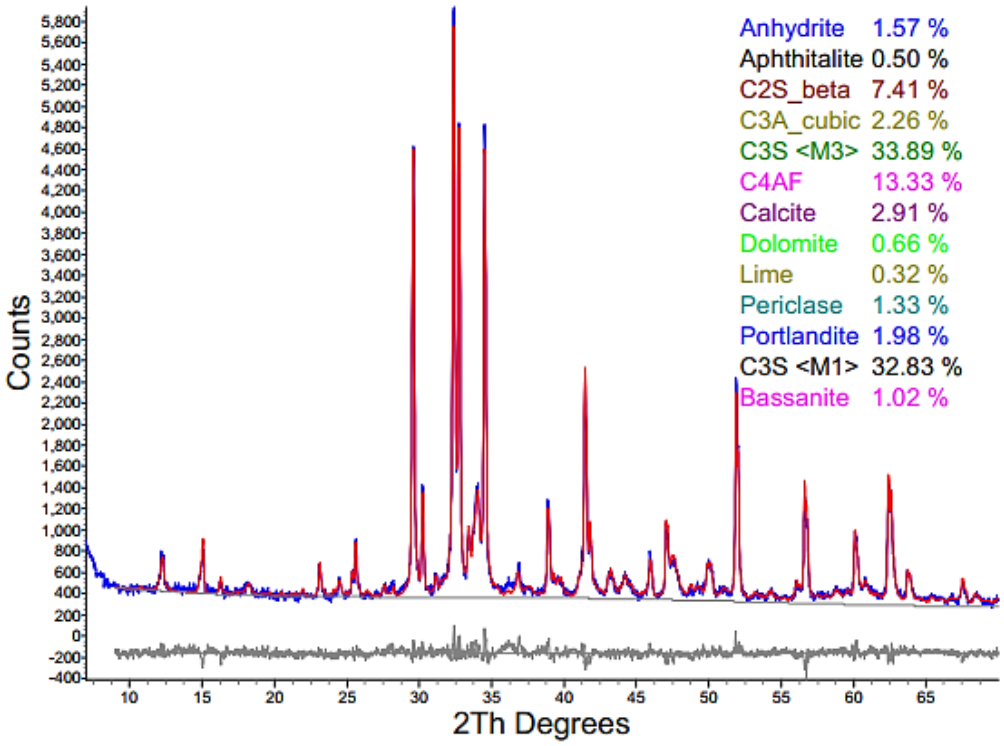

Figure 62. QXRD of Cement II/V 148.

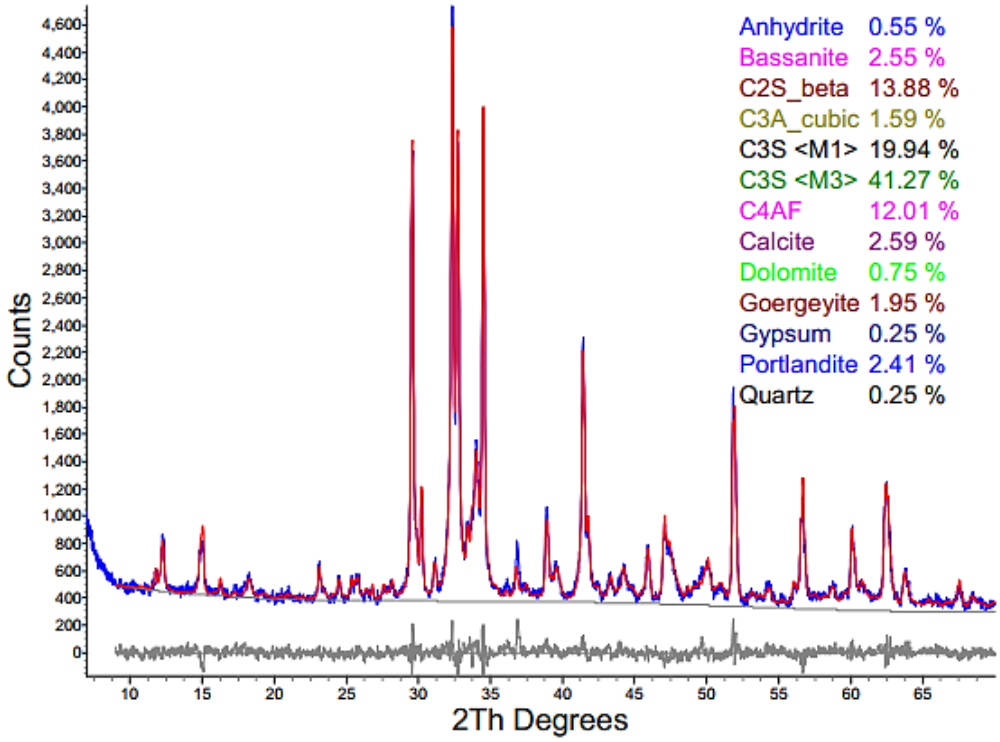

Figure 63. QXRD of Cement II/V 019.

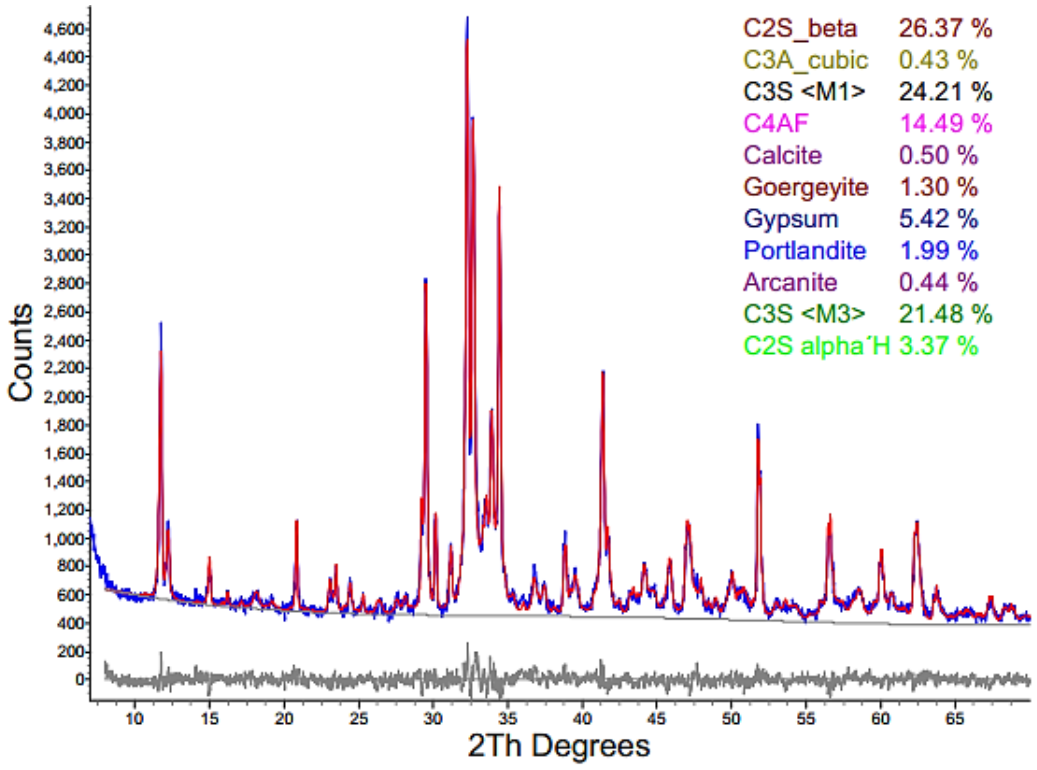

Figure 64. QXRD of Cement II/V 002.

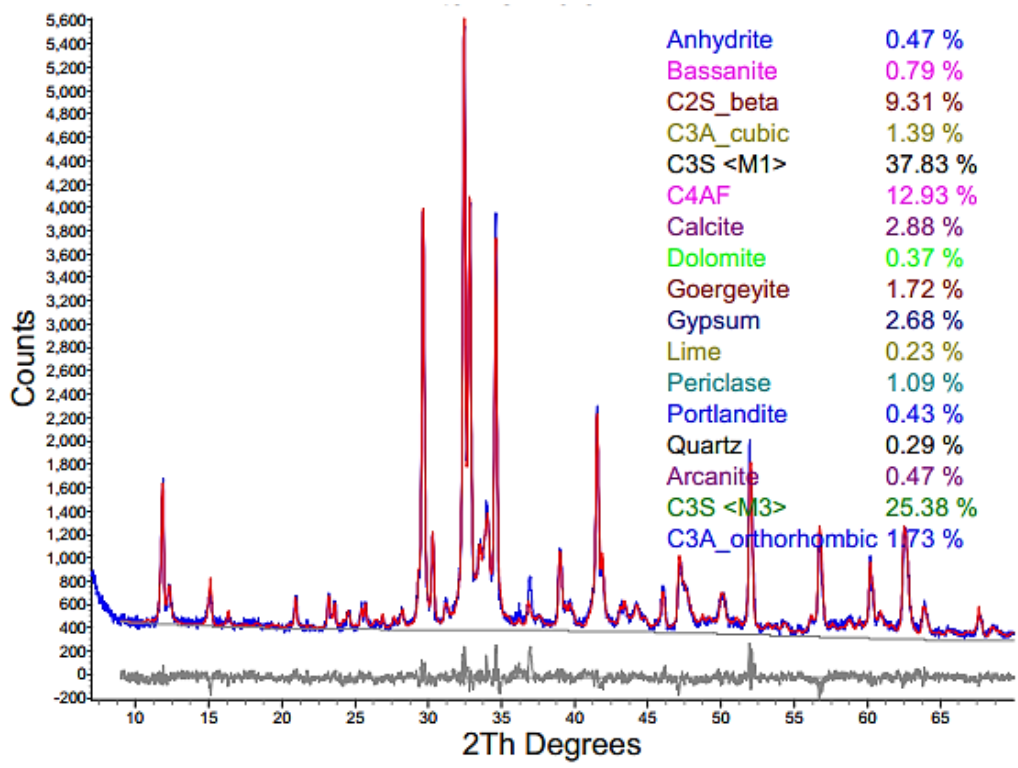

Figure 65. QXRD of Cement II/V 058.